

SRC-2006-32  
30 October 2006  
Contract/Order No: B2532534  
Void Detection Demonstration Projects

Technical Report  
Final Report

---

# Void Detection Technology Delta ElectroMagnetic Gradiometer

*Prepared for*

---

Jim Pfeifer  
MSHA Technical Support  
Mine Waste and Geotechnical Engineering Division  
P.O. Box 18233  
Cochrans Mill Road  
Pittsburgh, Pennsylvania 15236  
Pfeifer.james@dol.gov

*Prepared by*

---



Stolar Research Corporation  
848 Clayton Highway  
Raton, New Mexico 87740  
(505) 445-3607  
fax: (505) 445-2038  
stolar@stolarhorizon.com



## TABLE OF CONTENTS

Electromagnetic Gradiometer Demonstration .....	1
Task Summary .....	1
Background .....	2
Electromagnetic Gradiometer System Overview.....	3
Global Positioning System Overview .....	5
Electromagnetic Gradiometer Instrument Design .....	7
Electromagnetic Survey Operating Frequency .....	13
Field Tests and Data Analysis.....	16
Area 1 – 2 <sup>nd</sup> South CC38 .....	20
Area 2 - 2 <sup>nd</sup> South CC29 .....	22
Area 3 – 4 <sup>th</sup> East CC12 .....	25
Area 4 – 1 <sup>st</sup> South CC28 .....	27
Area 5 – 4 <sup>th</sup> East CC25 .....	30
Area 6 – 7 <sup>th</sup> North CC72.....	33
Old Workings Area.....	35
Data Plots and Interpretation .....	37
Conclusions.....	39
Survey Field Test Results .....	39
Confirmation Drilling .....	40
References.....	46

## APPENDICES

A. Spatial Plots.....	A-1
B. DeltaEM Gradiometer Specifications .....	B-1
C. Geological Log Data .....	C-1
D. EarthFax Report .....	D-1



## LIST OF FIGURES

<b>Figure 1.</b> Fundamental science.....	4
<b>Figure 2.</b> Top: DeltaEM Gradiometer receiver assembly components. Bottom: DeltaEM Gradiometer chassis and tripods in storage and shipping case. ....	8
<b>Figure 3.</b> DeltaEM gradiometer system antennas. ....	9
<b>Figure 4.</b> DeltaEM Gradiometer system transmitter components; 30-in.-diameter loop (left), and 31-ft-diameter loop coiled up (right). ....	9
<b>Figure 5.</b> Personal Data Assistant used for the DeltaEM Graphical User Interface. ....	10
<b>Figure 6.</b> GUI Graph page.....	11
<b>Figure 7.</b> GUI Setup page. ....	11
<b>Figure 8.</b> GUI GPS page. ....	12
<b>Figure 9.</b> GUI Data page. ....	12
<b>Figure 10.</b> Remote computer system.....	13
<b>Figure 11.</b> Emery Mine gradiometer survey areas.....	18
<b>Figure 12.</b> Area 1 survey location.....	21
<b>Figure 13.</b> Area 1 200-kHz survey lines spatially over mine workings.....	22
<b>Figure 14.</b> Area 2 survey location.....	23
<b>Figure 15.</b> Area 2 2-kHz survey lines spatially over mine workings.....	24
<b>Figure 16.</b> Area 2 20-kHz survey lines spatially over mine workings.....	25
<b>Figure 17.</b> Area 3 survey location.....	26
<b>Figure 18.</b> Area 3 2-kHz survey lines spatially over mine workings.....	27
<b>Figure 19.</b> Area 4 survey location.....	28
<b>Figure 20.</b> Area 4 2-kHz survey lines spatially over mine workings.....	29
<b>Figure 21.</b> Area 4 20-kHz survey lines spatially over mine workings.....	30
<b>Figure 22.</b> Area 5 survey location.....	31
<b>Figure 23.</b> Area 5 2-kHz survey lines spatially over mine workings.....	32
<b>Figure 24.</b> Area 5 20-kHz survey lines spatially over mine workings.....	33
<b>Figure 25.</b> Area 6 survey location.....	34
<b>Figure 26.</b> Area 6 2-kHz survey lines spatially over mine workings.....	35
<b>Figure 27.</b> Old Workings Area survey location.....	36
<b>Figure 28.</b> Old Workings Area 2-kHz survey lines spatially over mine workings.....	37
<b>Figure 29.</b> Delta Plotter user interface. ....	38
<b>Figure 30.</b> Diagram of the two geometric scenario modeled in the probability curves: #1 drill hole started at exact center of 14-ft-wide entry, #2 drill hole started at exact rib edge of 14-ft-wide entry.....	43



**Figure 31.** Scenario #1 Probability of intersecting mine entry with 3-in. drill string. Drill hole started at exact center of 14-ft-wide entry. .... 44

**Figure 32.** Scenario #2 probability of intersecting mine entry with 3-in. drill string. Drill hole started at exact rib-edge of 14-ft-wide entry. .... 45

### LIST OF TABLES

Table 1. Project Tasks and Status. .... 1

Table 2. Skin Depth Table. .... 14

Table 3. Summary of Small Loop Transmit Antenna Properties..... 15

Table 4. Summary of Large Loop Transmit Antenna Properties..... 16

Table 5. Summary of Survey Spatial Locations and Approximate Overburden. .... 19

Table 6. Drill hole predicted depths..... 41



## Electromagnetic Gradiometer Demonstration

The objective of this program, commissioned and overseen by the Mine Safety and Health Administration (MSHA) Technical Support Division, is to demonstrate the void-detection capabilities of Stolar’s Delta ElectroMagnetic (DeltaEM) Gradiometer survey system. This program was initiated in January 2005 and began active laboratory and field efforts in February.

A series of four field data collection tests have been completed at the Emery Mine on the following dates: 4-5 March 2005, 1-2 June 2005, 23-25 August 2005, and 28 February to 2 March 2006. The field tests were witnessed by MSHA representatives. This report is a summary of the field tests and fully documents activities, findings, and results of the demonstration. Appendices A through D provide supporting information.

### Task Summary

During contract negotiation, a list of project tasks was accepted as the statement of work. This list included DeltaEM system modifications (relevant to demonstration site/target specifications) and field testing (survey, preparation, site analysis, data collection/testing, final system demonstration, and ground-truthing). The project tasks are listed in Table 1 and their status is shown as percent complete.

Table 1. Project Tasks and Status.

<b>Project Task Title</b>	<b>Status (% Complete)</b>
Preliminary Site Data Collection	100
EM Gradiometer Assembly	100
Site Demonstration Plans	100
EM Gradiometer Demonstration – Emery	100
Ground Truth Determination	100
Draft Final Report	100
Confirmation Drilling	100
Final Report	100

## Background

Prior to this work, the DeltaEM gradiometer had been used successfully in a wide variety of military and industrial applications associated with subsurface void detection including clandestine tunnels, bunkers, underground utilities and voids, both natural and man-made (mined). The induction of current in these subsurface structures and/or conductors by the primary continuous wave (CW) of the magnetic dipole transmitter caused observable secondary EM waves on the surface. Analysis of the measured data at a variety of sites has determined that the centerlines and depth to the structures could be determined from their respective data sets. High signal-to-noise (S/N) ratios have been proven for many different types of structures and background geology. This has made possible the ability to analyze anomalous measurements during field data acquisition.

Clandestine tunnels and underground complexes (UGC) have been developed in recent years to conceal entries into embassies, border-crossing passageways, and military assets. The U.S. Army Belvoir Research and Development Engineering Center (BRDEC) have conducted tunnel-detection science and engineering investigations. These science and engineering investigations were reported in several conferences sponsored by BRDEC. In 1993, the USAE Waterways Experiment Station (now the Engineer Research and Development Center) received the Army's tunnel-detection mission. The discovery of drug-smuggling tunnels near San Diego, California, provided an opportunity to compare various geophysical techniques against these targets. The BRDEC (1993) report on the tunnel campaign found that "to be successful in detecting/locating a tunnel or cavity requires combining the use of high-resolution geophysical techniques having good depth of penetration with advanced signal processing and interpretation techniques." One of the conclusions of the BRDEC study was that the active frequency-domain (continuous wave) electromagnetic (EM)-gradiometer imaging system developed by Stolar clearly demonstrated the capability to detect and define tunnels.[1]

While the tunnels' conductors generally provide the strongest target, the surveys also demonstrated that a tunnel without conductors can be detected with high-frequency EM instrumentation. Ground-penetrating radar (GPR) technology was not able to detect the tunnels. In 1994, a panel of U.S. Department of Energy (DOE) National Laboratory geophysicists accepted an assignment to assess the state of the geophysical technologies that might be applied in the underground structure detection problem.

As a result of the DOE/NN-20 Benchmark Study [2], Sandia National Laboratories (SNL) continued the evolutionary development of the active EM gradiometer receiver design applied in the BRDEC tunnel work. Integral equation

and finite difference codes were used to determine the EM secondary response for underground tunnels and complexes. A laboratory EM gradiometer receiver was built and successfully acquired gradiometer data from the DOE Nevada Test Site (NTS) Cloud Chamber and the Yucca Mountain Tunnel[3]. The EM gradiometer was the only technology that successfully detected the Yucca Mountain Tunnel at a depth of 200 ft. The active EM gradiometer receiver design was revised in work sponsored by the Air Force Research Laboratory as part of the High-Frequency Active Aurora Research Project (HAARP). The tunnel sites in San Diego were selected as demonstration sites for the newly developed synchronized EM gradiometer receiver. The sync EM gradiometer instrumentation provided rapid real-time surface-based data collection and interpretation at the tunnel. The DeltaEM system used in this demonstration is the commercial version of that original gradiometer prototype. The commercial version has been continuously upgraded and demonstrated at dozens of UGC sites in the last 10 years, including mining and military sites.

## Electromagnetic Gradiometer System Overview

The DeltaEM Gradiometer survey system provides a tool that can generate subsurface geophysical imaging capabilities with greater sensitivity, range (distance), and flexibility than with existing instrumentation [2]. A couple of primary advantages of gradient measurements are: 1) the ability to detect the significant rate of change in gradient fields that do not exist in total field measurements, and 2) the ability to reject interfering, unwanted signals that would be summed in total field measurements. Also, in efforts using local radio sources (HAARP, civilian-band AM radio, etc.), EM gradiometry has been shown to be a promising technique.

The synchronized EM gradiometer instrumentation is a narrow-band receiver that can discriminate against the spectra noise components and operate in the low ionosphere-earth waveguide noise band, thus maximizing the detection threshold sensitivity of the instrumentation. Primary EM waves interact with underground infrastructures to create secondary EM waves that are detectable on the earth's surface with a gradiometer. Synchronization to the primary wave in the extremely low-frequency and very-low-frequency (ELF/VLF) bands enables very narrow-band detection with threshold detection sensitivity in the sub picotesla (pT) range [4]. The EM gradiometer capitalizes on its high threshold detection sensitivity to secondary EM waves in the ELF/VLF bands.\*

---

\* The ELF band is 30 to 300 Hz.  
The VLF band is 3 to 30 kHz.

Two important advantages in UGC detection have been achieved with this system. First, the magnitude of the scattered secondary wave from the UGC infrastructure increases as frequency decreases; thus, waves in the ELF/VLF bands have a significant advantage in the UGC detection. Second, the attenuation rate of EM waves in the ELF/VLF bands through soil/rock is very low so that deeply buried structures can be illuminated and detected. The structures may be empty passageways or may contain electrical conductors serving utility and ventilation needs.

Figure 1 depicts the fundamental science of this application. An underground tunnel or cave exists and contains a man-made or natural electrical path. The “channel” of electrical current flow ( $I$ ) is the source of the secondary EM field. Primary EM waves induce current into the electrical path. In the empty tunnel case, the higher conductivity layer underlying the tunnel “channels” current. The high electrical conductive layers underlying the tunnel are caused by soluble salts. The result is a cylindrically spreading EM wave that is observable on the surface. In either case, the subsurface induced current results in a surface detectable secondary EM wave.

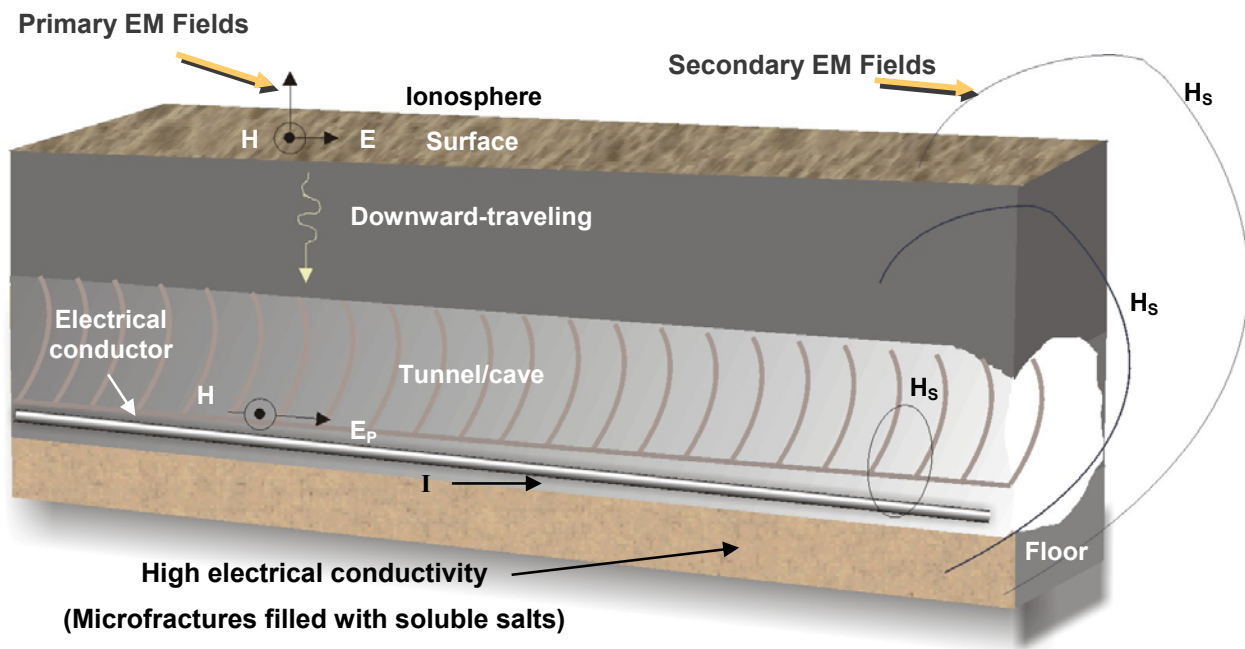


*Figure 1. Fundamental science.*

The DeltaEM electromagnetic gradiometer for underground structure detection is a mobile unit, comprising a dual receiver and a separate transmitter. Setting up any underground detection survey requires preplanning, which must be specific to the location of the survey. Before the survey, the surveyor must note the location of



any obvious metallic conductors, such as overhead power lines. These structures will be detected by the DeltaEM system and will create “false positives” in the profile. Corrections can be made to the final data set to eliminate the effects of such structures. However, if a structure’s position is delineated in the data file, its occurrence in the final profile typically can be ignored. The distance from these surface features to the survey traverse can be predicted from the profile plot and correlated to the actual distance as measured in the field. This way the surface conductor can be discriminated and subsurface anomalies can be better identified.

The DeltaEM gradiometer survey setup involves a selected survey method and a selected survey grid. The basic system survey methods are a linear traverse or an arc traverse with a fixed-offset transmitter, and a bi-static traverse where the receiver and transmitter move in unison. DeltaEM rejects the primary wave while measuring the gradient of the secondary scattered EM wave. This secondary wave radiated out and away in a cylindrical wave-front from any linear subsurface conductive source. The DeltaEM system will provide the most optimal response to this wave-front if carried along a traverse line that passes over the conductor in a perpendicular orientation. If the traverse line passes over the conductor at an angle other than 90 degrees, the conductor is still detected however the shape of the response curve will not be symmetric and its amplitude will decrease as the angle approaches zero. If the traverse line is quasi-perpendicular but does not pass directly over the void, the response may still be perceivable but its amplitude will decrease proportionally to the distance from the traverse line to the conductor. **For the purpose of this report, the detectable subsurface voids (mine workings) are approximated as a conductive EM-wave scattering source resulting from conductivity contrasts between the background rock and the air- or water-filled void cavity.**

## Global Positioning System Overview

The two predominant types of global positioning system (GPS) receivers are classified as “code” and “carrier.” The satellite code pattern has a granularity of about 1 m, while the carrier pattern has a granularity of about 1 mm; these are the absolute maximum accuracies.

Sources of error add up to degrade the accuracy of the GPS system. These error sources include satellite clock, receiver clock, satellite orbit error, atmospheric error, geometric error, and signal multipath error. Some cures for the sources of error include differential mode, kinematic mode, and signal processing techniques.

Autonomous mode does not use any aiding whatsoever. Differential mode requires the use of two receivers. A fixed base receiver transmits correction data to the mobile rover receiver. The accurate knowledge of the base position directly

impacts the accuracy of the position computed by the rover. Differential mode with code tracking is known as differential GPS (DGPS) and differential mode with real-time carrier tracking is known as real-time kinematic (RTK). The differential mode will remove most errors except multipath and receiver errors. Multipath errors are reduced with the receiver's signal processing techniques. With code DGPS, results are instantaneous but not as accurate as carrier RTK. In RTK, receiver computations are much more complex because of the problem of resolving the carrier phase integer cycles. With RTK mode, an initialization or start-up period must take place and a minimum number of satellites must be tracked continuously to resolve ambiguities reliably and quickly.

Only RTK systems can return to the "exact" location spatially and indefinitely. However, the base station must always be positioned in the same spot to achieve this. So the base station location typically also is surveyed. Rover accuracy does degrade with distance from the base station and is dependent on manufacturer specifications, but typically is 1 mm/km. The base and rover must be line-of-sight (typically up to 10 km range) for reliable communication. If the rover loses communication with base or loses satellite track (5 continuously), it must re-initialize and will lose accuracy during re-initialization. The cold start initialization time can be up to 30 minutes on the RTK setup and systems with a fast restart are desirable.

GPS satellites transmit information on the L1 and L2 frequency bands. Precision receivers track both signals to remove the effect of the ionosphere. Non-precision receivers track only the L1 signal. Autonomous receivers track only the L1 code and do not implement differential aiding. Some GPS receivers can track the Russian Federation's global navigation satellite system (Glonass) in conjunction with the United States' global positioning system. With this combination, accuracy is increased because more satellites are available to the receiver.

The Federal Aviation Administration and the Department of Transportation have developed the Wide Area Augmentation System (WAAS) program for use in precision flight approaches. The system became operational in July of 2003. WAAS is a system of satellites and ground stations that provide GPS signal corrections that result in better position accuracy. No additional receiving equipment or service fees are required to use WAAS. WAAS consists of approximately 25 ground reference stations positioned across the United States that monitor GPS satellite data. Two master stations, one located on each coast, collect data from the reference stations and create a GPS correction message. This correction accounts for GPS satellite orbit and clock drift plus signal delays caused by the atmosphere and ionosphere. The corrected differential message is then broadcast through one of two geostationary satellites, or satellites with a fixed position over the equator. The information is compatible with the basic GPS signal structure, which means any



WAAS-enabled GPS receiver can read the signal. The WAAS signal-in-space covers the entire Continental U.S. and Alaska.

GPS receiver position horizontal accuracy (90 percentile circular error probability) depends widely on manufacturer specifications, but typical numbers are: RTK mode is 1 cm to 10 cm, DGPS mode is less than 1 m, WAAS DGPS mode is less than 3 m, and Autonomous mode is greater than 3 m. The GPS receiver position vertical accuracy is typically twice the horizontal accuracy.

## Electromagnetic Gradiometer Instrument Design

The DeltaEM™ Gradiometer system consists of a custom transmitter and receiver, each with a number of component parts, and support equipment. Integrated into the DeltaEM are a GPS receiver and a 2.4-GHz band radio frequency (RF) modem.

A Garmin WAAS DGPS receiver (model GPS 18 LVC) was used for this demonstration and has an accuracy of 3 m horizontal and 6 m vertical, both at the 90 percentile statistic, as specified in the manufacturer data sheet. An optional, more accurate, sub-meter GPS receiver can be provided by the user and installed on the gradiometer. An additional hand-held GPS receiver (Garmin GPSmap 76) also was used in survey work for data collection, but was not intended to improve the overall accuracy of the data point positioning. An RF modem inside the DeltaEM system provides the capability to transmit the collected gradiometer data to a remote computer for display and logging. Gradiometer data files always are written to the local removable memory card.

The DeltaEM instrument measures the gradient of horizontal magnetic field strength. A vertical magnetic dipole (VMD) transmit antenna is used to illuminate the intended features. The VMD transmit antenna has horizontal electric fields that optimally couple to horizontal subsurface features. The transmitting antenna is physically located by reading its signal strength at the receiver location. The transmitting antenna is moved to discrete positions to keep its signal in range of the receiver.

The DeltaEM system maintains operation for 8 hours on the rechargeable battery pack. The system is packaged to address ergonomic sensibilities and ease-of-use functionality. The system is sealed for water and dust resistance and all connectors are hermetic sealed. The receiver is a man-portable unit carried with a harness worn over the shoulders. The battery pack can be worn around the shoulder or on a belt around the waist. The gradiometer receiver is shown in Figure 2.

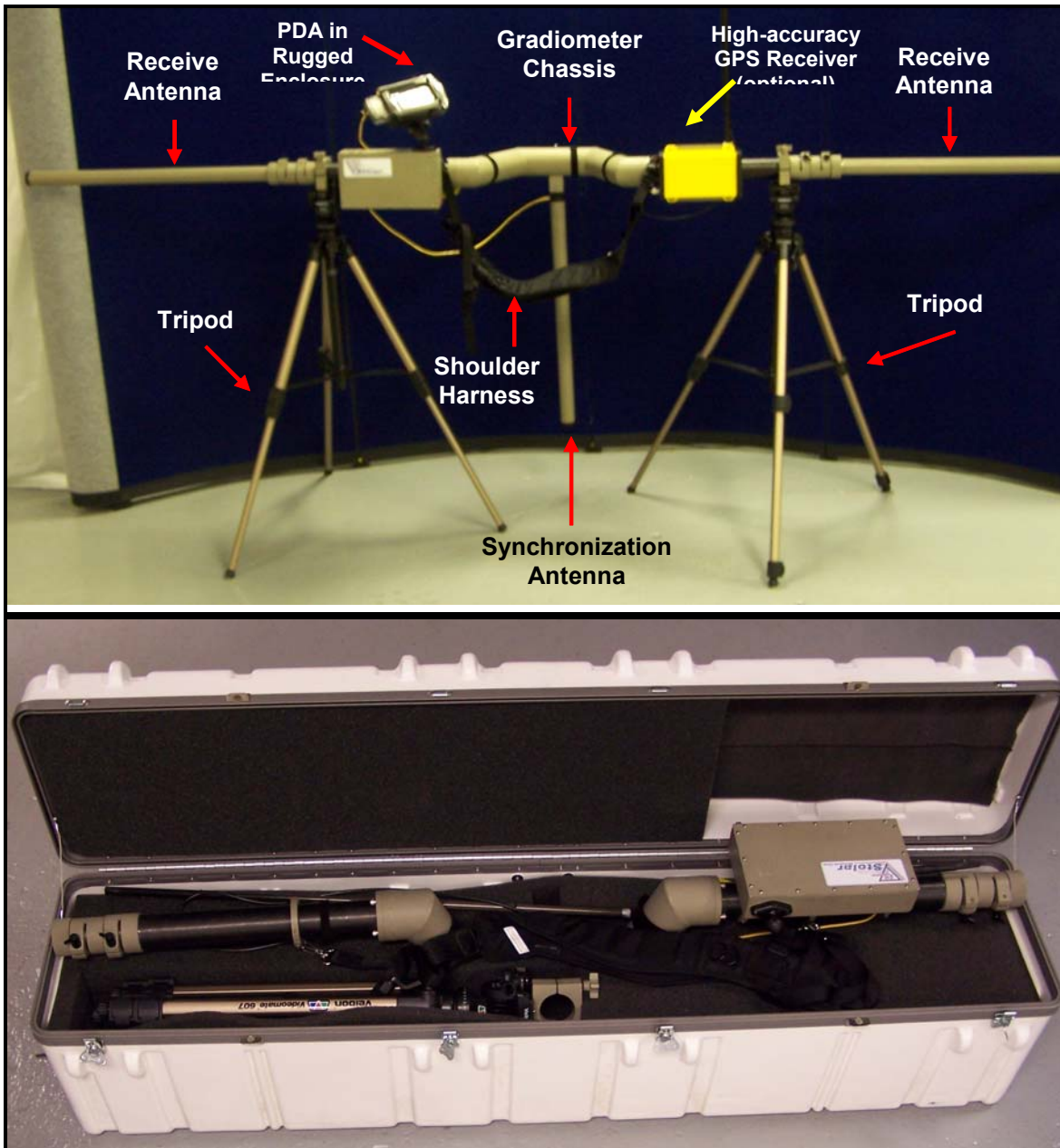


**Figure 2.** Top: DeltaEM Gradiometer receiver assembly components.  
Bottom: DeltaEM Gradiometer chassis and tripods in storage and shipping case.

The gradiometer system antennas are shown in Figure 3.





*Figure 3. DeltaEM gradiometer system antennas.*

The transmitter, shown in Figure 4, consists of transmit air-core loop antennas, the transmitter control box, the connecting cable, and the battery pack.



*Figure 4. DeltaEM Gradiometer system transmitter components; 30-in.-diameter loop (left), and 31-ft-diameter loop coiled up (right).*

The custom Delta software application runs on a personal digital assistant (PDA) with Microsoft Windows Mobile 2005\* operating system using the landscape mode display. The Delta application is stored on the secure digital (SD) memory card and can be copied to the PDA internal memory. Data files are written to the removable SD memory card when it is installed, otherwise they are written to the PDA memory in the “My Documents” folder. The PDA is shown in Figure 5. The PDA is housed in a rugged enclosure when mounted on the gradiometer. Once the user accesses the application, input is via the touch-screen or the four buttons located on the front of the PDA.

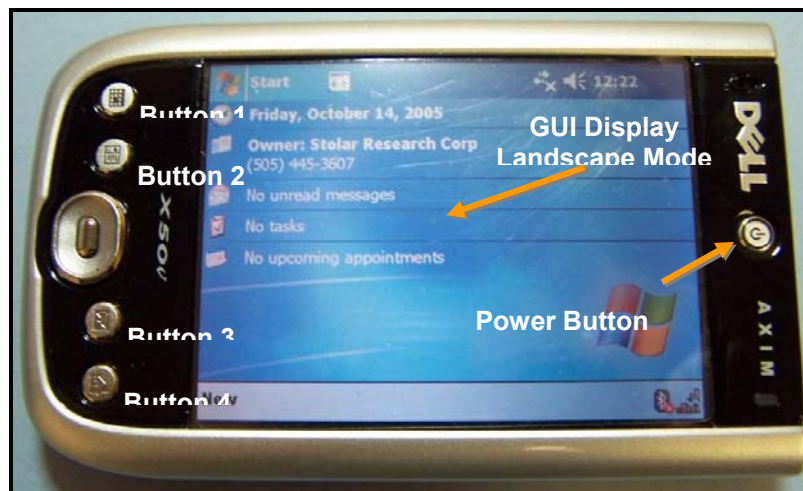


*Figure 5. Personal Data Assistant used for the DeltaEM Graphical User Interface.*

The Graph page shows a plot of every data sample on the display. The display is updated at the refresh rate selected on the Setup page graph frequency. The white trace shows the magnitude data values and the red trace shows the phase data values. The vertical (Y) axis corresponds to the magnitude data in millivolts, and the horizontal (X) axis is time in seconds. The Y axis is auto-scaled according to the magnitude values in the current open file. The phase data trace is for “trend” information and does not have corresponding Y axis values. The graph display is a plot of the current open file. Data are plotted in real time as they are acquired. Data files recalled from memory also are plotted. Figure 6 shows the GUI Graph page of the DeltaEM system.

---

\*Microsoft Windows Mobile 2005 is a trademark of Microsoft Corporation, Redmond, Washington.

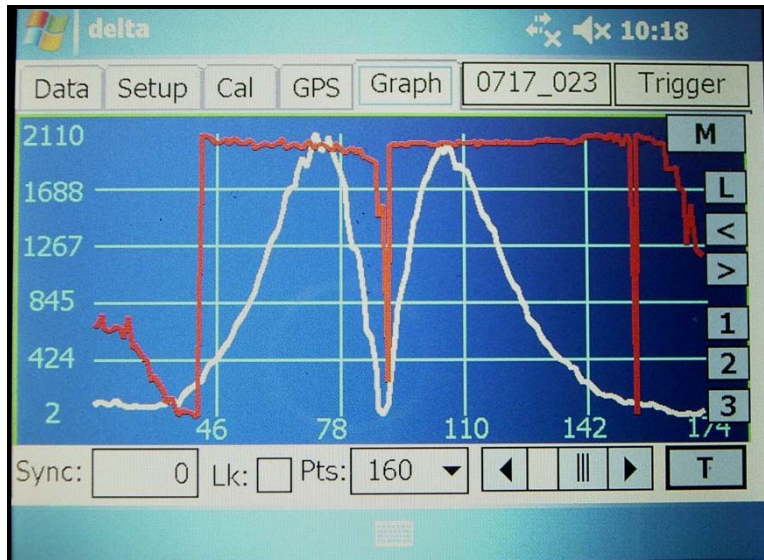


*Figure 6. GUI Graph page.*

The GUI Setup page contains the instrument control variables. The gain setting is the only variable that is typically adjusted during the survey. Figure 7 shows the GUI Setup page of the DeltaEM system.

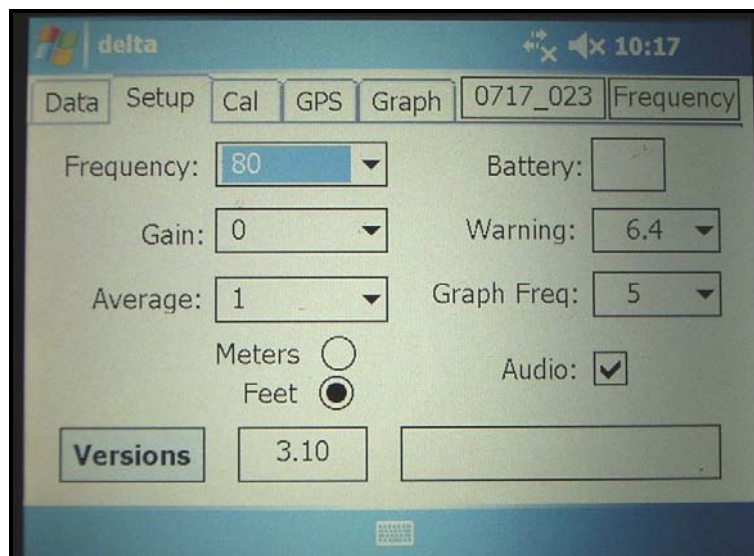


*Figure 7. GUI Setup page.*

Figure 8 shows the GUI GPS page of the DeltaEM system.



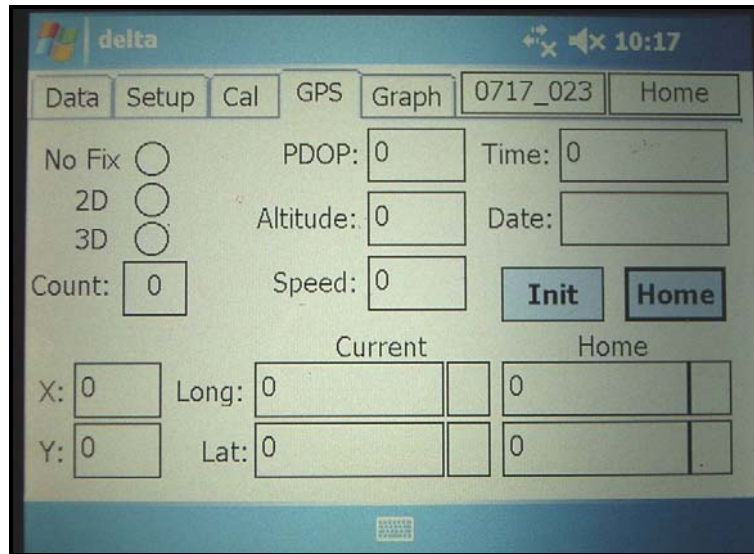


**Figure 8.** GUI GPS page.

Figure 9 is the GUI Data page of the DeltaEM system. The center of the GUI Data page displays a textual data window where data values are displayed as they are acquired in real time. New files are created and opened using the Data page. Data files are named in the month, day, number format. Data files are numbered automatically using the current month and day. A sequential number from 1 to 999 is appended to the file name; the number assigned is the next unused value. A new file cannot be created if the current open file is empty. Data written to a file are always appended to the data in the current open file.

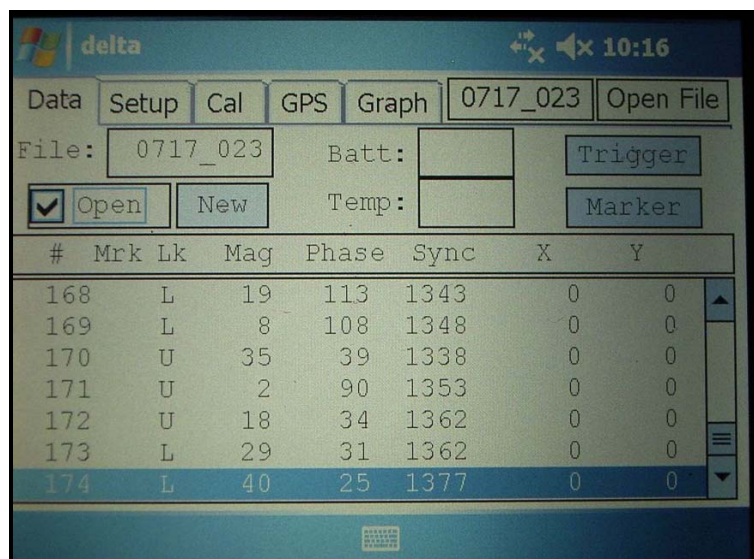


**Figure 9.** GUI Data page.



The remote computer display presents measured data from the DeltaEM system in graphical and textual form in real time. Software for the remote computer has been written in LabView. The software logs data, indicates gradiometer status, and displays a graphical plot—all in real time. The remote computer can provide additional computations and decision levels with more software development. The modem is from Max Stream and operates at 2.4 GHz. Data also can be routed by the remote computer to Ethernet and accessed by any networked computer. Figure 10 shows a laptop computer with the external RF modem.

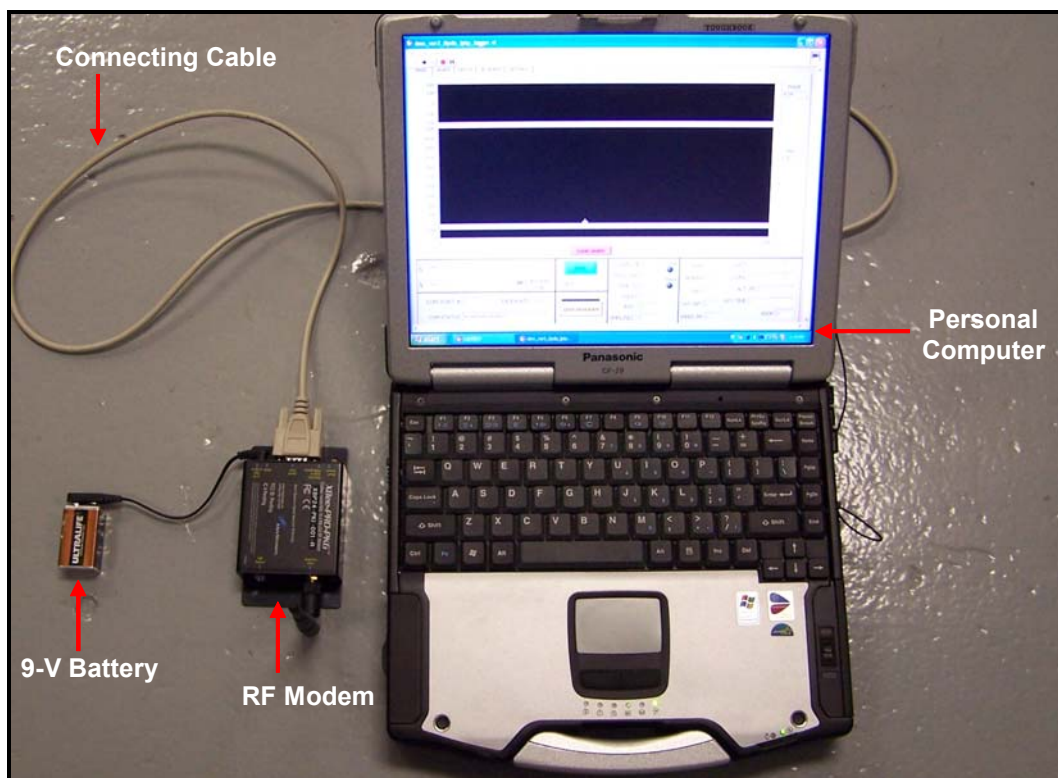


*Figure 10. Remote computer system.*

## Electromagnetic Survey Operating Frequency

The electromagnetic gradiometer system was set up to conduct surveys over coal mine workings. It was anticipated that several operating frequencies would be required to detect shallow and deep voids. Survey frequencies at 2, 20, 40, 80, and 200 kHz could be used. Frequency of operation is selected, in part, based on skin depth calculations. Skin depth is defined as the distance at which an electromagnetic wave penetrating a material has decayed to  $1/e$ , or 36.8%, of its original amplitude. Equation 1 defines the relationship between skin depth ( $\delta$ ), permeability ( $\mu_o$ ), conductivity ( $\sigma$ ), and frequency ( $f$ ) for common soil types. The

composition includes loose or solid formations. Table 2 provides the calculated results.

$$\delta = \sqrt{\frac{2}{\mu_0 \sigma \omega}} = \frac{1}{\sqrt{\mu_0 \sigma \pi f}} \quad (1)$$

Table 2. Skin Depth Table.

	Nominal Conductivity [Resistivity]			
	clay 0.01 [100]	clay-silt 0.0067 [150]	silt 0.003 [333]	sand 0.001 [1000]
Freq (Hz)	Skin Depth (feet)			
2,000	369	451	674	1167
20,000	117	143	213	369
40,000	83	101	151	261
80,000	58	71	107	185
200,000	37	45	67	117

Each frequency requires tuning of the gradiometer receive antennas, the synchronization antennas, and the transmitting antennas independently. The antennas on the gradiometer are ferrite-core, wire-wound loops. The type of wire, gauge of wire, number of turns, and spacing of turns are optimized for each frequency of operation. The antennas are then tuned to operate at resonance. The phase and magnitude of the gradiometer antennas are balanced inside an isolated radio frequency screen room.

Two configurations of air-core transmit loop antennas were used. The first is a 30-in.-diameter loop, and the second is a 31-ft-diameter loop. Again, the type of wire, gauge of wire, number of turns, and spacing of turns are optimized for each frequency of operation. Each of these antennas may be used in direct contact with the surface unless the ground is wet, muddy, or icy. In these cases the antenna will need to be elevated no more than a few feet or higher if desired. The presence of vegetation is not detrimental to antennas performance unless it too is high in moisture (i.e., visibly wet or covered in ice or snow). Surface topography must be measured and considered during data collection because the transmitting antenna orientation should remain constant relative to the gradiometer antennas. The distance between these two antennas may be variable over some practical range, as determined by operating frequency (typically 50 to 300 ft for commonly used operating frequencies).

The air-core transmit antenna characteristics are analyzed. The antenna is connected to the output of a Class-L power amplifier. The radiated power, in air, generated by the antenna is determined from:

$$P_R = R_R \times I^2 \quad (2)$$

where

$P_R$  = radiated power,

$R_R$  = radiation resistance,

$I$  = maximum sinusoidal current.

The radiation resistance of air-core,  $N$ -turn loop is given by:

$$R_R = N^2 \left( 31,000 \frac{\pi^2 A^4}{\lambda^4} \right) \quad (3)$$

where

$N$  = number of turns,

$A$  = area of loop (*length x height*) or ( $\pi \times \text{radius}^2$ ),

$\lambda$  = free-space wavelength (speed of light  $\div$  operating frequency).

The 30-in.- and 31-ft-diameter air-core loop antennas have the following properties shown in Tables 3 and 4.

Table 3. Summary of Small Loop Transmit Antenna Properties.

<i>30-inch diameter loop</i>					
$A = \pi \left( \frac{15}{0.0254} \right)^2 = 0.456m^2$					
$f$	$\lambda$	$N$	$ I _{Measured}$	$R_R$	$P_R$
2 kHz	150 km	120	2.5 A	376E-15 $\Omega$	2.4 <i>pW</i>
20 kHz	15 km	20	3.4 A	105E-12 $\Omega$	1.2 <i>nW</i>
200 kHz	1.5 km	10	1.6 A	261E-9 $\Omega$	0.7 $\mu W$

Table 4. Summary of Large Loop Transmit Antenna Properties.

31-foot diameter loop $A = \pi \left( \frac{15.5}{3.2808} \right)^2 = 70m^2$					
$f$	$\lambda$	$N$	$ I _{Measured}$	$R_R$	$P_R$
2 kHz	150 km	3	7.0 A	131E-9 $\Omega$	6.4 $\mu W$
20 kHz	15 km	3	1.0 A	131E-5 $\Omega$	1.3 $mW$
200 kHz	1.5 km	3	0.25 A	13 $\Omega$	0.8 $W$

## Field Tests and Data Analysis

Field testing was conducted over four different time periods at the Emery Mine near Salina, Utah. The test dates were: 4-5 March 2005, 1-2 June 2005, 23-25 August 2005, and 28 February to 2 March 2006. The Emery mine is a Consol Energy property at which the current MSHA demonstration program for DeltaEM has been entirely performed. Complete data collection and debugging activity over the mine's active workings have been completed, as well as data collection over the mine's old workings. **The data analysis has been reviewed between the draft and final versions of this report. The existing correlations have been determined to be valid.**

The DeltaEM gradiometer surveys were carried out over seven separate locations above the Emery Mine, as shown in Figure 11. The locations were selected for ease of accessibility and for variations in depth of overburden. The surveys were nonintrusive to both the environment and any ongoing mine activities. All the response profiles in the following section were collected using a continuous data stream from the gradiometer with real-time spatial coordination and data logging. Approximately 10 samples per second are logged continuously. These data included the amplitude (also referred to as Mag) and synchronous signal phase of the receiver gradiometer based on the secondary radiated signal from the induced current along the walls of the mine workings. The response profiles themselves are typical of this methodology.

Multiple passes at a normal walking speed over the same traverse line are always conducted with each frequency. This provides a larger data set for the analysis and identification of features. Multiple frequencies not only vary the skin depth of soil penetration but at the same time provide different resolutions.

The objective for each survey is to create an “M-Curve” response over the mining void, or show a phase-shift response related to the mine-void. The M-Curve is a double-peak response centered on a “null-point.” The null point is the position on the surface where the secondary radiation from the underground structure is directly beneath the gradiometer. At this location, both of the gradiometer’s receiver antennas are detecting equal signal levels, therefore, their gradiometric (differential) response is to equally cancel the signals out, or create a null value. This null is seen **anywhere** the receiver antennas detect an **equal** signal level. This can occur **directly** over the conductive structure or completely away from the structure for **no target**. A null point results only from structure detection if the characteristic double magnitude peaks are represented; each indicate the reception of the target’s magnetic field by either antenna, depending on traverse direction. And then, the detected structure can only be said to represent the mine-void if the depth evaluation correlated to the known seam depth. This allows some discrimination to be made with shallow conductors, surface or aerial conductors, and environmental effects.

Minimal corrections were made to the final data sets to compensate for surface topography or electrical structures. Typical survey environments were open fields adjacent to mine-site structures but did not pass over or beneath these structures, lines, or utilities. Significant elevation change over the length of a traverse line must also be corrected for because the distance from the instrument to the mine void will inversely affect the magnitude of the gradiometric response.

**The success of the survey work will be defined as a proven ability to discriminate between the coal pillars and the mining-related voids of the Emery Mine using the DeltaEM data profiles in comparison to spatially known information.**



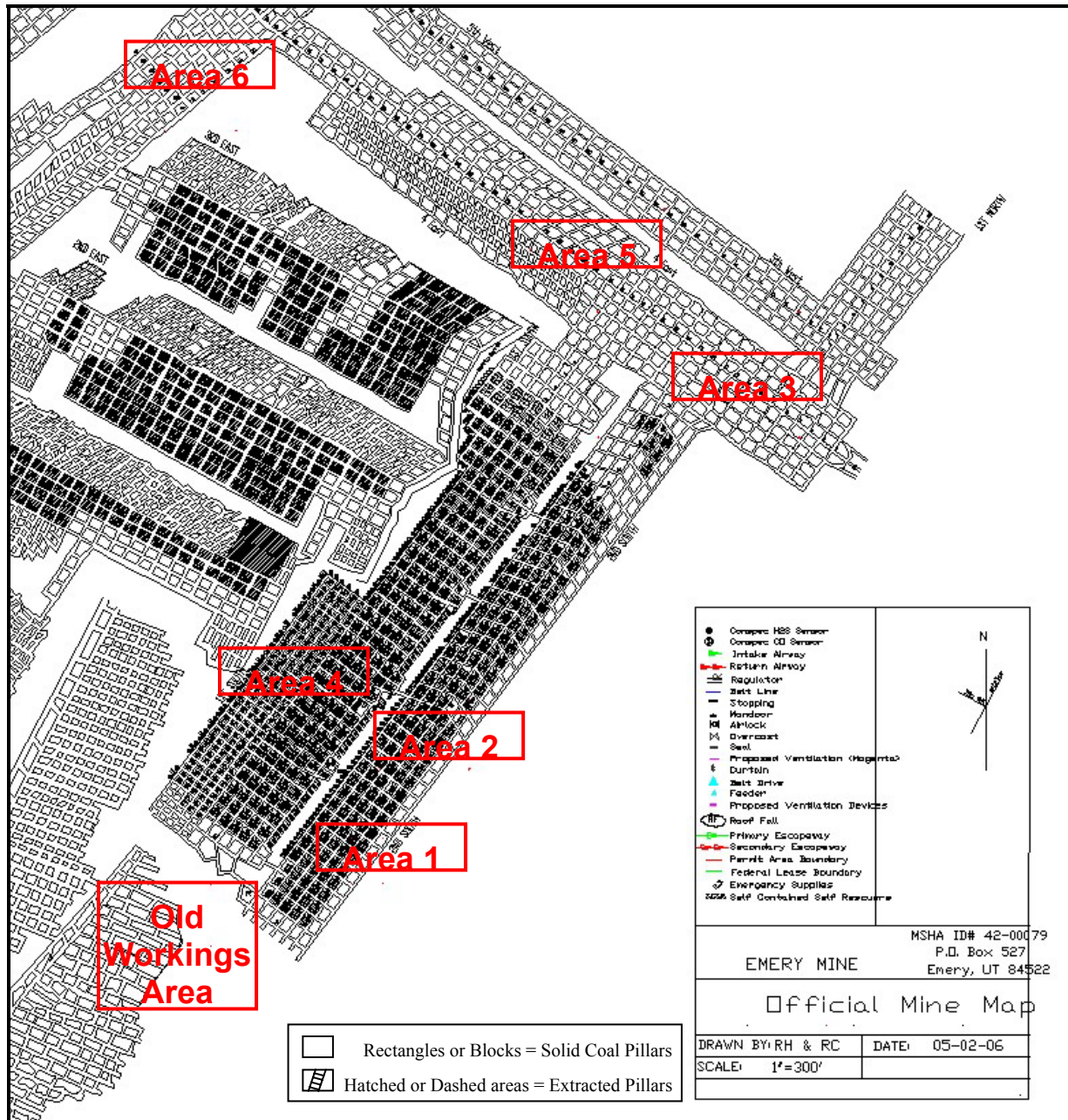


Figure 11. Emery Mine gradimeter survey areas.

The approximate mine locations, the GPS points for the surface stakes, and the approximate amount of overburden at each location is summarized in Table 5.

Table 5. Summary of Survey Spatial Locations and Approximate Overburden.

Location	Latitude (NAD83 Deg)	Longitude (NAD83 Deg)	Stake Number	Area on Mine	Approx. Depth
4th Est CC12	N 38.87558	W 111.23745	1	3	100'
	N 38.87452	W 111.23848	2		
2nd Sth CC29	N 38.86832	W 111.24390	3	2	130'
	N 38.86894	W 111.24495	4		
2nd Sth CC38	N 38.86636	W 111.24580	5	1	40'
	N 38.86629	W 111.24566	6		
4th Est CC25	N 38.87754	W 111.24030	7	5	200'
	N 38.87724	W 111.24118	8		
7th Nth CC72	N 38.88048	W 111.24985	9	6	400'
	N 38.87997	W 111.24931	10		
1st Sth CC28	N 38.86962	W 111.24731	11	4	200' (flooded)
	N 38.86991	W 111.24779	12		
Old Workings	N 38.86573	W 111.24962			185'
	N 38.86499	W 111.25040			

Field test data are presented below for each of the seven separate locations. Spatial plots have been generated with GPS track logs of each survey line. **The starting location for each survey line is indicated by a small dot.** The spatial plots have been plotted separately for every survey location and also for each operating frequency at that location. Each spatial plot has been graphically overlaid on the corresponding Emery Mine Map AutoCAD\* file area so that the surface survey traverse lines are shown spatially over the mine workings and with identified null points from the traverse response plots. **The identified null points are shown as small pink triangles on the traverse lines and indicate the point on the profile where an air-coal boundary is suspected.** These air-coal boundaries are the points at which the coal pillar contacts the open entry of the mining void.

It is fairly easy to correlate the individual markers (small pink triangles) between the spatial plots and response plots. Each survey line on the spatial plot is a unique color and the starting point is known. The response plot starting point is always the beginning of the plot, so the traverse distance increases from left to right (distance from start is the x axis). Then the first marker located on the response

---

\* AutoCAD is a trademark of Autodesk, Inc., Suasalito, California.

plot, again moving from left to right, is the correlated marker on the spatial plot when moving away from the starting point. The same procedure is used to locate any remaining markers. While it is somewhat important to see the individual markers as they relate between a response plot and spatial plot, it is much more important to see the distribution of many markers on the spatial plot. **The grouping of distributed markers on the spatial plots proves the ability of the gradiometer to discriminate between the coal pillars and the mining-related voids.** Therefore, the spatial plots are kept in the main body of this document, while the response plots are in Appendix A for complete reference.

The spatial graphic overlay was accomplished by converting the four corners of the GPS track log plot from geodetic latitude and longitude in decimal degrees (WGS84) to State Plane Utah Central Zone (NAD83) in inches. The four converted points were then marked in the Emery Mine Map AutoCAD file and the area was captured as a picture file. The two picture files were finally overlaid and spatially lined up with the corners of the GPS plot and the associated marks in the captured AutoCAD file. This technique was validated to be accurate by manually plotting individual spatial points from the GPS track directly on the digital mine map and comparing the results to the graphical overlay. **Note: These GPS data contain up to 3 m of error.**

### **Area 1 – 2<sup>nd</sup> South CC38**

This area, known as the wash location, is positioned near cross-cut 38 of the 2<sup>nd</sup> South workings. The survey was conducted down in a river wash bed, above shallow mine workings. Figure 12 shows this location.





*Figure 12. Area 1 survey location.*

The survey traverse lines, in Figure 13, are shown spatially over the mine workings and with identified null points from the traverse response plots. The identified null points are shown as small pink triangles on the traverse lines and indicate the point on the profile where an air-coal boundary is suspected.

Figure 13 shows 3 traverse lines with 7 total identified null points. The null point's locations have been related to intended subsurface features by measuring the distance between the null point and the nearby feature. The measured distance must be within the error (3 meters or 9.9 feet) of the GPS. The following results are given: 6 null points over air-coal boundaries, and 1 null point over no feature. Note that GPS reception was very poor on traverse line 03\_05\_21, which contained the identified null point over no feature.

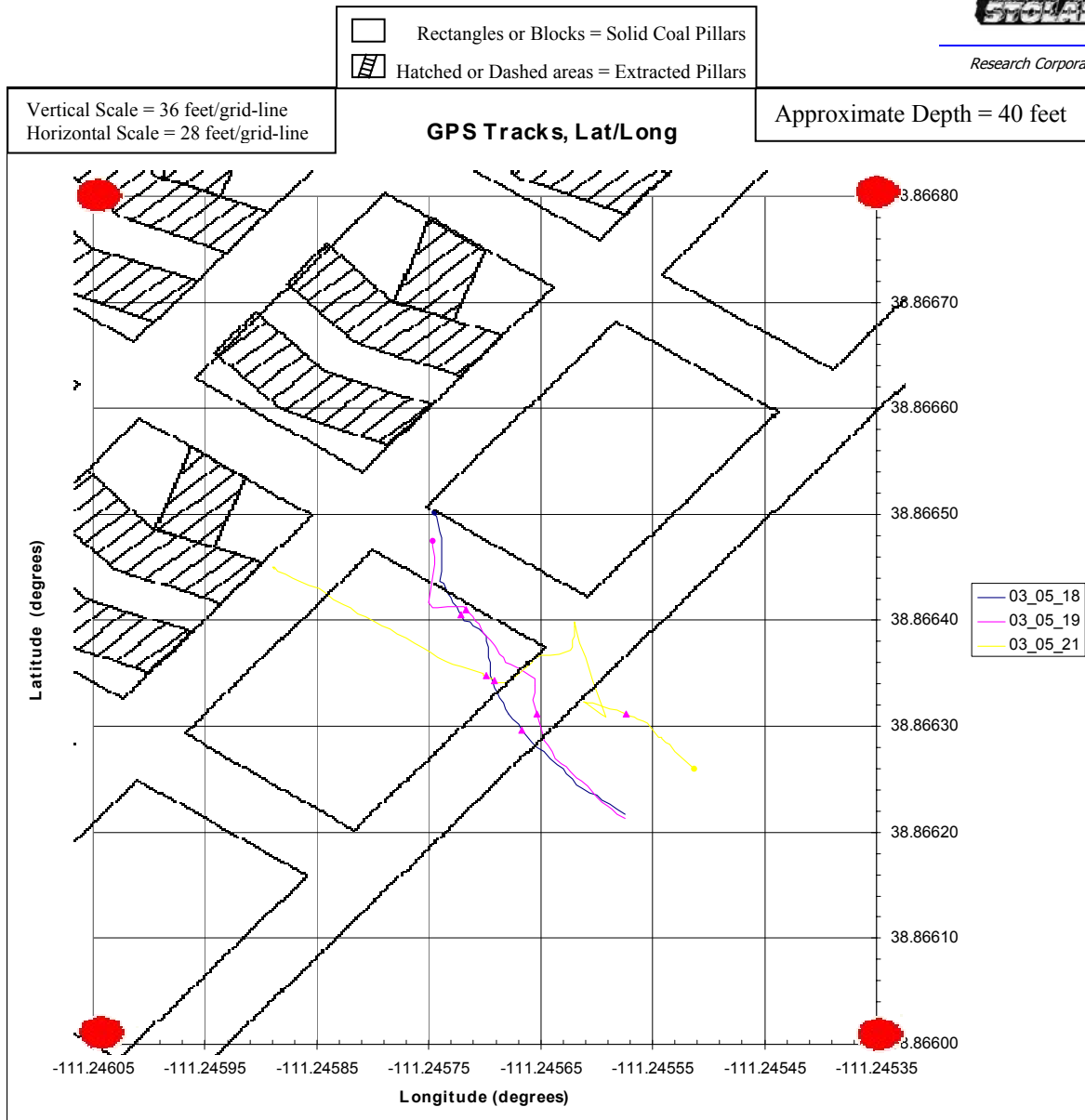


**Figure 13.** Area 1 200-kHz survey lines spatially over mine workings.

The traverse response plots are shown in Appendix A, Figures A-1 to A-3.

### Area 2 - 2<sup>nd</sup> South CC29

This area is located near cross-cut 29 of the 2<sup>nd</sup> South workings. The survey was conducted above deep mine workings. Figure 14 shows this location.

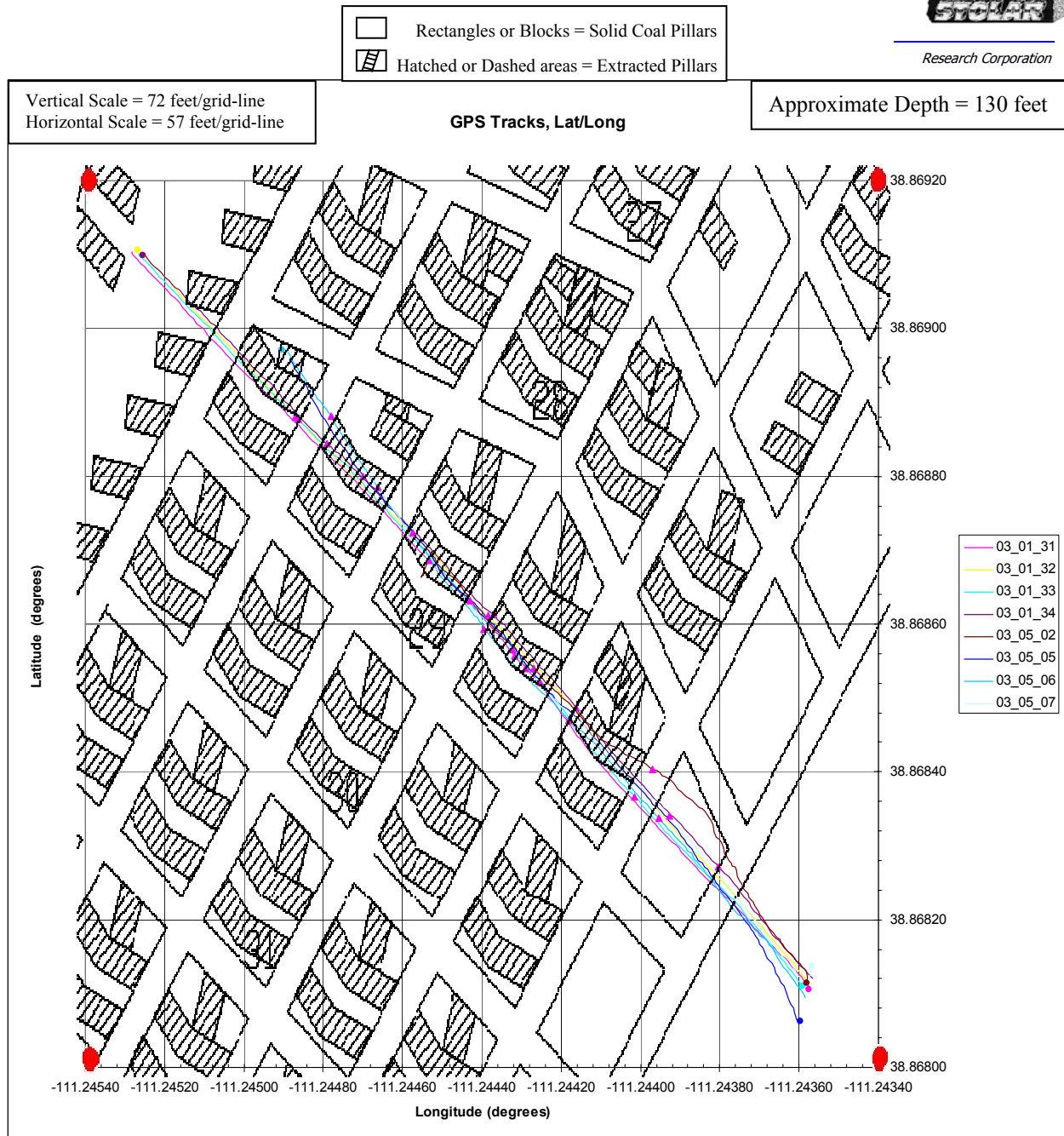


*Figure 14. Area 2 survey location.*

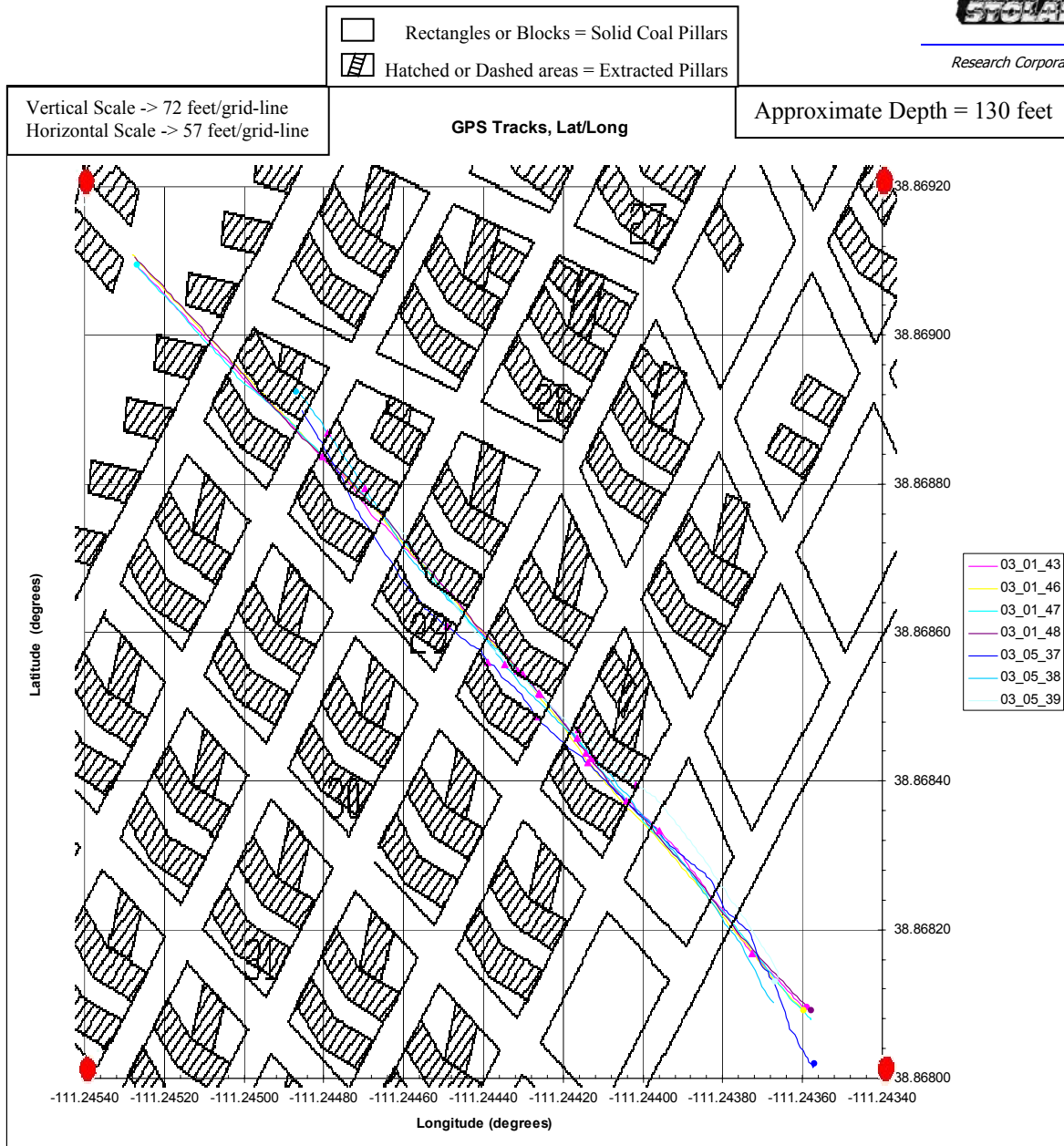
The survey traverse lines, in Figures 15 and 16, are shown spatially over the mine workings and with identified null points from the traverse response plots. The identified null points are shown as small pink triangles on the traverse lines and indicate the point on the profile where an air-coal boundary is suspected.

Figure 15 shows 8 traverse lines with 24 total identified null points. The null point's locations have been related to intended subsurface features by measuring the distance between the null point and the nearby feature. The measured distance must be within the error (3 meters or 9.9 feet) of the GPS. The following results are given: 22 null points over air-coal boundary, 1 null point over a coal pillar, and 1 null point over no feature.

Figure 16 shows 7 traverse lines with 20 total identified null points. The following results are given: 19 null points over air-coal boundaries, and 1 null point over no feature.



*Figure 15. Area 2 2-kHz survey lines spatially over mine workings.*



**Figure 16.** Area 2 20-kHz survey lines spatially over mine workings.

The traverse response plots are shown in Appendix A, Figures A-4 to A-18.

### Area 3 – 4<sup>th</sup> East CC12

This area, known as the stockpile/water-tank location, is positioned near cross-cut 12 of the 4<sup>th</sup> East workings. The survey was conducted above deep mine workings. Figure 17 shows this location.





*Figure 17. Area 3 survey location.*

The survey traverse lines, in Figure 18, are shown spatially over the mine workings and with identified null points from the traverse response plots. The identified null points are shown as small pink triangles on the traverse lines and indicate the point on the profile where an air-coal boundary is suspected.

Figure 18 shows 2 traverse lines with 28 total identified null points. The null point's locations have been related to intended subsurface features by measuring the distance between the null point and the nearby feature. The measured distance must be within the error (3 meters or 9.9 feet) of the GPS. The following results are given: 20 null points over air-coal boundaries, 7 null points over coal pillars, and 1 null point over no feature.

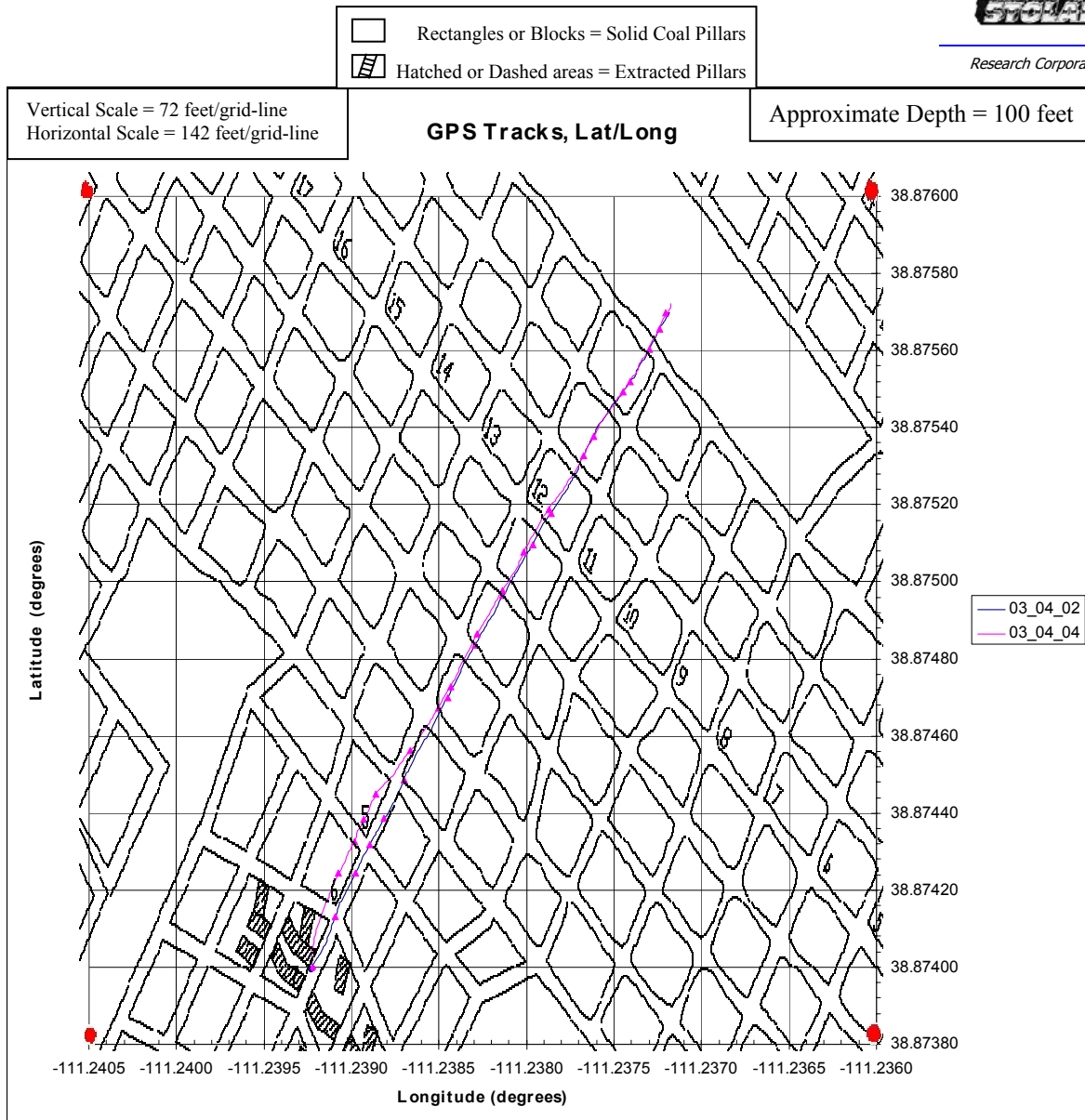


*Figure 18. Area 3 2-kHz survey lines spatially over mine workings.*

The traverse response plots are shown in Appendix A, Figures A-19 and A-20.

#### Area 4 – 1<sup>st</sup> South CC28

This area is located near cross-cut 28 of the 1<sup>st</sup> South workings. The survey was conducted above deep mine workings. Figure 19 shows this location.



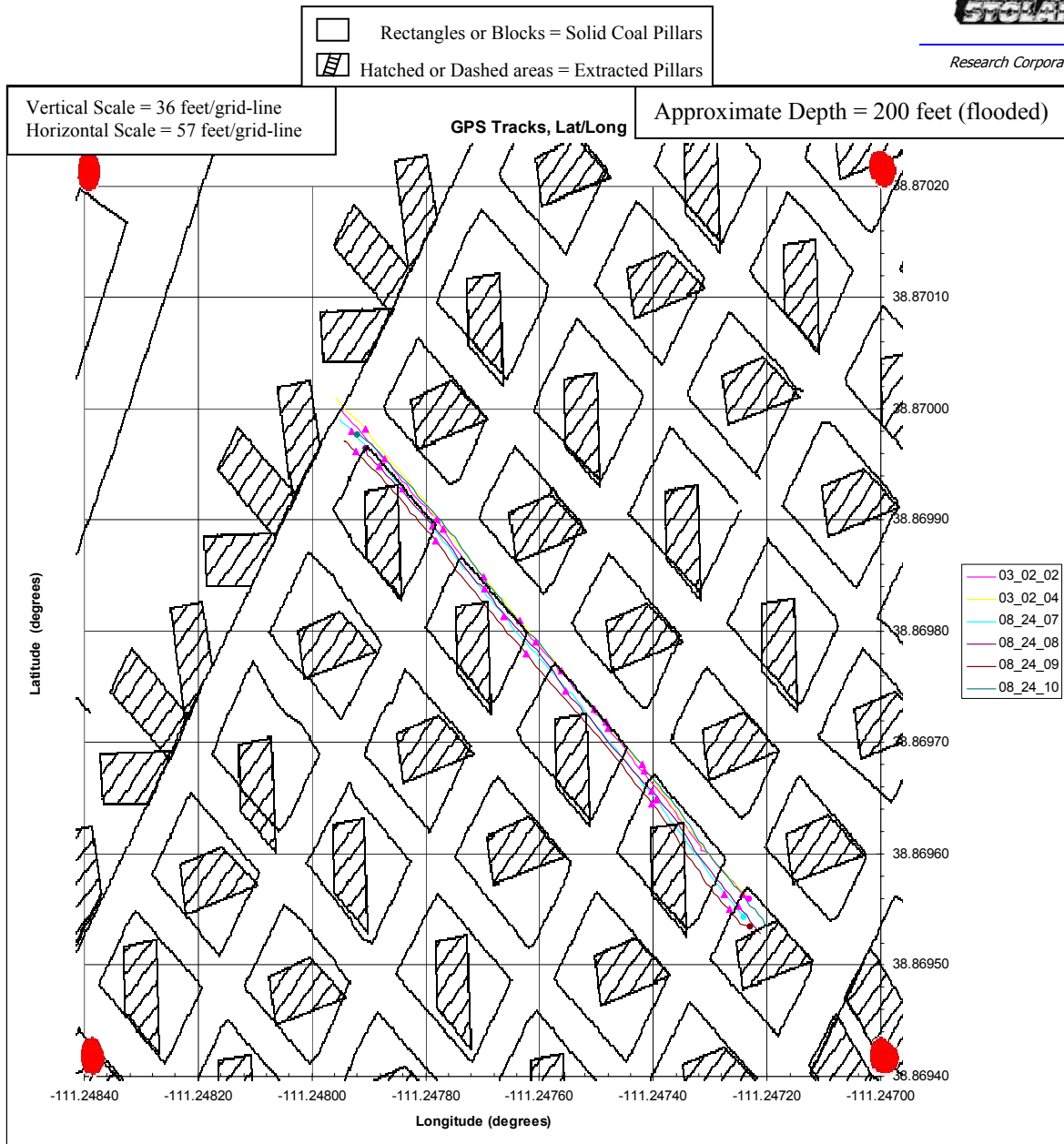
*Figure 19. Area 4 survey location.*

The survey traverse lines, in Figures 20 and 21, are shown spatially over the mine workings and with identified null points from the traverse response plots. The identified null points are shown as small pink triangles on the traverse lines and indicate the point on the profile where an air-coal boundary is suspected.

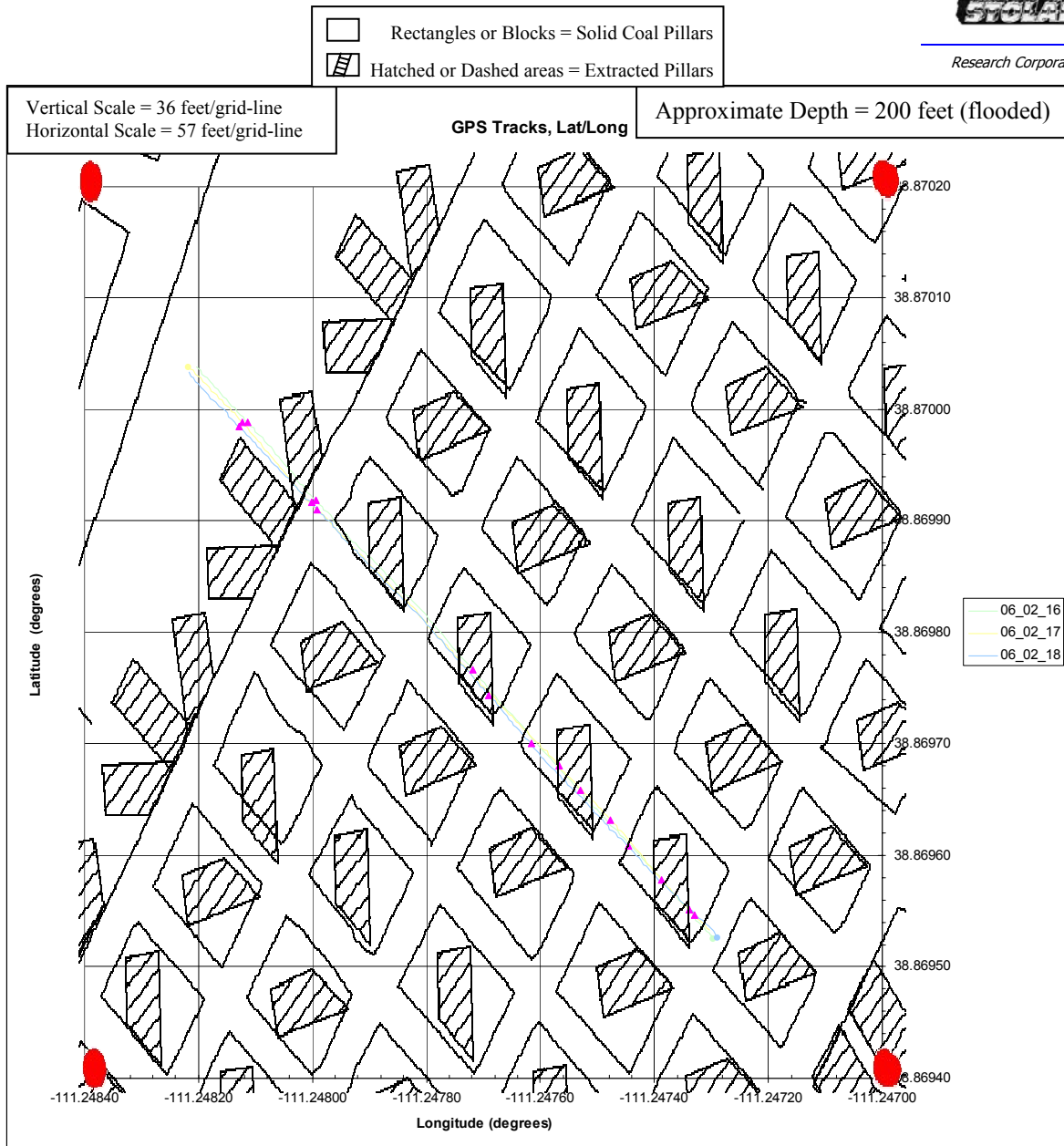
Figure 20 shows 6 traverse lines with 30 total identified null points. The null point's locations have been related to intended subsurface features by measuring the distance between the null point and the nearby feature. The measured distance must be within the error (3 meters or 9.9 feet) of the GPS. The following results are given: 28 null points over air-coal boundary, and 2 null points over no feature.

Figure 21 shows 3 traverse lines with 16 total identified null points. The following results are given: 15 null points over air-coal boundaries, and 1 null point over no feature.





*Figure 20. Area 4 2-kHz survey lines spatially over mine workings.*



**Figure 21.** Area 4 20-kHz survey lines spatially over mine workings.

The traverse response plots are shown in Appendix A, Figures A-21 to A-29.

### Area 5 – 4<sup>th</sup> East CC25

This area is located near cross-cut 25 of the 4<sup>th</sup> East workings. The survey was conducted above deep mine workings. Figure 22 shows this location.

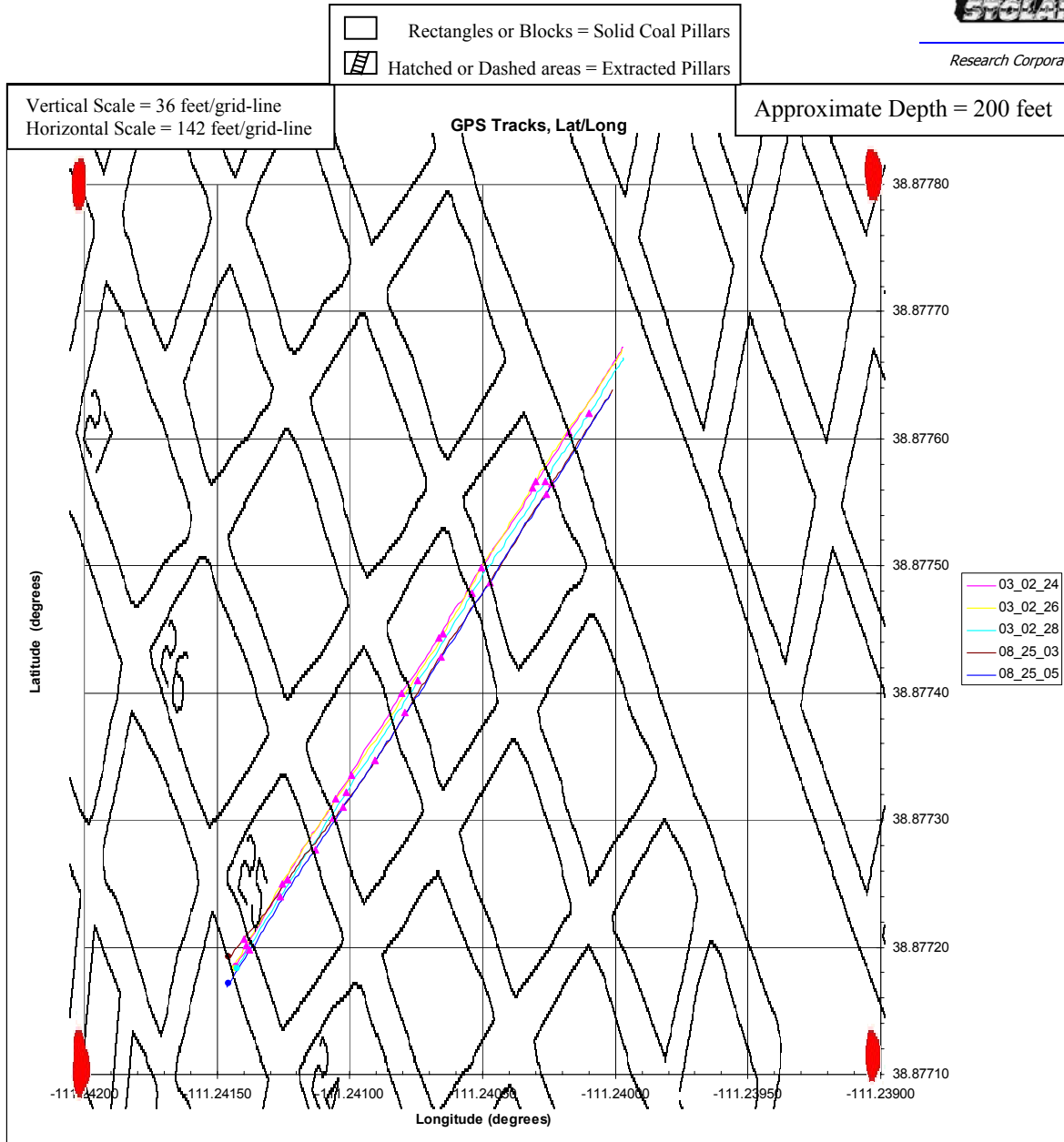


*Figure 22. Area 5 survey location.*

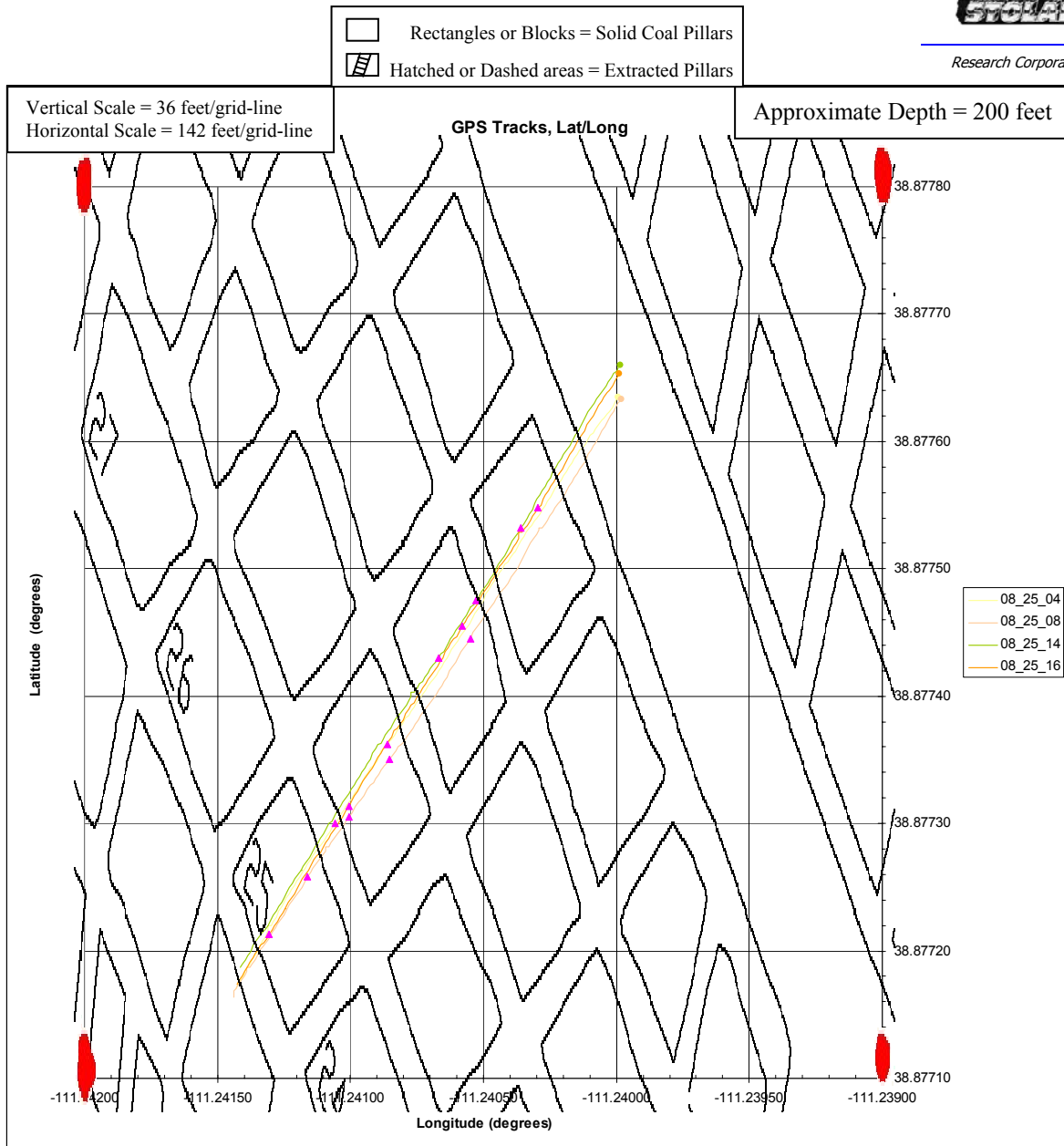
The survey traverse lines, in Figures 23 and 24, are shown spatially over the mine workings and with identified null points from the traverse response plots. The identified null points are shown as small pink triangles on the traverse lines and indicate the point on the profile where an air-coal boundary is suspected.

Figure 23 shows 5 traverse lines with 29 total identified null points. The null point's locations have been related to intended subsurface features by measuring the distance between the null point and the nearby feature. The measured distance must be within the error (3 meters or 9.9 feet) of the GPS. The following results are given: 16 null points over air-coal boundaries, 11 null points over coal pillars, and 2 null points over no feature.

Figure 24 shows 4 traverse lines with 13 total identified null points. The following results are given: 4 null points over air-coal boundaries, and 9 null points over coal pillars.



*Figure 23. Area 5 2-kHz survey lines spatially over mine workings.*



**Figure 24.** Area 5 20-kHz survey lines spatially over mine workings.

The traverse response plots are shown in Appendix A, Figures A-30 to A-38.

### Area 6 – 7<sup>th</sup> North CC72

This area is located near cross-cut 72 of the 7<sup>th</sup> North workings. The survey was conducted above deep mine workings. Figure 25 shows this location.

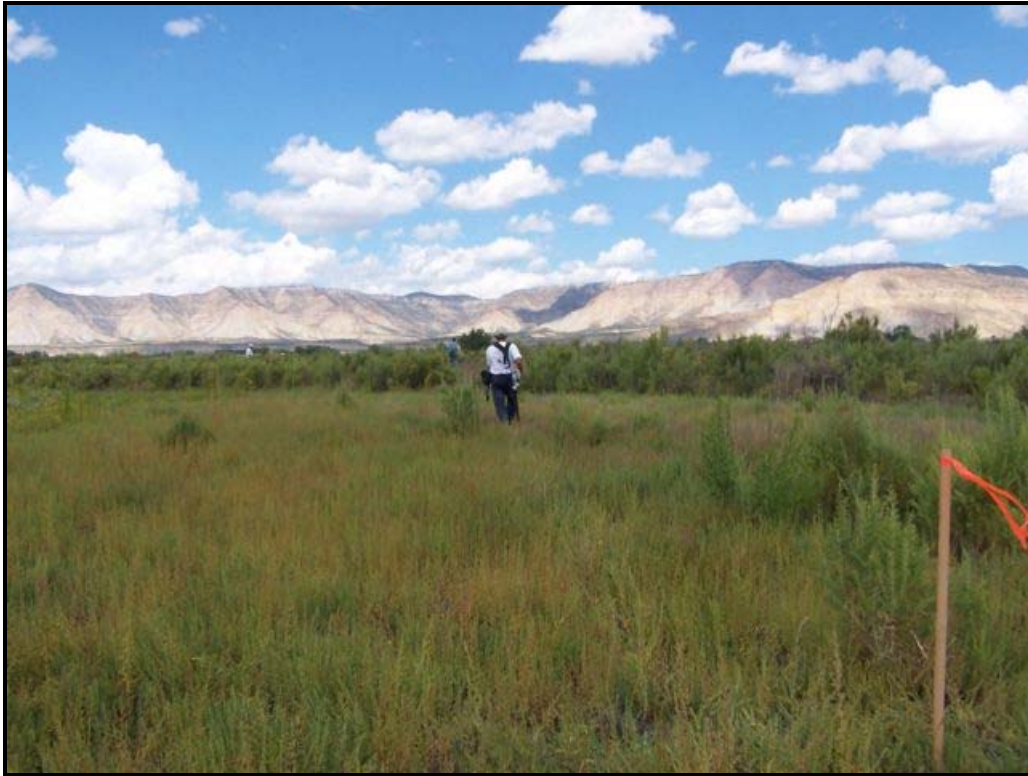


*Figure 25. Area 6 survey location.*

The survey traverse lines, in Figure 26, are shown spatially over the mine workings and with identified null points from the traverse response plots. The identified null points are shown as small pink triangles on the traverse lines and indicate the point on the profile where an air-coal boundary is suspected.

Figure 26 shows 3 traverse lines with 17 total identified null points. The null point's locations have been related to intended subsurface features by measuring the distance between the null point and the nearby feature. The measured distance must be within the error (3 meters or 9.9 feet) of the GPS. The following results are given: 8 null points over air-coal boundaries, 5 null points over coal pillars, and 4 null points over no feature.

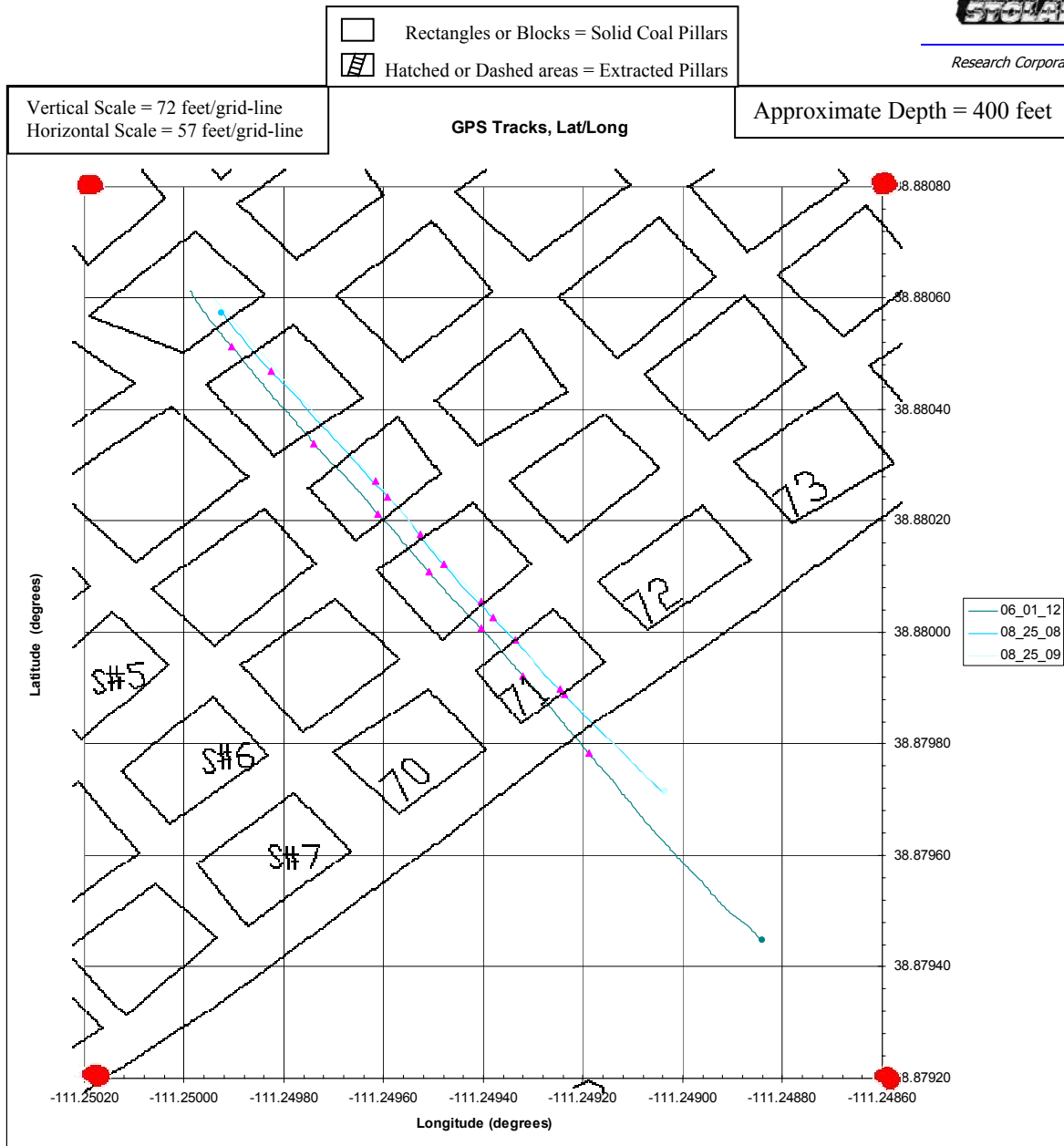


**Figure 26.** Area 6 2-kHz survey lines spatially over mine workings.

The traverse response plots are shown in Appendix A, Figures A-39 to A-41.

### Old Workings Area

This area is located near the southern end of the 1<sup>st</sup> South and 2<sup>nd</sup> South workings. The survey was conducted above deep mine workings. Figure 27 shows this location.





*Figure 27. Old Workings Area survey location.*

The survey traverse lines, in Figure 28, are shown spatially over the mine workings and with identified null points from the traverse response plots. The identified null points are shown as small pink triangles on the traverse lines and indicate the point on the profile where an air-coal boundary is suspected.

Figure 28 shows 2 traverse lines with 6 identified null points over old existing workings and 6 identified null points over a suspect area. The null point's locations have been related to intended subsurface features by measuring the distance between the null point and the nearby feature. The measured distance must be within the error (3 meters or 9.9 feet) of the GPS. The following results are given: 4 null points over air-coal boundaries, and 2 null points over coal pillars.

Figure 28 also shows the 2 identified drill site locations.



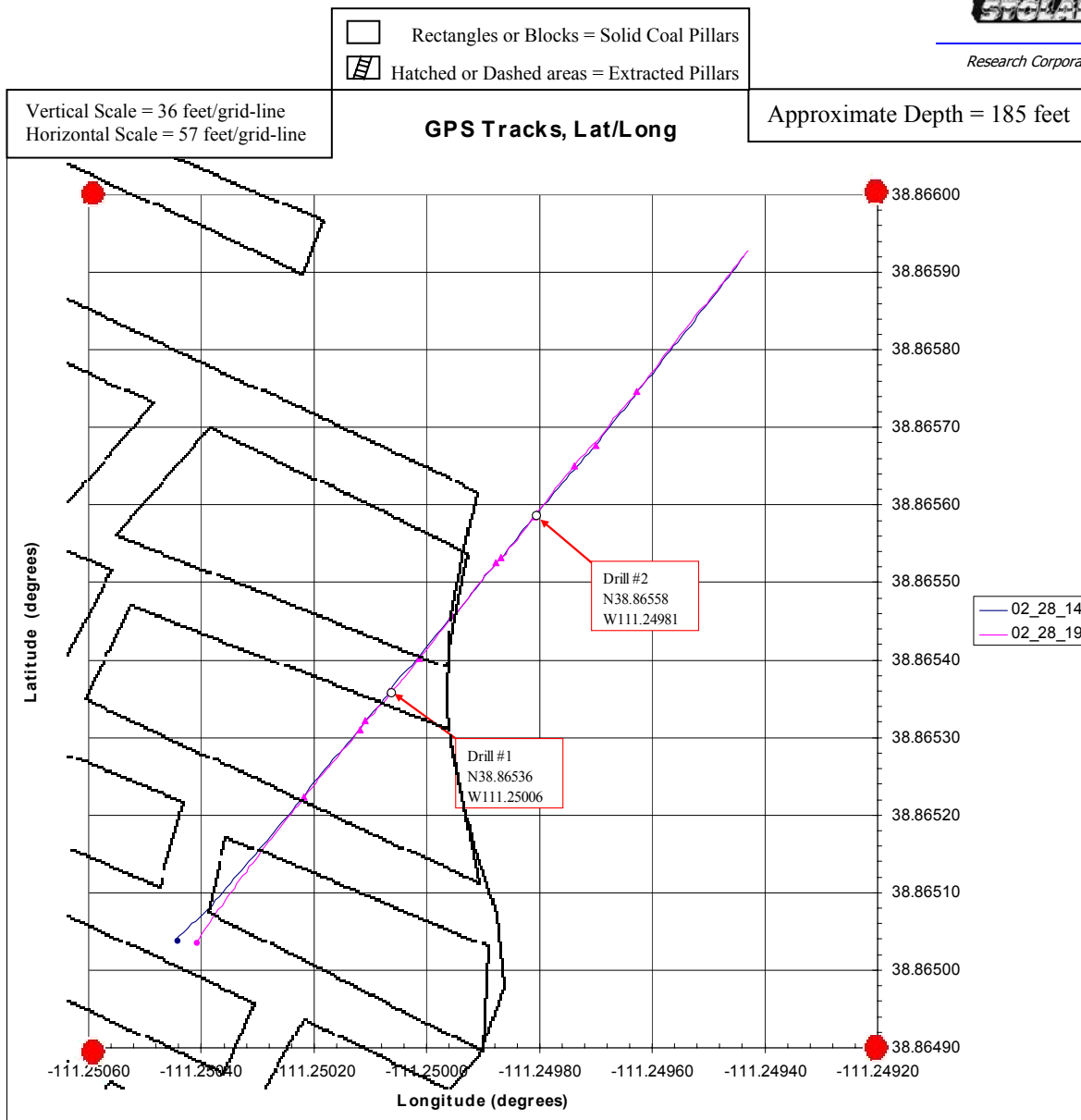


**Figure 28.** Old Workings Area 2-kHz survey lines spatially over mine workings.

The traverse response plots are shown in Appendix A, Figures A-42 and A-43.

## Data Plots and Interpretation

The inherent high signal-to-noise (S/N) ratio of the gradiometer design provides data with a large dynamic range so that little post-processing is required. The resulting plots showed the locations at which the gradiometer response peaked and nulled. The detection can be characterized by a null or trough in the profile. The null indicates the approximate location of the underground anomaly surface projection on the traverse.

Traverse response plots have been batch generated with Microsoft Excel. A custom software script known as Delta Plotter runs with Excel and allows the user to plot large numbers of raw data files automatically. \*A user interface has been implemented and is shown in Figure 29.

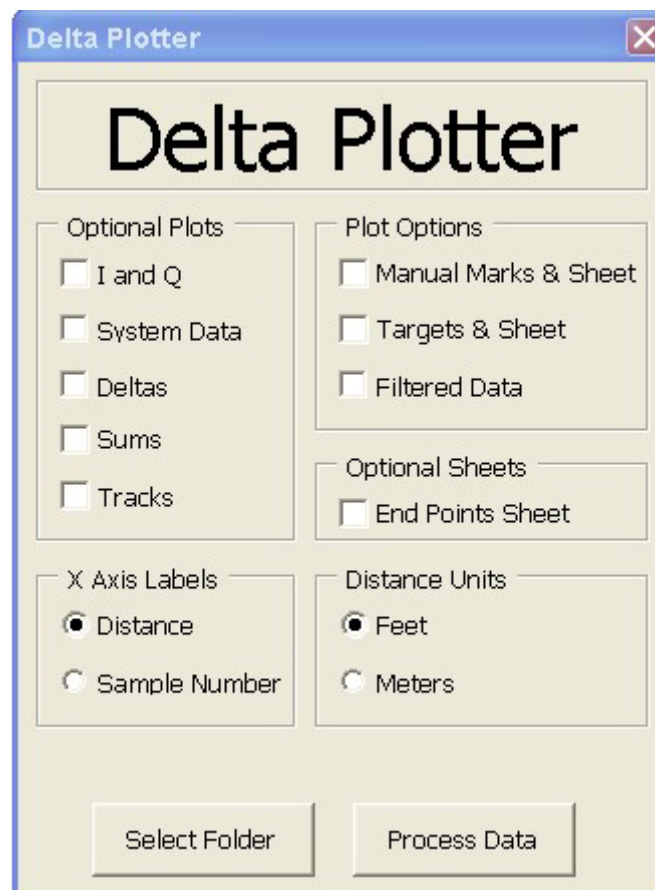


**Figure 29.** *Delta Plotter user interface.*

Interactive spatial analysis has been implemented by allowing the user to select anomalies when analyzing response plots and the corresponding location is automatically placed on the GPS track log plot. Raw sensor data is collected by the DeltaEM instrument along each survey line. Header information above each generated plot gives specific details about the survey. The graphs display signal magnitude (Mag), signal phase (Phase), and the receiver synchronization (Sync) automatic gain control (AGC). Unexpected variations in the signal magnitude can be explained by the corresponding variations in the phase or sync AGC signals. The changes in magnitude and phase result from the response of the secondary

---

\* Excel is a trademark of Microsoft Corporation, Redmond, Washington.

scattered wave of the anomaly. The sync AGC signal is from the primary wave of the local source transmitter. The sync AGC signal is inversely proportional to signal strength and should be fairly constant. Significant changes in the sync AGC signal are a result of the primary local source transmitter signal being too weak or too strong. The phase signal is affected by the polarized orientation of the gradiometer antennas and the transmitter antenna with respect to each other and with respect to the target. Phase shifts can occur when the gradiometer antennas cross the target boundary.

The identified null points were selected manually for each traverse line. The criteria for selecting these points have been experimentally determined to be 1) A change in Mag greater than or equal to 200 mV on each side of the null, with or without a corresponding phase change, and 2) Multiple null points must be greater than or equal to 30 ft apart, otherwise the feature is near surface. These two criteria were used to quickly and consistently select null points in the response profile plots.

The intended purpose of the linear traverse response plots is to identify possible targets, not to position truth data. Truth data locations must be and are positioned on spatially correct grid plots. The response plots for a given traverse area have the same horizontal scale, with some variation due to GPS positioning error. Note also that the auto-scale feature in Excel does impact the labeling of the horizontal scale values.

Noise in the Mag traces on the profile plots is a direct result of the quality of the Sync data. The Sync data provides the coherent timing information to the receiver. The Sync channel is not immune to external noise sources that are local to the traverse area. In continuation, noise in the Mag traces translates to noise in the Phase traces, since the latter is computed from the former. The Phase traces were eliminated from some of the profile plots because of noise. Also, in one instance traverse lines were not over the same survey line (some offset) because the surface stakes were moved due to obstacles.

## Conclusions

### Survey Field Test Results

A total of 43 traverse lines have been analyzed in relating 190 total identified null points in the profile plots to the physical locations in spatial plots that have been overlaid with the mine workings. The following results are given: 142 (75%) of the null points are over air-coal boundaries, 35 (18%) of the null points are over coal pillars, and 13 (7%) of the null points are over no obvious features.

The shallow workings, up to 50 ft, at Area 1 proved to be a good site for the high frequency gradiometer survey. The useful frequency used here was 200 kHz. The boundaries at the coal and air interface were distinguishable from most of the profiles with some errors resulting from either GPS inaccuracy or geologic/environmental incongruities which slightly shifted the null points on the profile. The high frequencies provided adequate resolution to nail down the delineations in shallow workings as indicated in the profile plots.

The deeper workings, from 100 to 200 ft, at 5 of the survey areas proved to be good sites for the lower frequency gradiometer survey. The useful frequencies used here were 2 kHz and 20 kHz. The low frequencies do not have the resolution to pinpoint boundaries. Multiple gradiometer surveys over the same traverse line filled in data points over the coal barrier pillars as indicated in the profile plots.

The deepest workings, from 200 to 400 ft, at Area 6 required the lowest frequency gradiometer survey of 2 kHz. Again, multiple gradiometer surveys over the same traverse line filled in data points over the coal barrier pillars. Several barrier pillars were identifiable as indicated in the profile plots.

These electromagnetic gradiometer surveys have shown that identified null points in the signature profile plots over a coal mine indicate the air-coal boundary of the entry walls. Multiple surveys over the same traverse line must be taken to fill in the target boundary locations (air-coal or water-coal) and the non-target locations (solid coal). The procedures and results of these demonstration surveys are typical of this type of void-detection work. This method can be extended to unknown area and environments in non-demonstrative capacities.

### **Confirmation Drilling**

Based on DeltaEM data profiles, two positive void-detection areas were selected for confirmation drilling. The confirmation drill holes at the Emery Site were coordinated by EarthFax Engineering of Midvale Utah. These included two drill holes (#1 and #2) that reached to a level at least 5 ft below the LI-5 Coal Seam (about 170 ft deep). Each drill hole anticipated intersecting the top of the coal seam void at about 154 ft. Table 6 provides the predicted depth of the key layers of intersection. The drilling records for these holes are given in their entirety in Appendix D.

Table 6. Drill hole predicted depths.

Predicted Depths (ft)	Drill Hole #1	Drill Hole #2
Top of Ferron Sandstone Layer	36.3	37.1
Bottom of Ferron Sandstone	141.3	128.9
Top of Detected Void Space	153.5	153.9
Bottom of Coal Seam	168.5	168.9
End of Hole	172	174

No Voids  
Actually  
Encountered

The drilling method was Sonic, or Vibratory, Drilling. This methodology can be several times faster than other drilling techniques (depending on soil conditions) and does not use drilling mud in its application. Sonic drilling is able to provide continuous core samples to depths typical in shallow coal exploration. Sonic drilling uses controllable high-frequency resonant vibrations at the drill bit to optimize penetration based on soil/rock geology. The resonance magnifies the amplitude of the drill bit, fluidizing soil particles at the bit face.

While EarthFax worked very hard to ensure an accurate drilling path, it is anticipated that the drill holes may have deviated from their intended vertical path by some small angle. This common phenomenon, while controllable, is not avoidable. Deviation is caused by the mechanical factor in the drilling process and by changes in geologic conditions. The drill bit can react to foliation and structure within the rock and because of refraction as the bit moves from different rock units of varying density. Surveying the azimuth and dip of a borehole is the only way to quantify the degree and direction of deviation. The deviation of these drill holes greatly affects the usefulness of the information returned.

The conclusions made by EarthFax during the drilling exercise indicate that no actual mining-related voids were encountered. Given the errors associated in the positioning of the DeltaEM positive responses, combined with the errors associated with the pin-point drilling, the geometry of the confirmation drilling sets up a very risky, low-probability endeavor. The following graphics illustrate a very important limitation to the method of confirmation drilling. These involve the mathematical probability of actually intersecting a void space with a drill string given the two principle errors in (1) selecting a drilling location and (2) anticipating some modest level of drill hole deviation.

The detection of a void space by the DeltaEM unit is based on a minimum threshold in its gradiometric magnitude or phase response. As previously

discussed, the null points were typically selected manually for each traverse line based on the following criteria: 1) a change in magnitude greater than or equal to 200 mV on each side of the null, with or without a corresponding phase change, and 2) multiple null points must be greater than or equal to 30 ft apart, otherwise the feature is near surface. These two criteria best provide null point selections intended to be the spatial locations that best represent the actual boundaries at the coal and air interface. However, two main sources of error can result from this technique. The first involves the actual point of a void-related magnitude null. This point may have some lateral error associated with the actual radiated magnetic field created by the void space. It must be remembered that the induced current, and its resulting backscattered field, depend entirely on the electrical structure of the coal-void model, and not on its physical structure. To assume that the peak of the total magnetic field aligns perfectly with the center of a mine-related void space, given all the geologic and geometric factor, would be wrong. Therefore some leeway must be given to the positioning of the null point.

The second major source of error in detection and location is the coordinate points themselves. As stated early in this report the GPS inaccuracy must be considered when projecting the profile null points onto a map. The GPS system using in this demonstration was woefully inaccurate given the tolerances implied by the mine maps and the intention of confirmation drilling. These two principle error sources made actually picking the location of a drill hole fairly low probability. Coupled with errors associated with drill hole deviation, the fact that void spaces were not intersected by EarthFax is not surprising and far from conclusive.

To illustrate the deviation error possible in the confirmation drilling it is common to look at the typical cross-sectional areas created by angular deviation which may be drilled at specific depths. This was done here for deviation between 1 and 7 degrees (3 to 5 degrees are common). As common-sense dictates, the greater the deviation the wider the possible area created by the drill hole at depth. So given the size of the drill hole and the anticipated width of the mine entries (void targets), the probability of intersecting the void is significantly less than perfect. The plots presented in Figures 30 through 33 show the void-intersection probabilities for a small range of possible deviation angles as a function of depth. The coal seam was anticipated to be at around 155 to 165 ft. The probability of intersecting the void decreased with depth and deviation as indicated in the plots. These probabilities have nothing to do with the errors associated with the DeltaEM instrument, its data processing, or null point delineation; these are strictly drilling-related probabilities. To illustrate the possible effects of null-point placement two different scenarios are given for the probability curves. One is based on drilling directly over the void (centered on the 14-ft-wide entry) and the second is based on drilling over the edge of the entry rib. Figure 30 diagrams these two scenarios.



Figures 31 and 32 then show the probability curves for void-intersection based on these two geometric models.

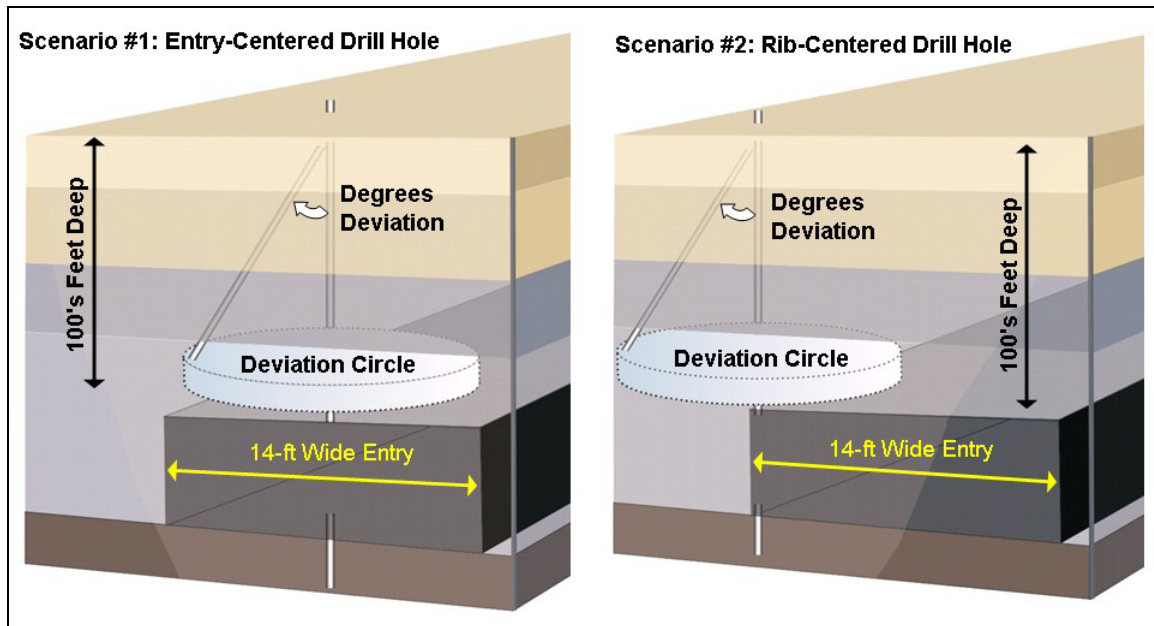


**Figure 30.** Diagram of the two geometric scenario modeled in the probability curves:  
 #1 drill hole started at exact center of 14-ft-wide entry,  
 #2 drill hole started at exact rib edge of 14-ft-wide entry.

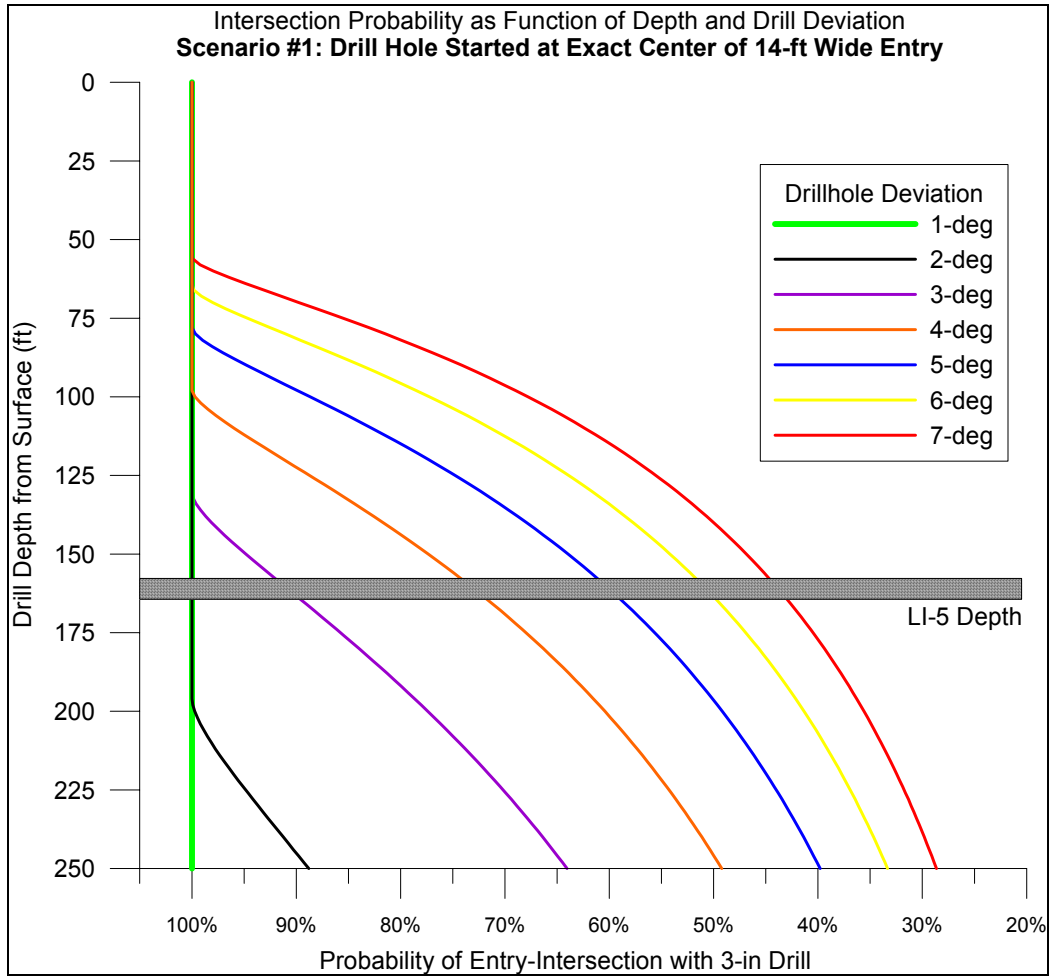


**Figure 31.** Scenario #1 Probability of intersecting mine entry with 3-in. drill string. Drill hole started at exact center of 14-ft-wide entry.

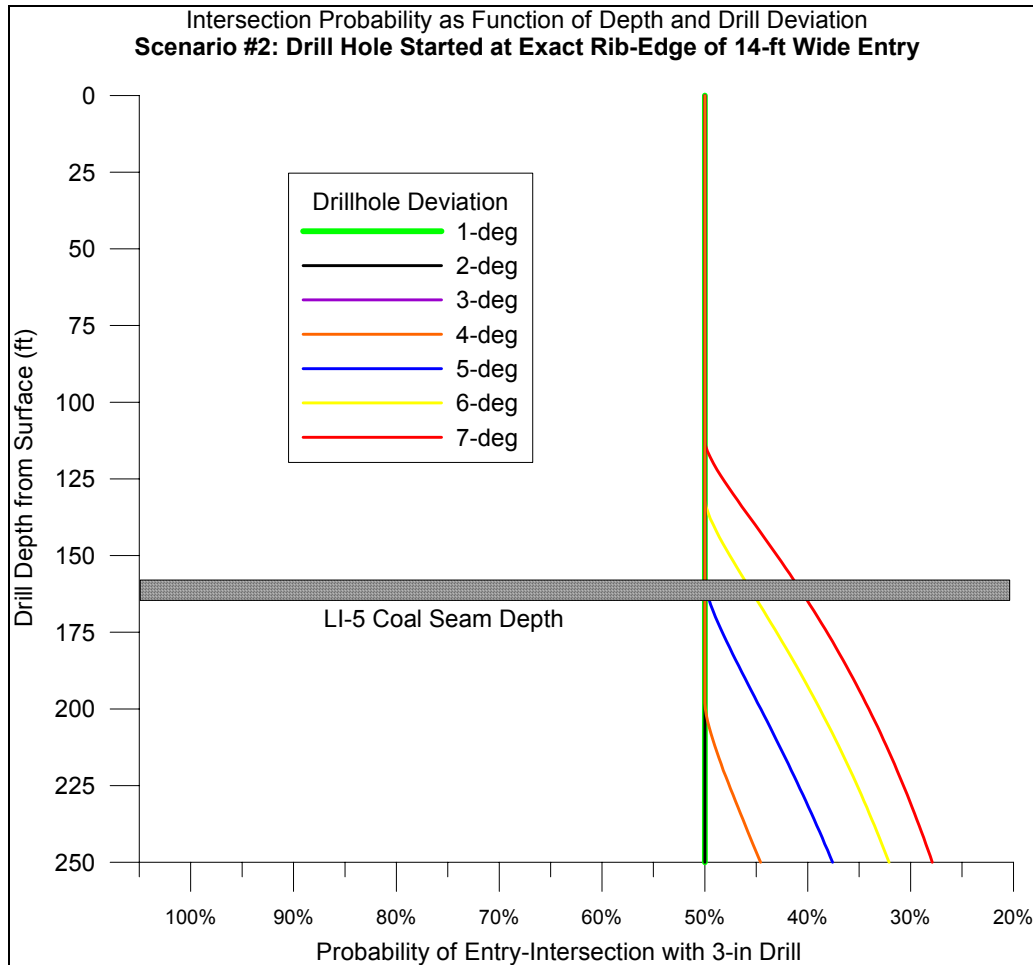


**Figure 32.** Scenario #2 probability of intersecting mine entry with 3-in. drill string. Drill hole started at exact rib-edge of 14-ft-wide entry.

If the drill hole started directly centered on the entry, a guarantee that the void was intersected would only occur if the deviation was less than 2 degrees. If the deviation was closer to 5 degrees, the probability drops to less than 60%. As the drill hole placement moves toward the edge of the entry (toward either of the ribs), the probability of intersects obviously goes down. With the drill hole at the edge of the rib itself the plot shows that for a 5-degree deviation, the likelihood of intersecting the entry at 155-ft depth is less than 50%. This is a very important fact when considering the implications and conclusions of this confirmation study: if the null-point corresponds to the coal-air interface (the rib), and this point is drilled for confirmation, the likelihood of intersecting the entry can **never** be better than the likelihood of correctly calling a coin flip.



Research Corporation

## References

1. *Summary Report Evaluation of Additional Tunnel Detection Research Techniques at the California Tunnel Site*. U.S. Army Belvoir RD&E Center (BRDEC) Physical Security Equipment Division Geophysics Team. 18 August–3 September 1993.
2. *Benchmark Study of Technical Capabilities, Research Efforts, and Recommendations for Underground Target Detection using Geophysical Techniques*, US Department of Energy Report DOE/NN-20/001, 1994.
3. Bartel, L. C., and D. H. Cress. *An Electromagnetic Induction Method for Underground Target Detection and Characterization*. Sandia Report SAND97-0054, January 1997.
4. Kelly, Robert E. *Underground Structure Detection by Surface Magnetic Gradient Measurements*. Los Alamos National Laboratory. LDRD final report, 26 April 1999.

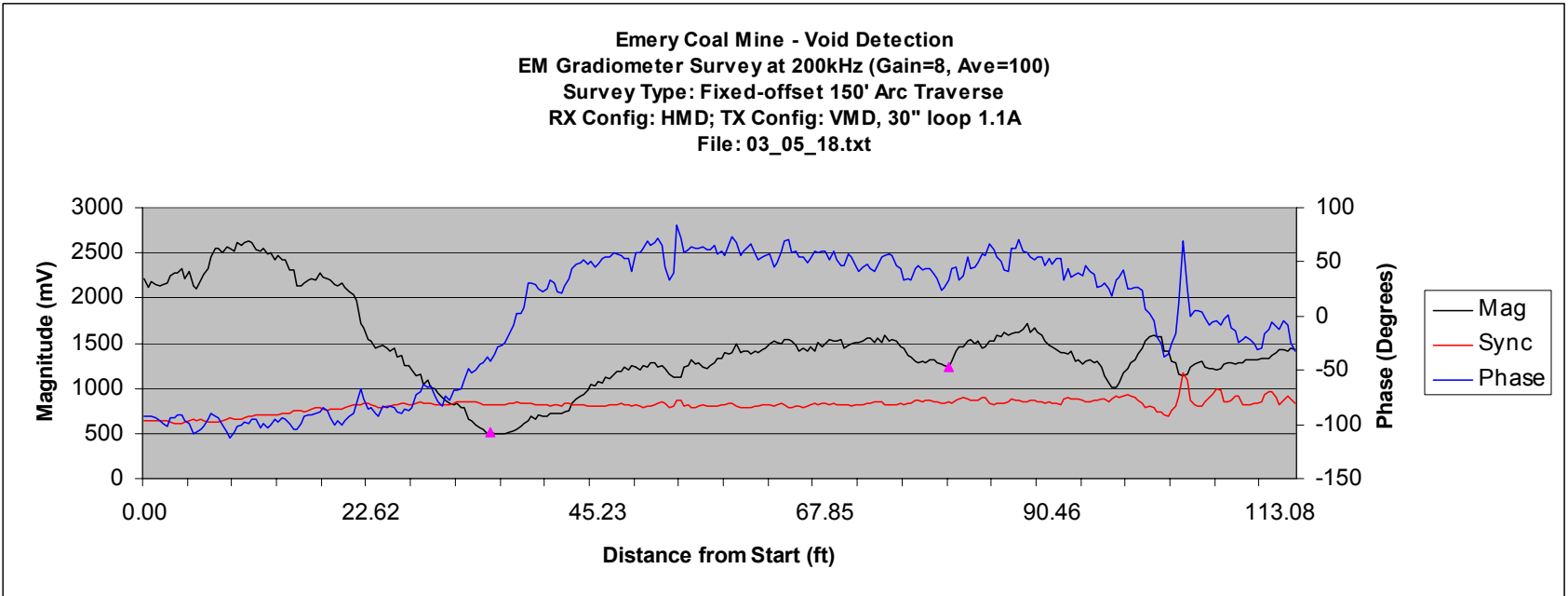


Research Corporation

## **APPENDIX A SPATIAL PLOTS**

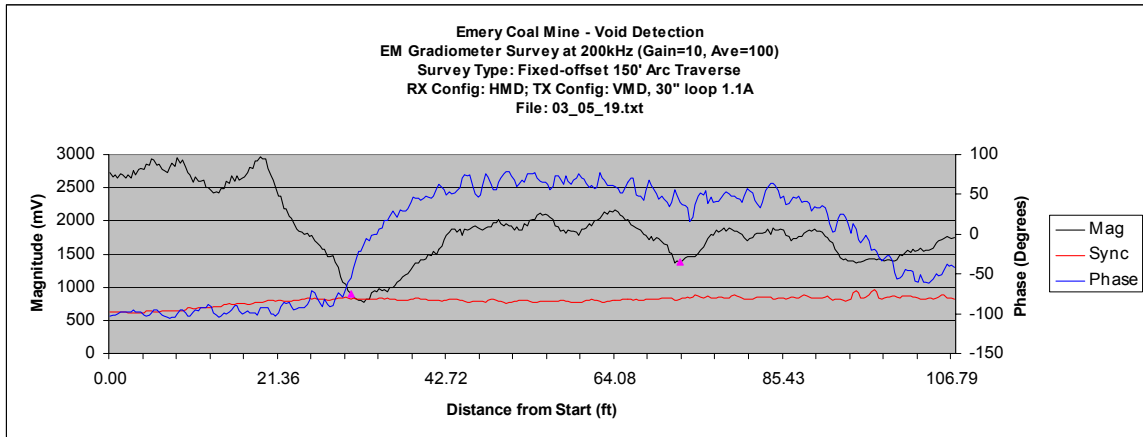
Figures A-1 through A-43 are the spatial plots from the Emery Coal Mine electromagnetic gradiometer survey.



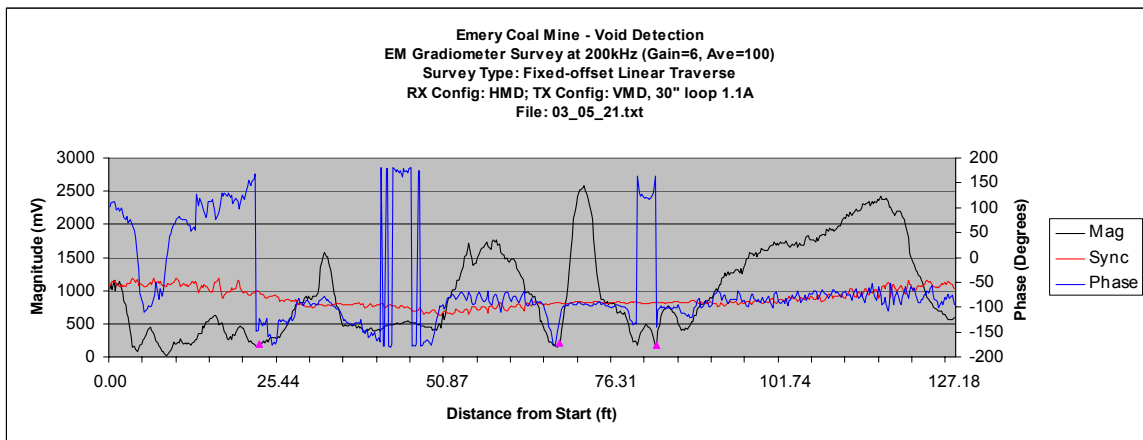


*Figure A-1. Area 1 200-kHz traverse response plot 1.*

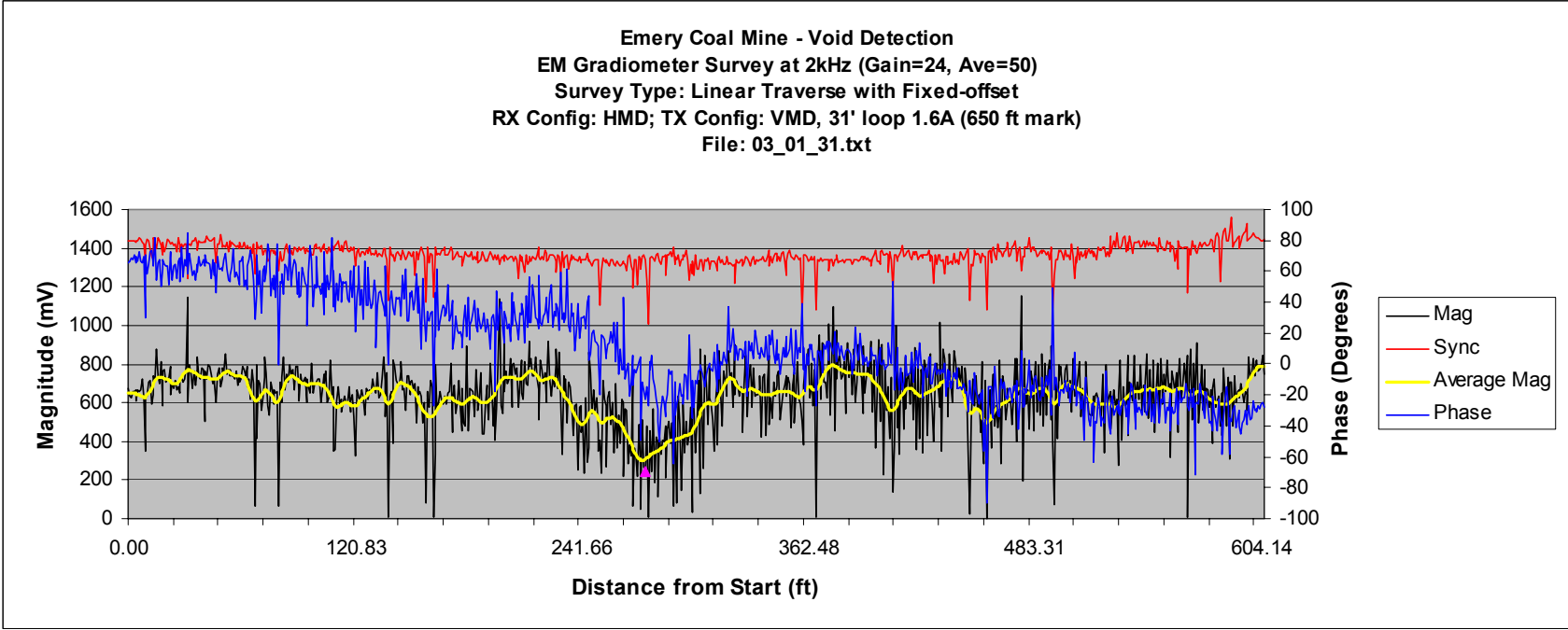




*Figure A-2. Area 1 200-kHz traverse response plot 2.*

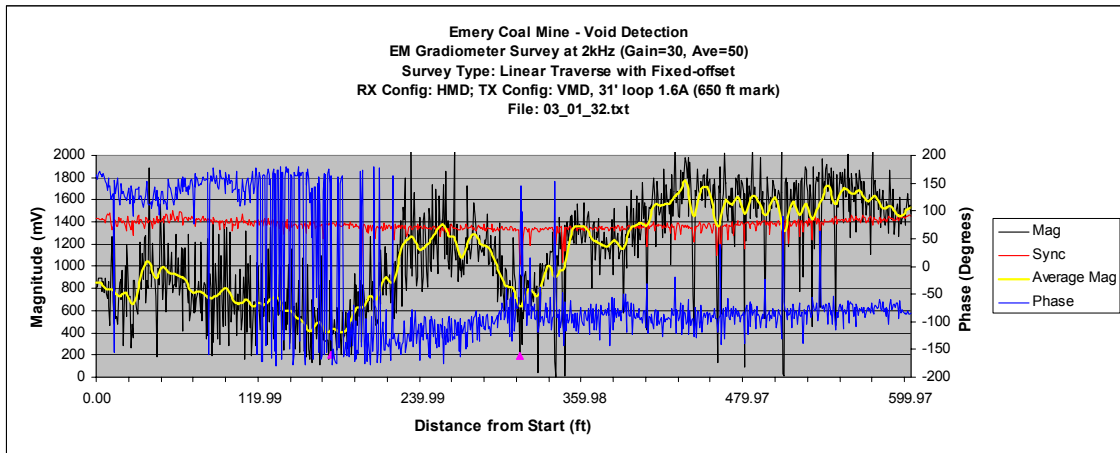


*Figure A-3. Area 1 200-kHz traverse response plot 3.*

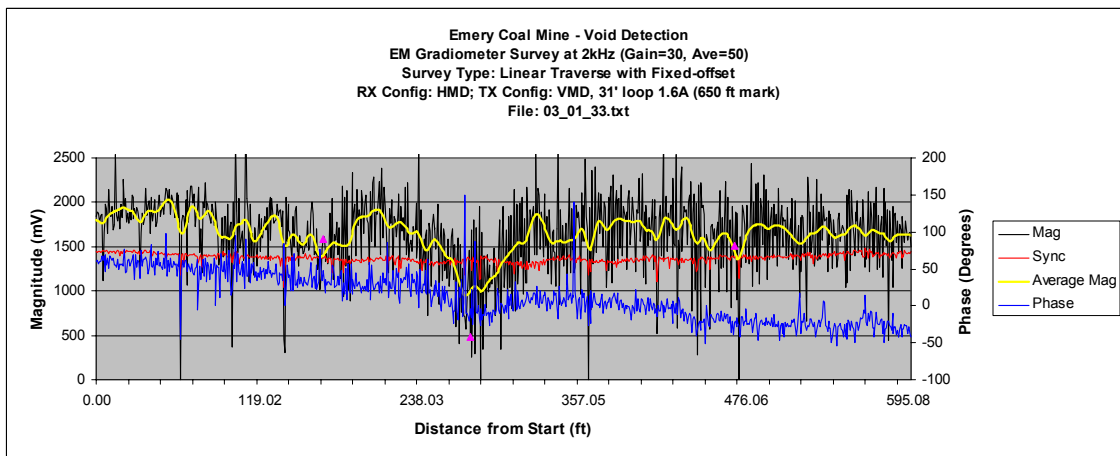


*Figure A-4. Area 2 2-kHz traverse response plot 1.*

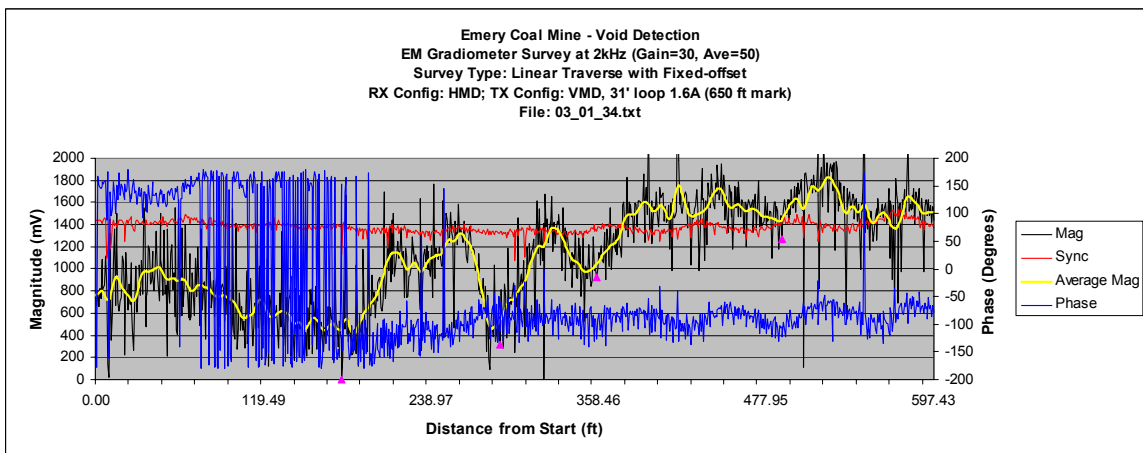




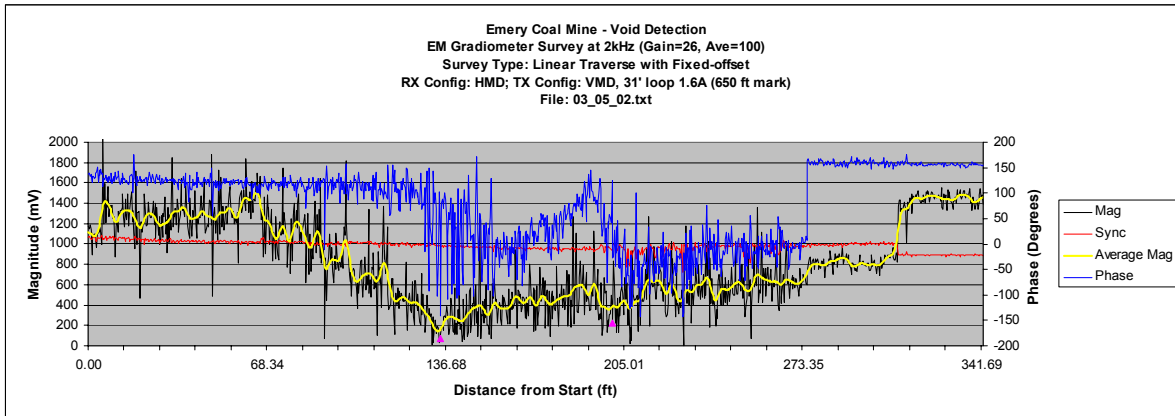
*Figure A-5. Area 2 2-kHz traverse response plot 2.*



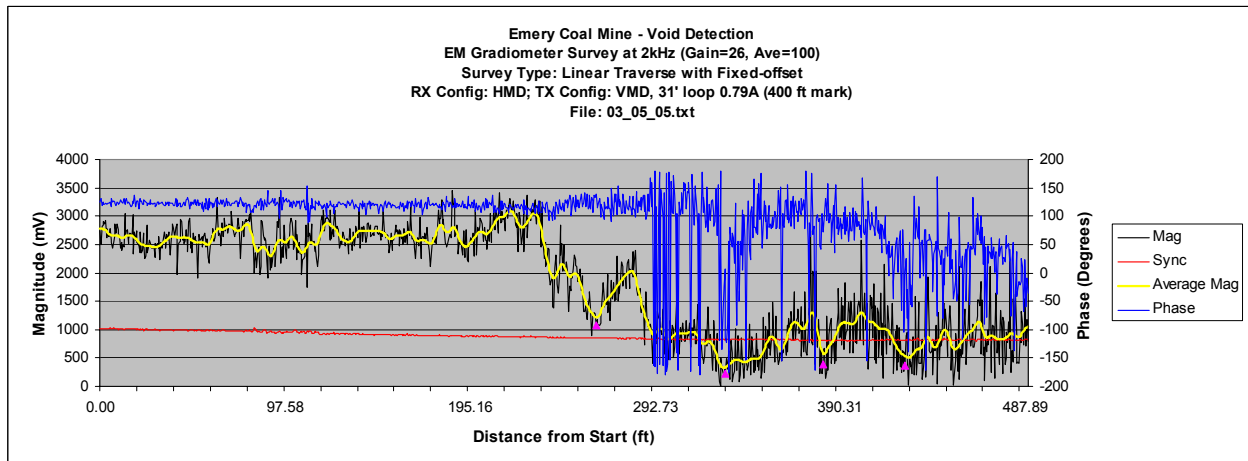
*Figure A-6. Area 2 2-kHz traverse response plot 3.*



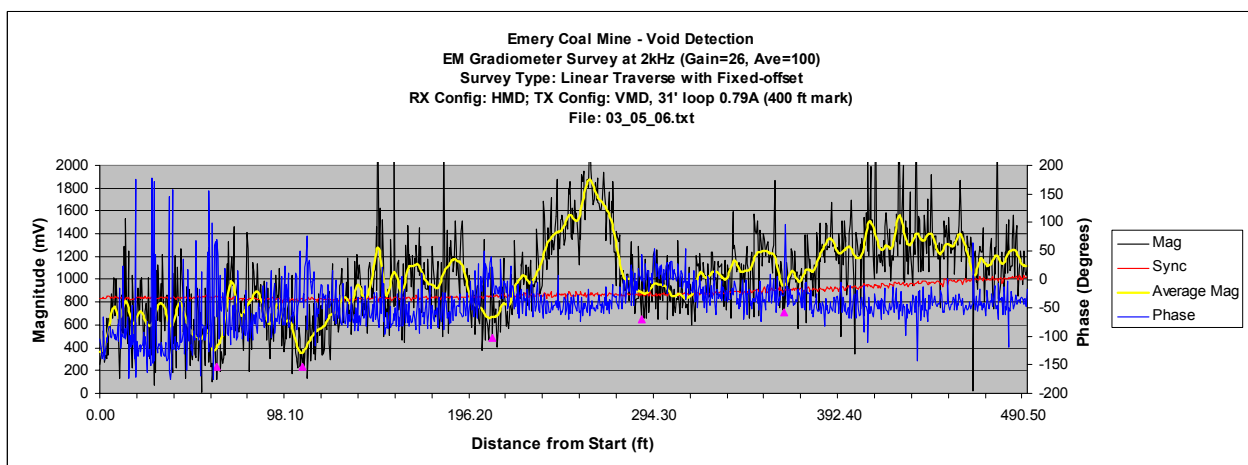
*Figure A-7. Area 2 2-kHz traverse response plot 4.*



*Figure A-8. Area 2 2-kHz traverse response plot 5.*

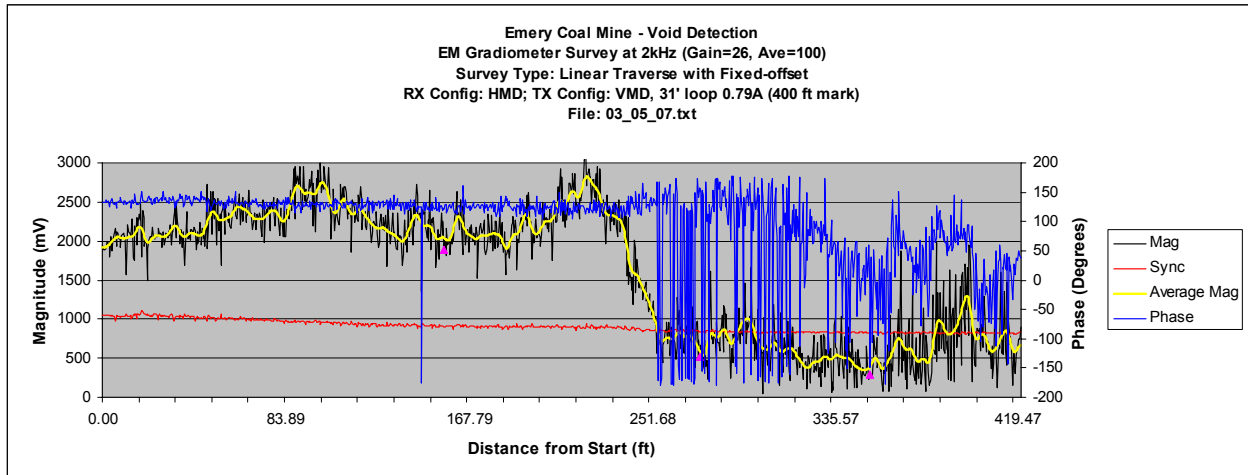


*Figure A-9. Area 2 2-kHz traverse response plot 6.*

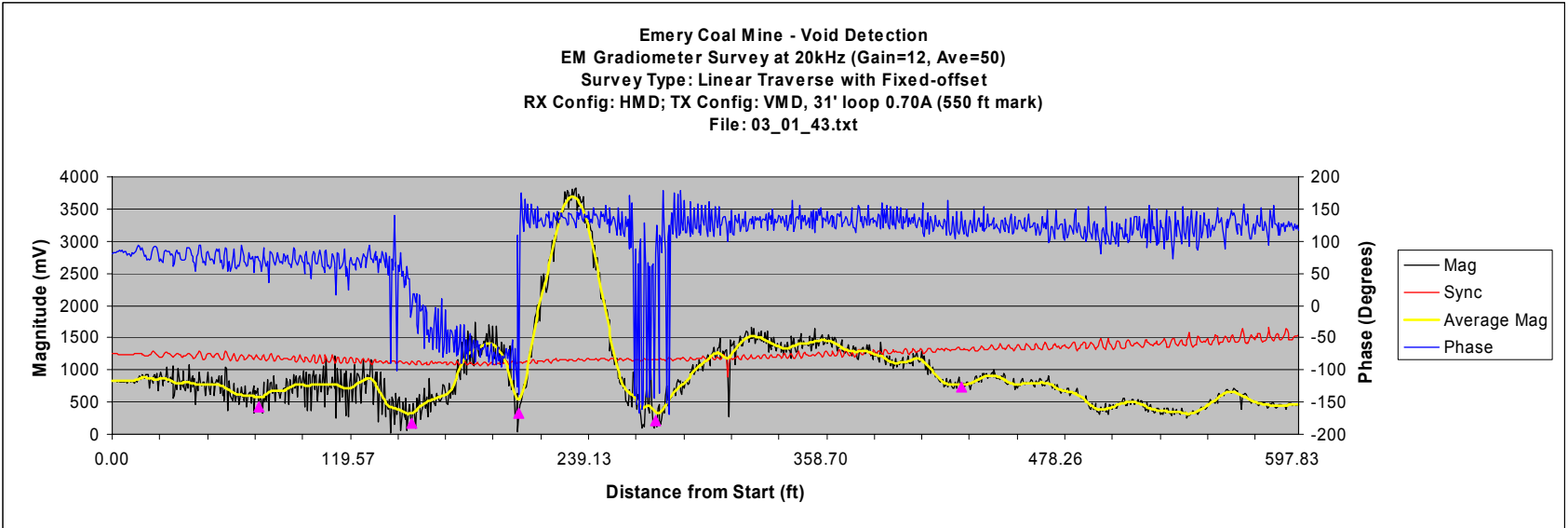


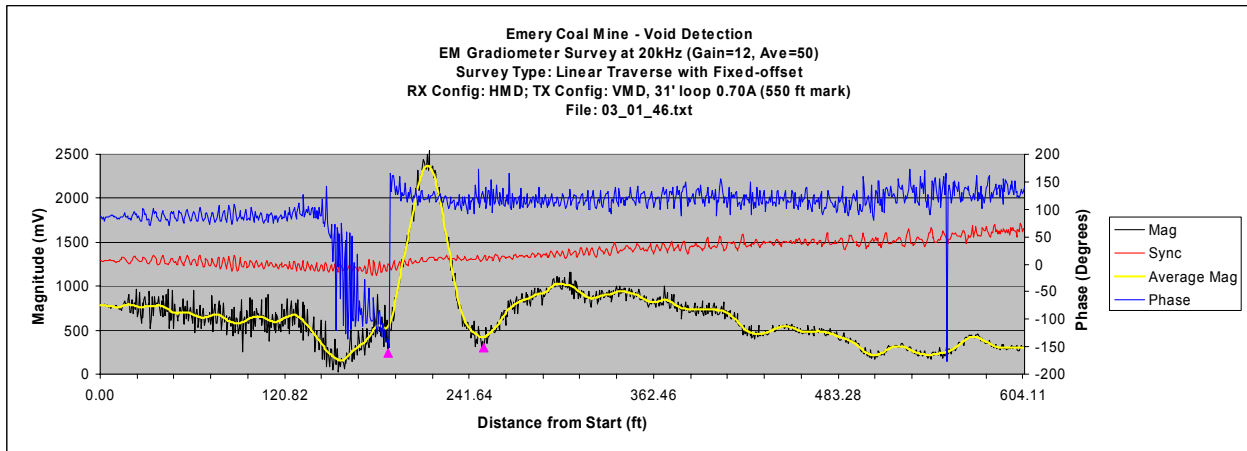
*Figure A-10. Area 2 2-kHz traverse response plot 7.*



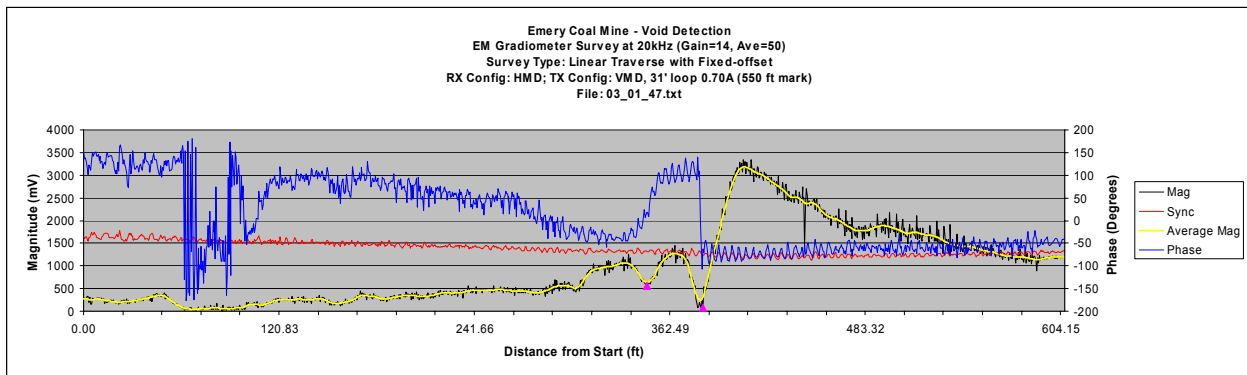


*Figure A-11. Area 2 2-kHz traverse response plot 8.*

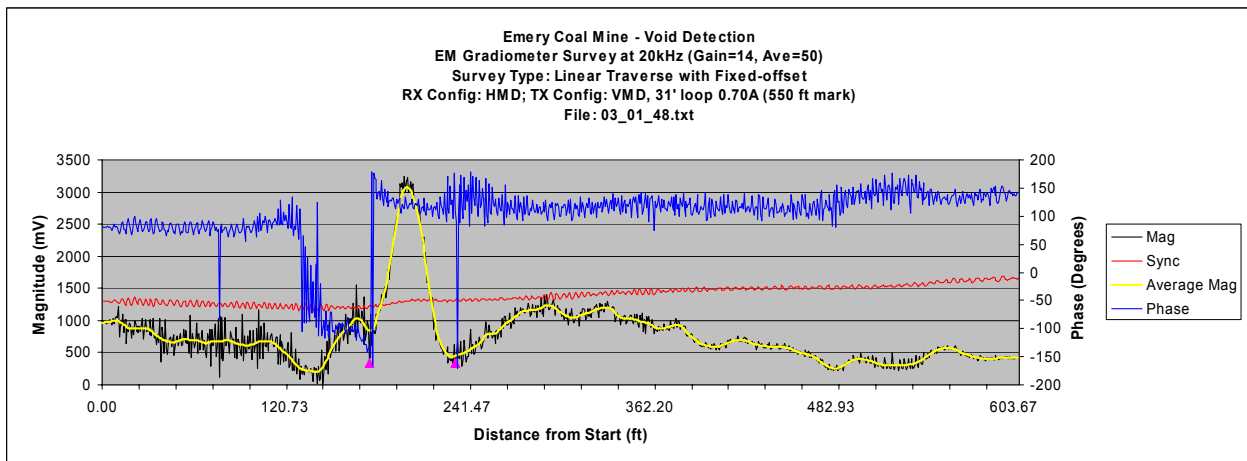




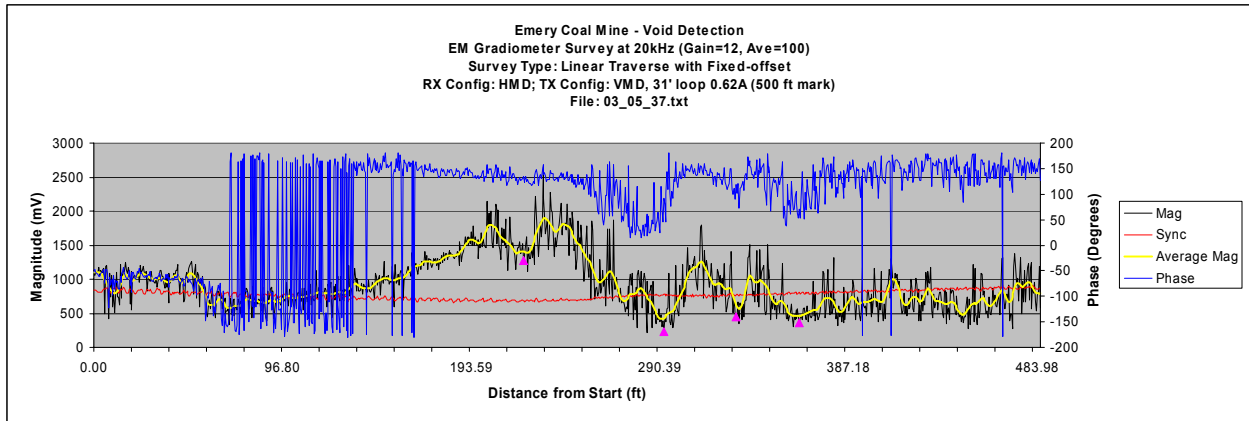
*Figure A-13. Area 2 20-kHz traverse response plot 2.*



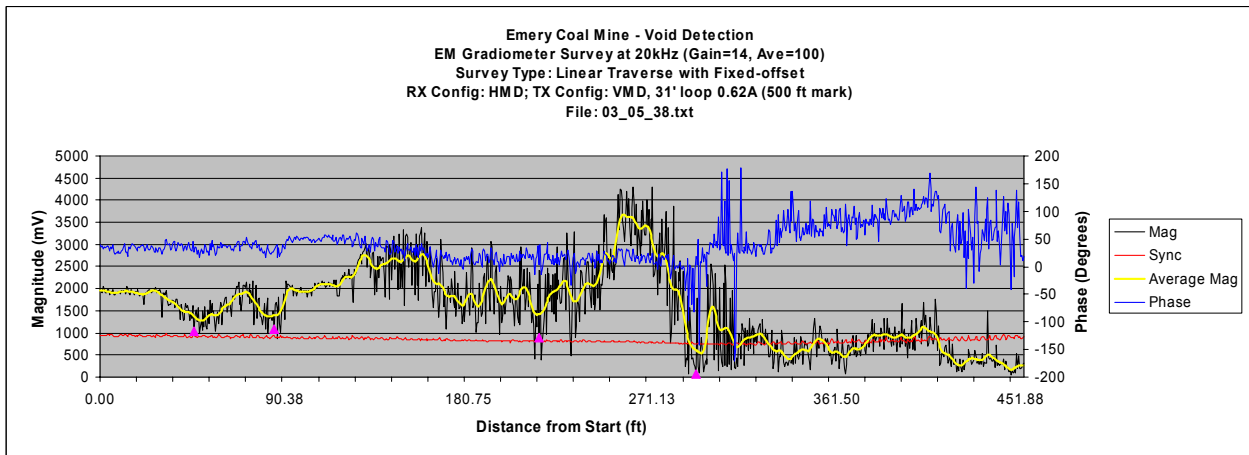
*Figure A-14. Area 2 20-kHz traverse response plot 3.*



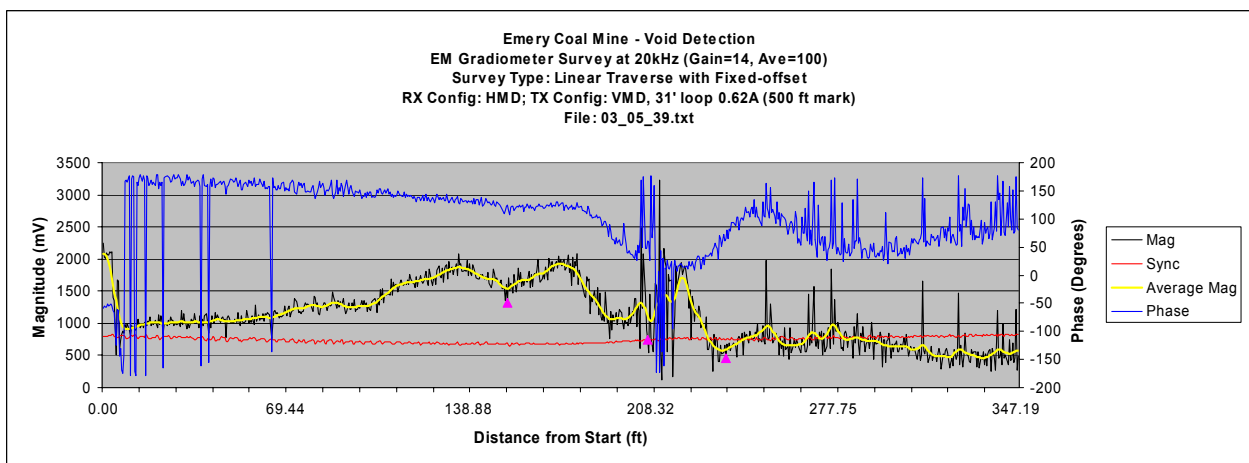
*Figure A-15. Area 2 20-kHz traverse response plot 4.*



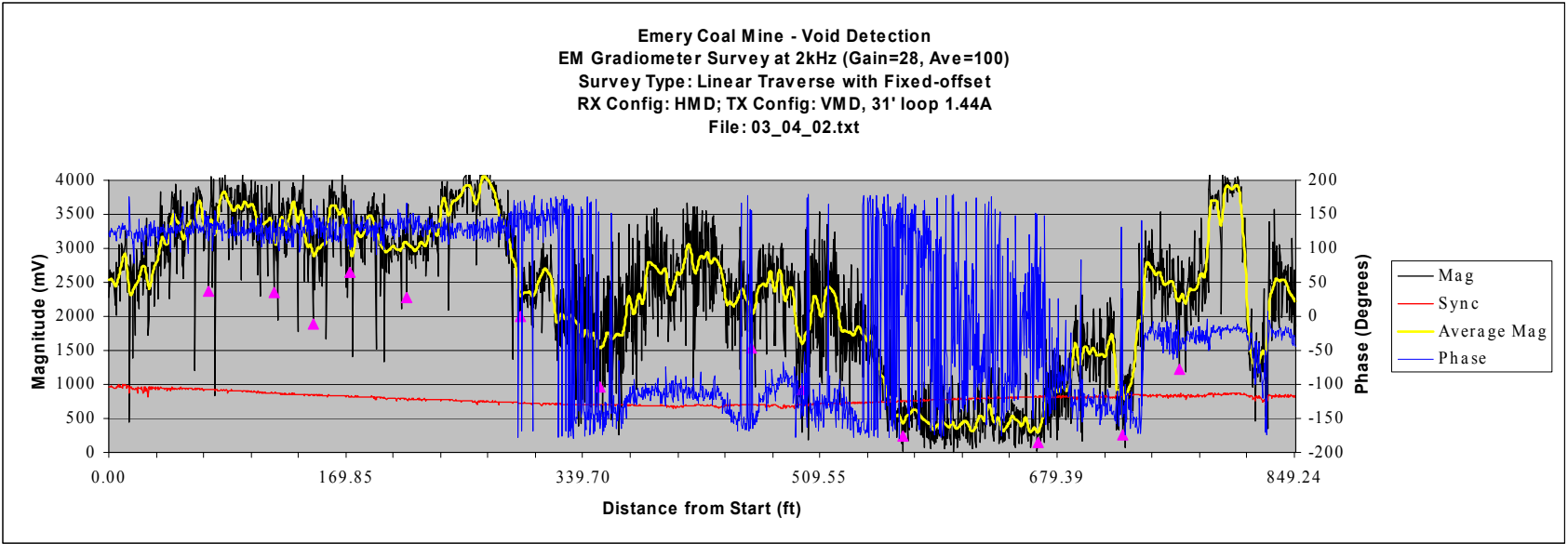
*Figure A-16. Area 2 20-kHz traverse response plot 5.*



*Figure A-17. Area 2 20-kHz traverse response plot 6.*



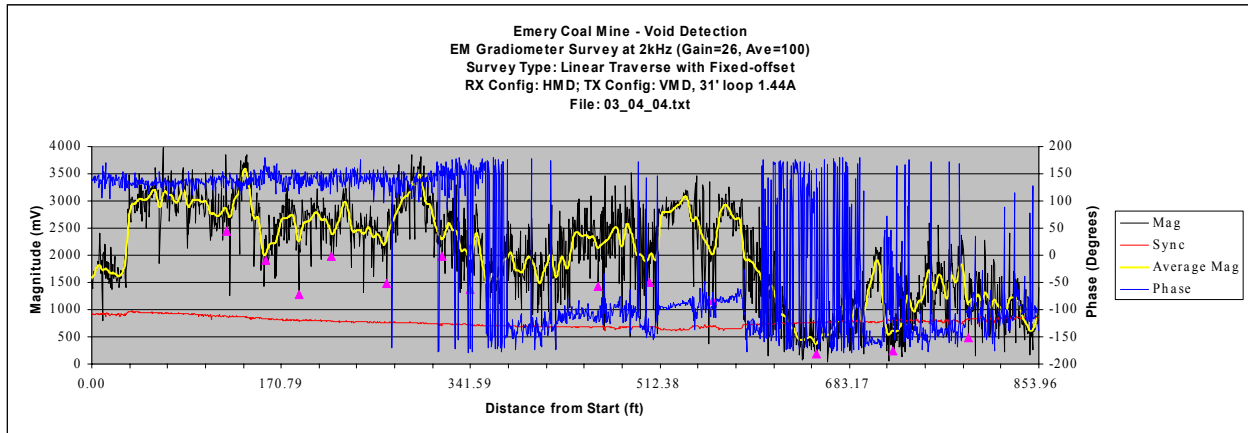
*Figure A-18. Area 2 20-kHz traverse response plot 7.*



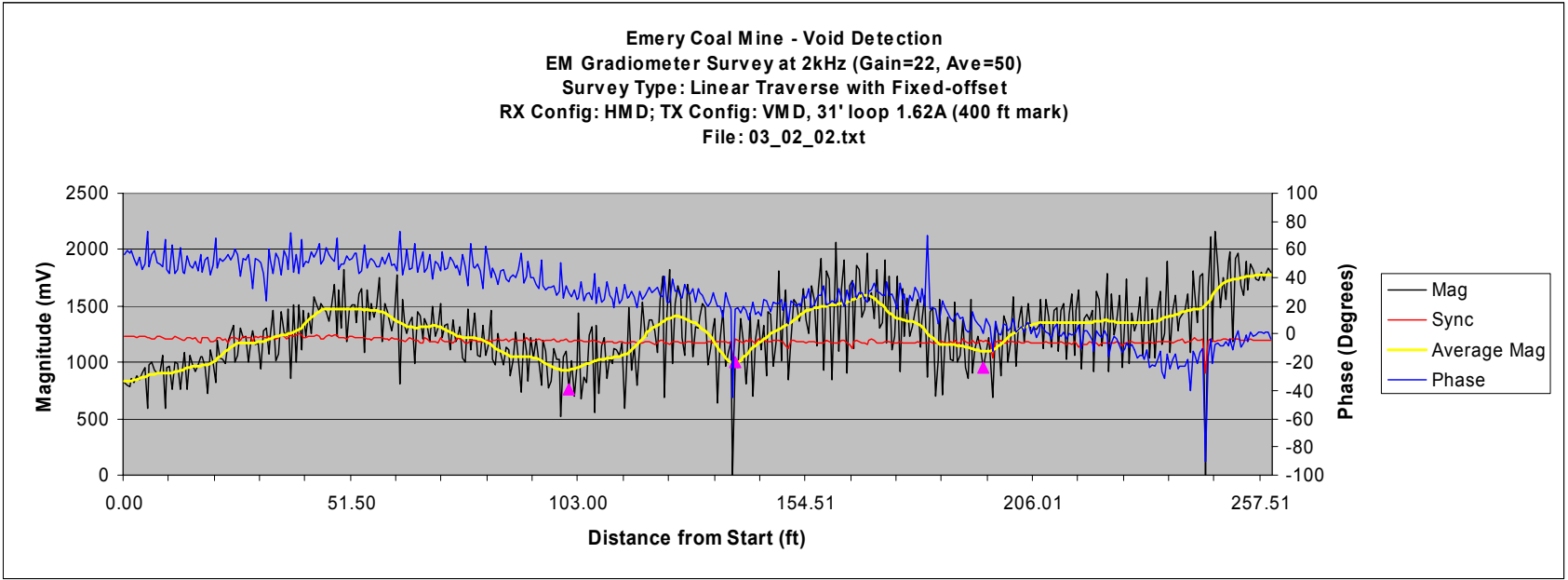
*Figure A-19. Area 3 2-kHz traverse response plot 1.*



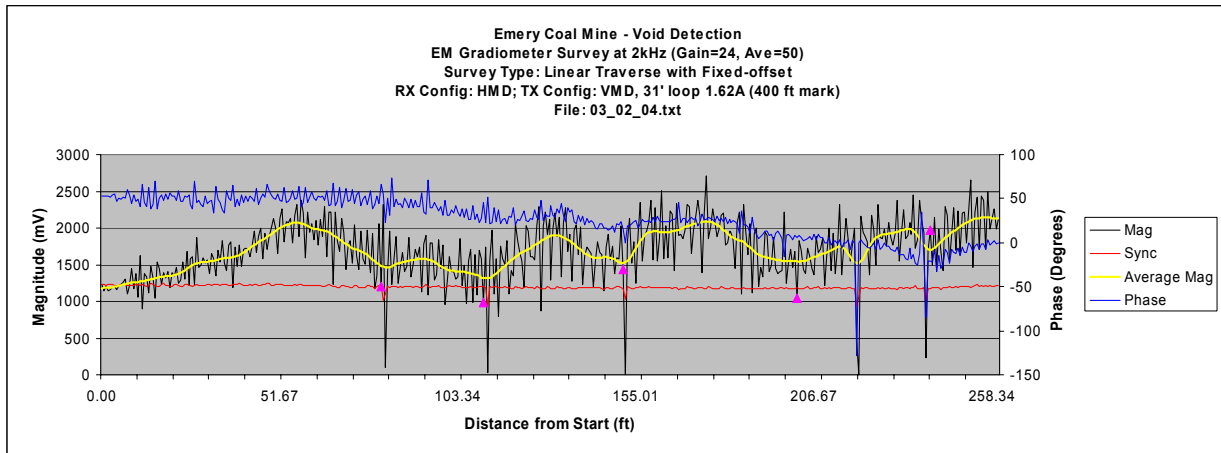




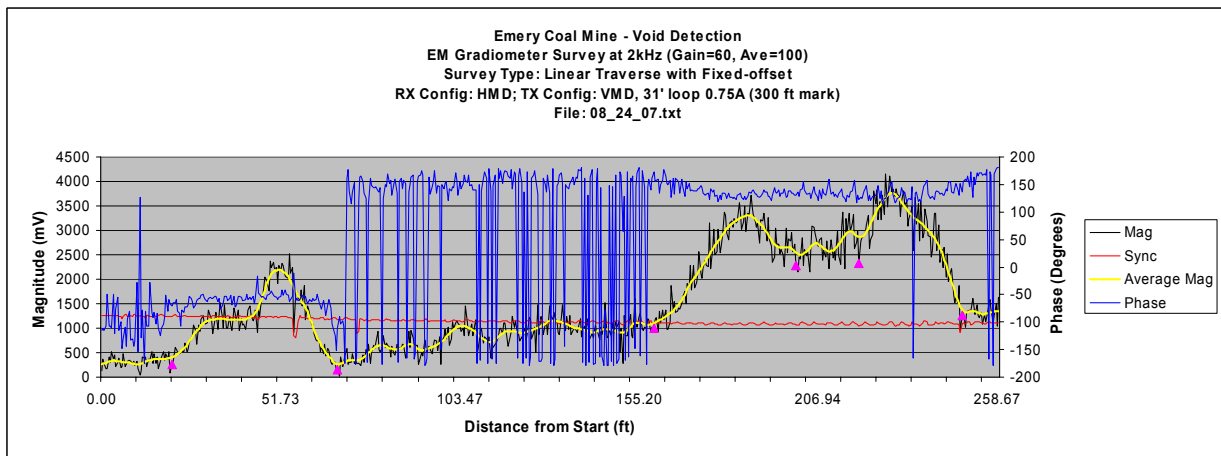
*Figure A-20. Area 3 2-kHz traverse response plot 2.*



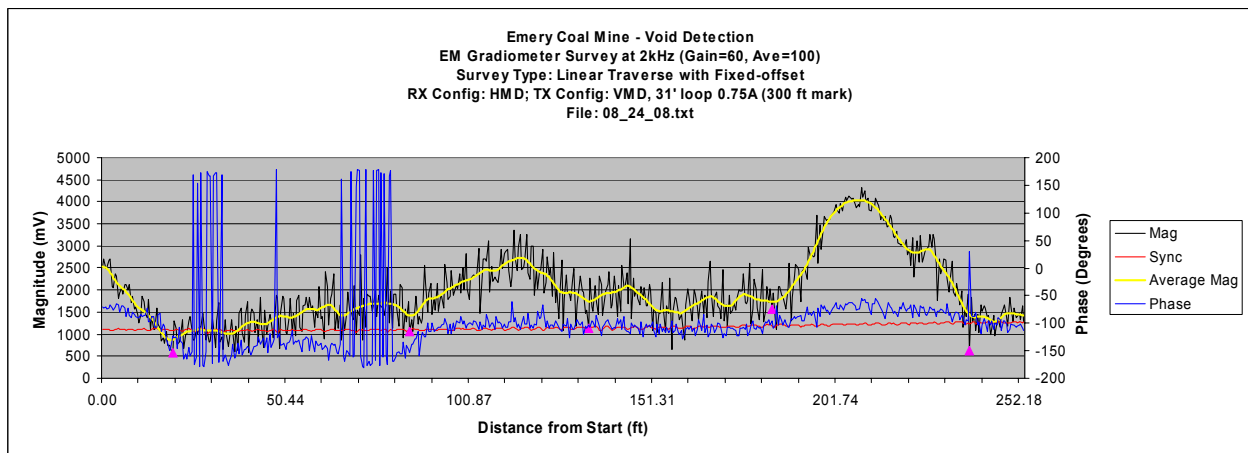
*Figure A-21. Area 4 2-kHz traverse response plot 1.*



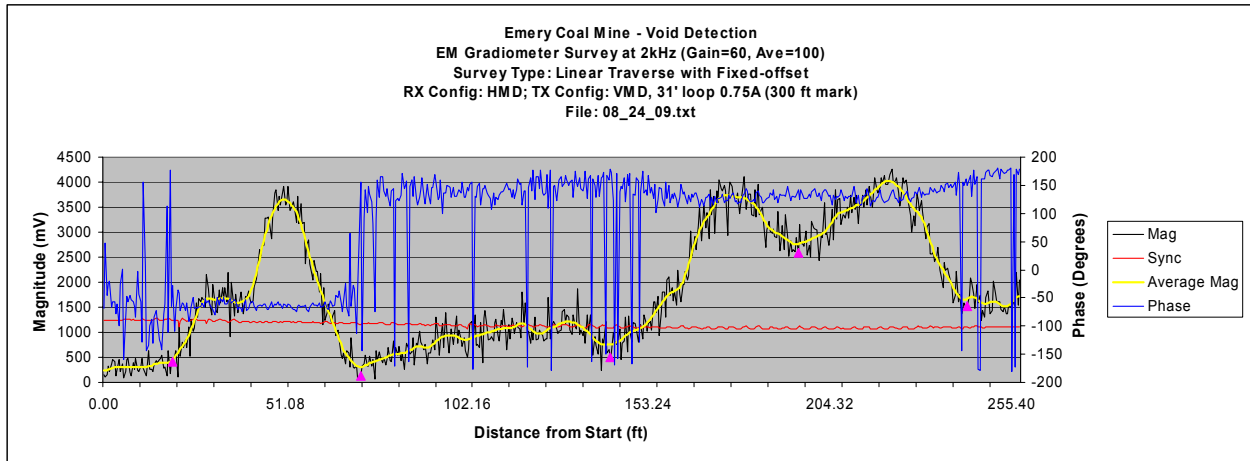
*Figure A-22. Area 4 2-kHz traverse response plot 2.*



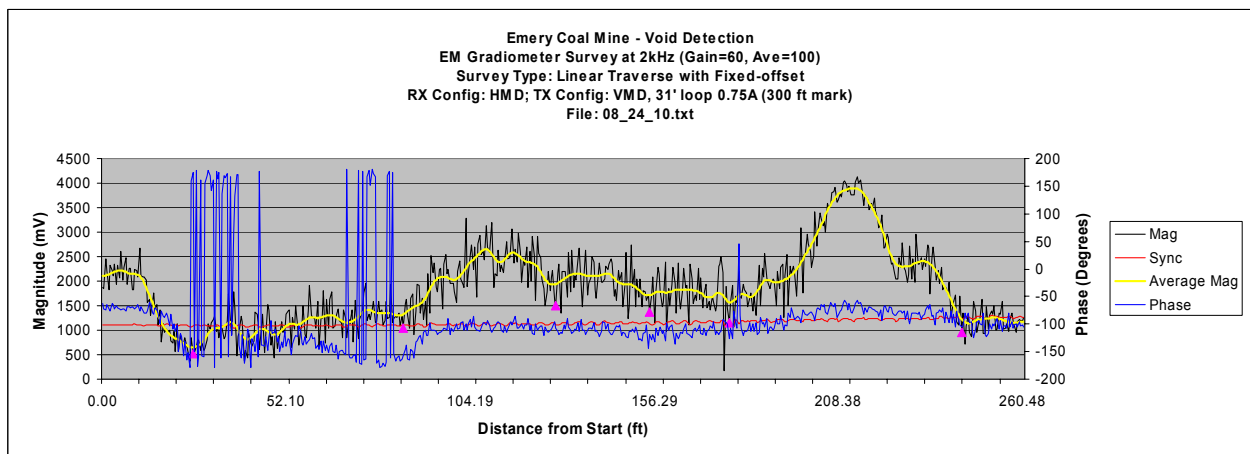
*Figure A-23. Area 4 2-kHz traverse response plot 3.*



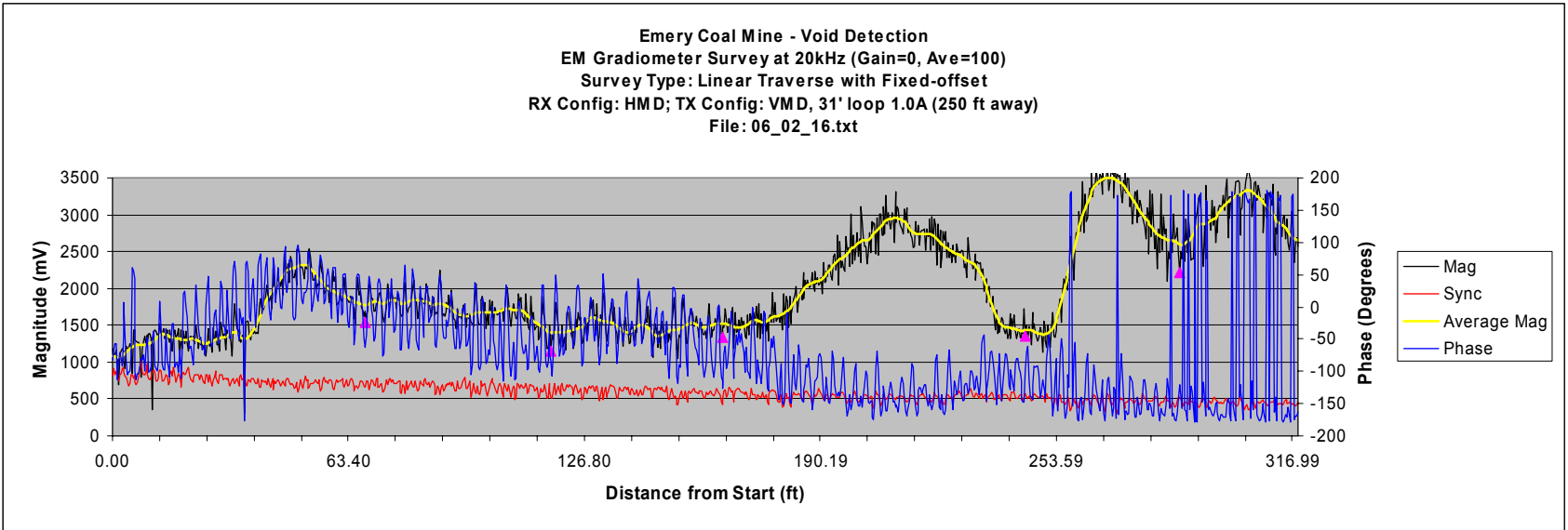
*Figure A-24. Area 4 2-kHz traverse response plot 4.*



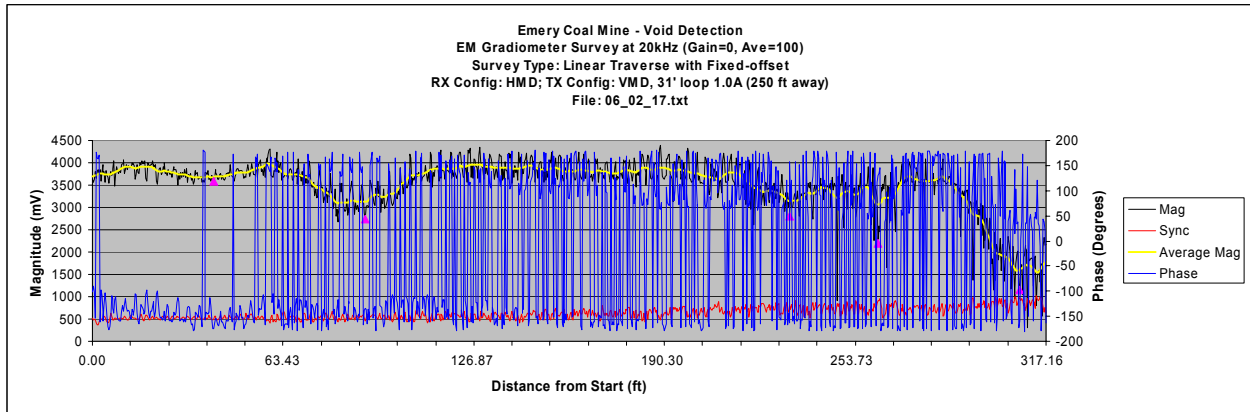
*Figure A-25. Area 4 2-kHz traverse response plot 5.*



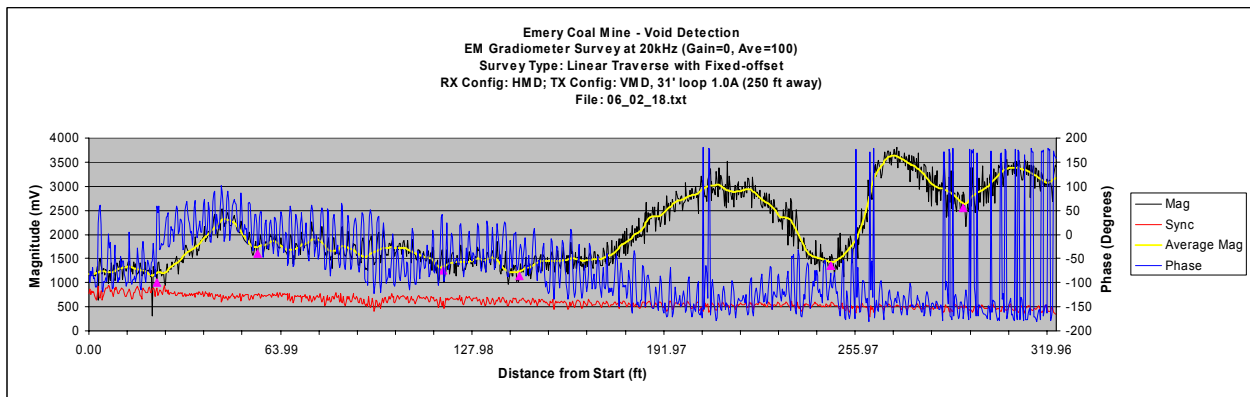
*Figure A-26. Area 4 2-kHz traverse response plot 6.*



*Figure A-27. Area 4 20-kHz traverse response plot 1.*

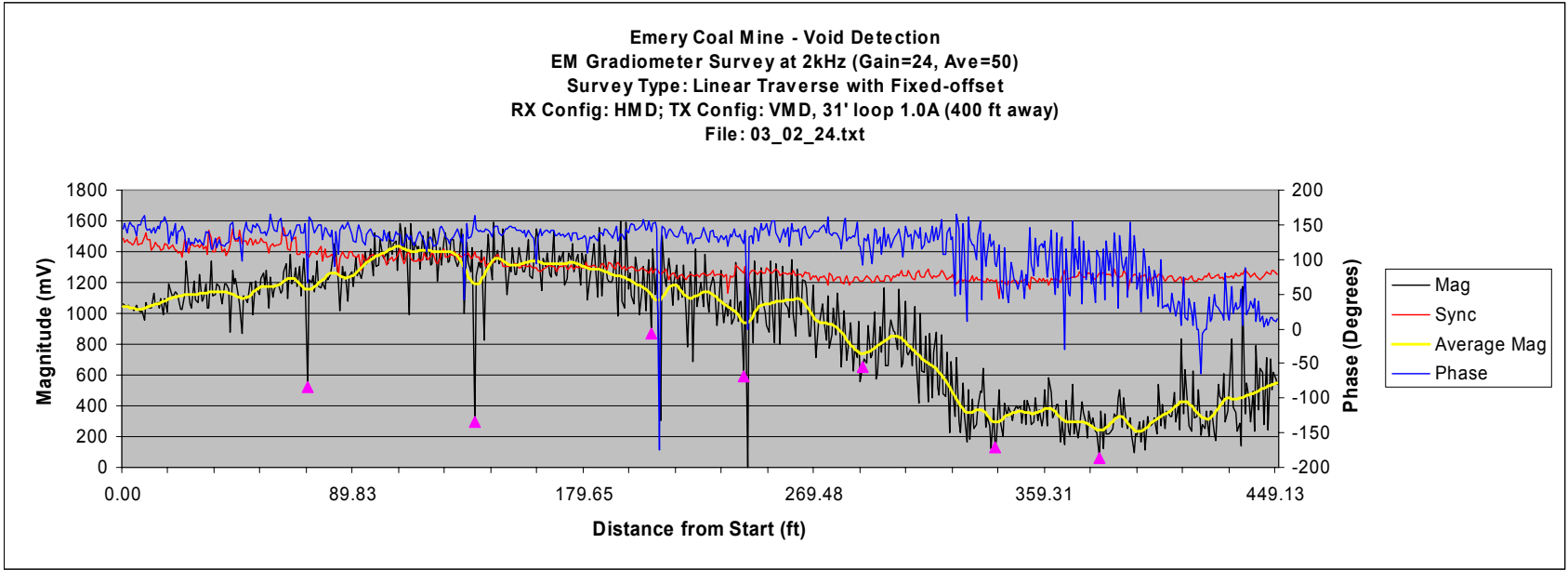


*Figure A-28. Area 4 20-kHz traverse response plot 2.*

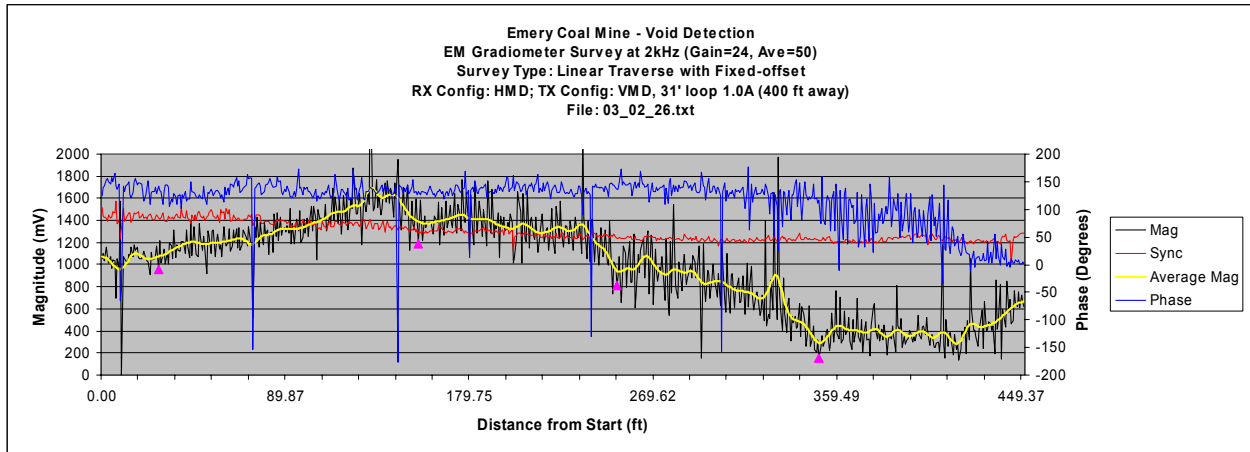


*Figure A-29. Area 4 20-kHz traverse response plot 3.*

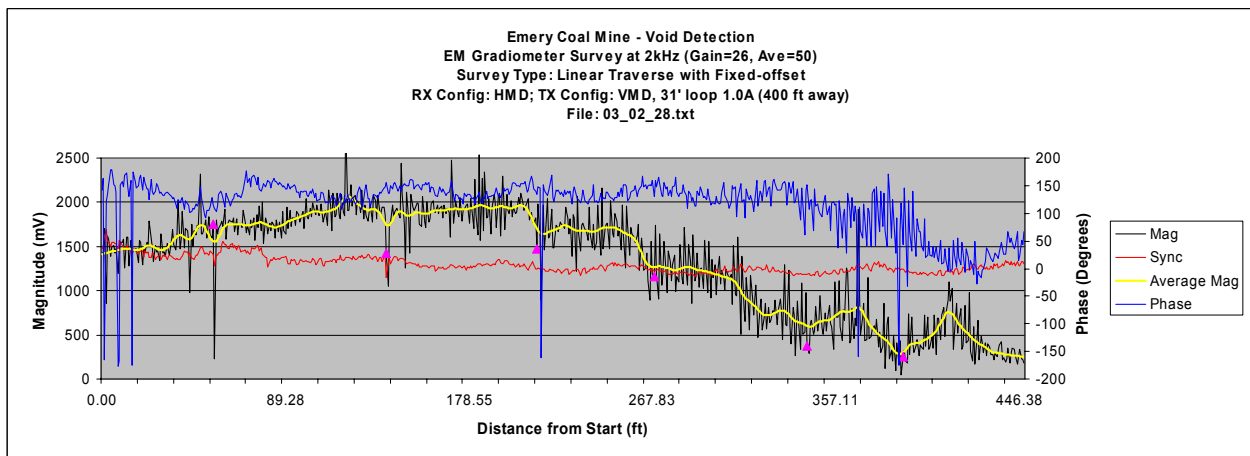




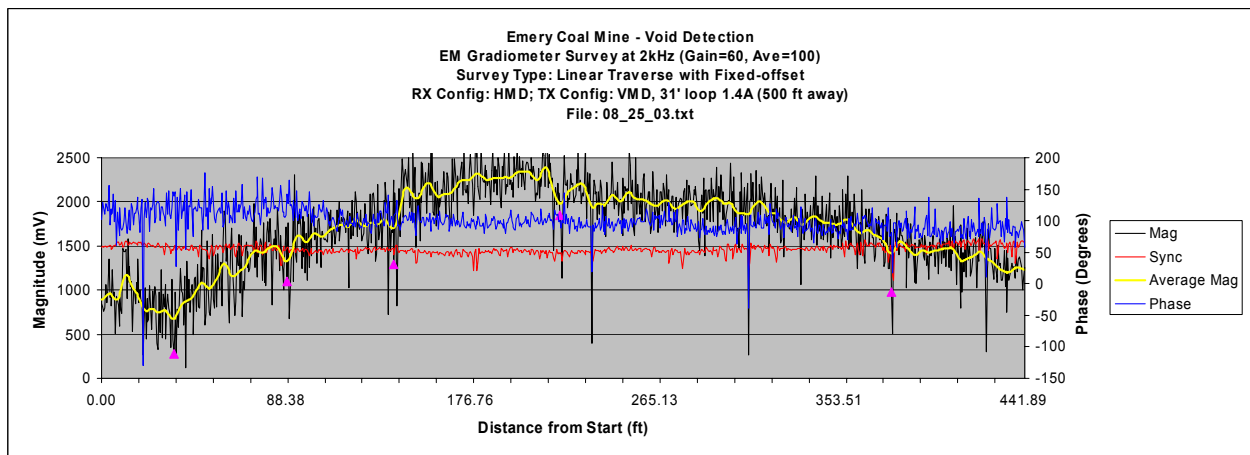
*Figure A-30. Area 5 2-kHz traverse response plot 1.*



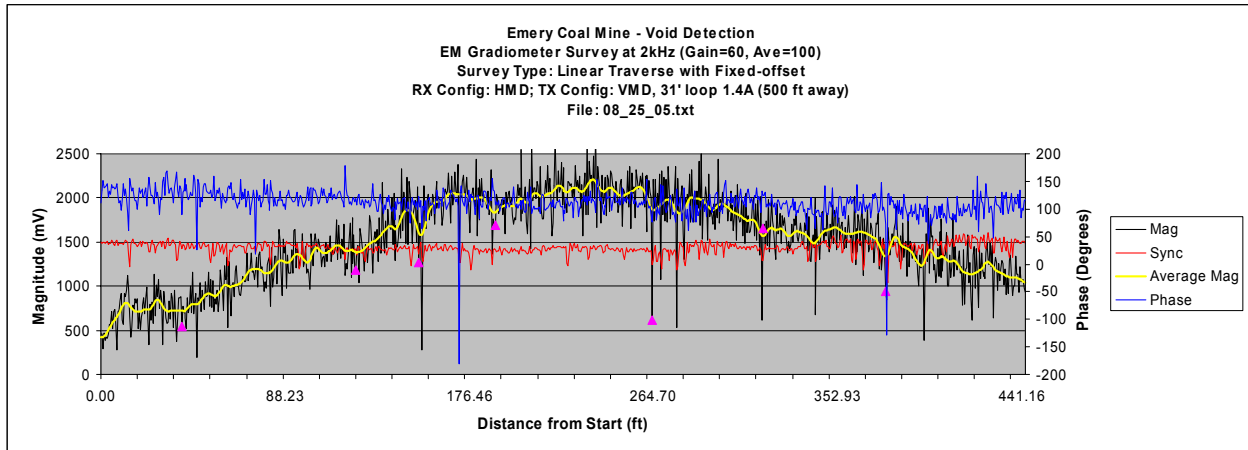
*Figure A-31. Area 5 2-kHz traverse response plot 2.*



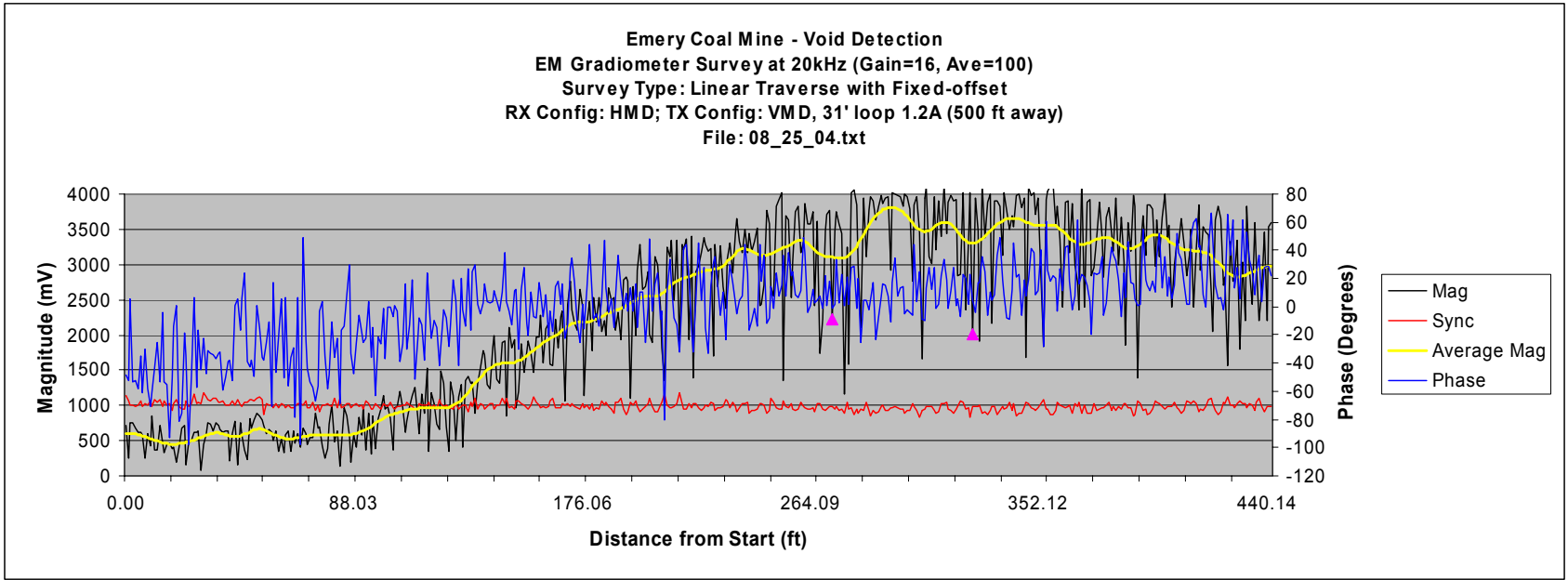
*Figure A-32. Area 5 2-kHz traverse response plot 3.*



*Figure A-33. Area 5 2-kHz traverse response plot 4.*



*Figure A-34. Area 5 2-kHz traverse response plot 5.*



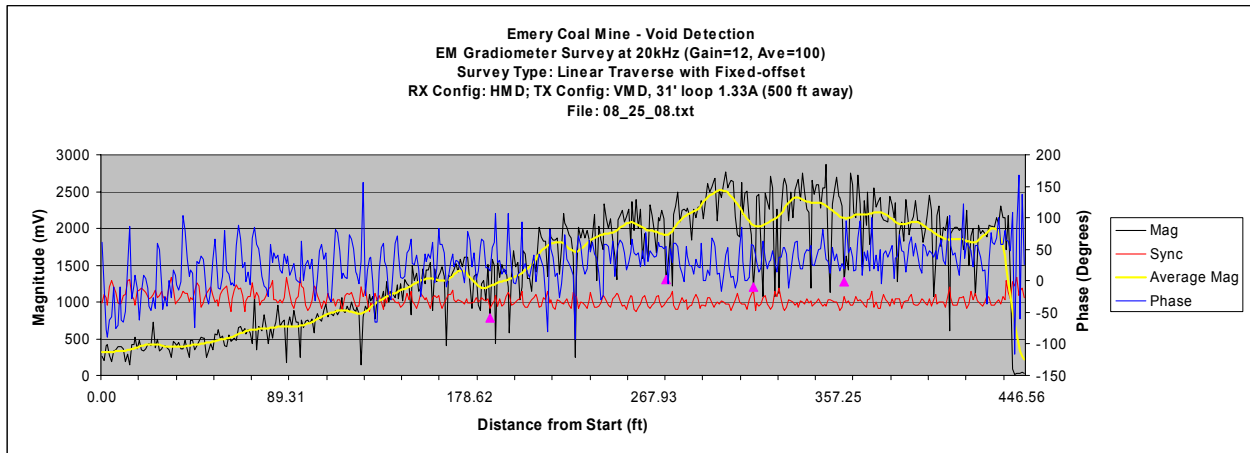


*Figure A-36. Area 5 20-kHz traverse response plot 2.*

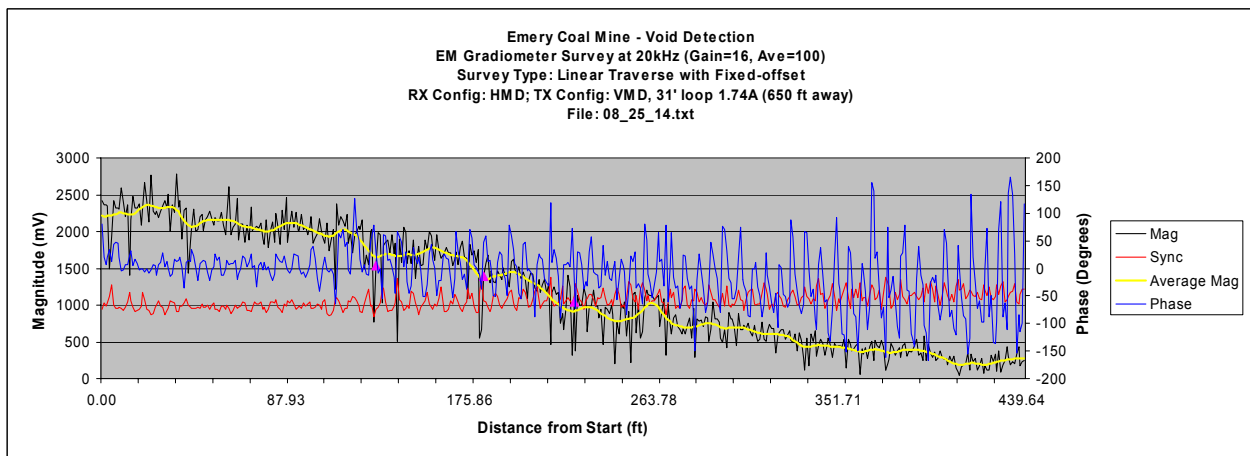


*Figure A-37. Area 5 20-kHz traverse response plot 3.*

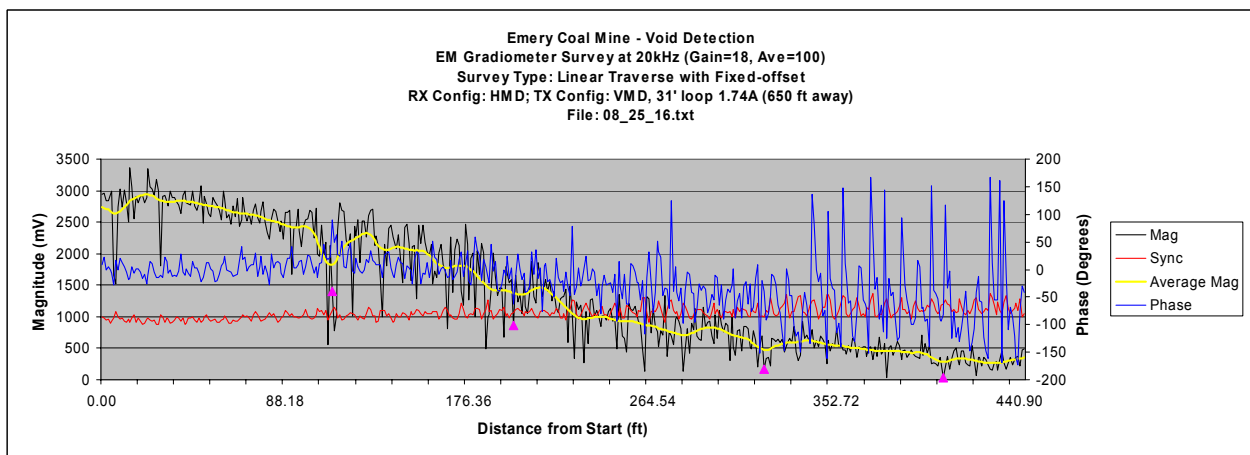


*Figure A-38. Area 5 20-kHz traverse response plot 4.*

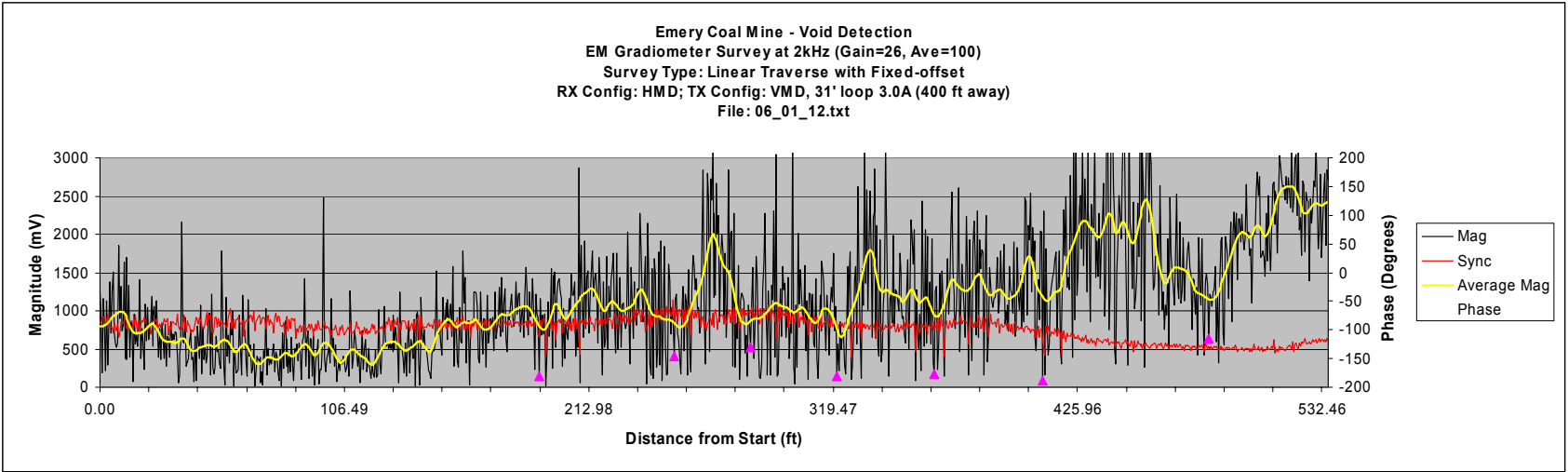


*Figure A-39. Area 6 2-kHz traverse response plot 1.*





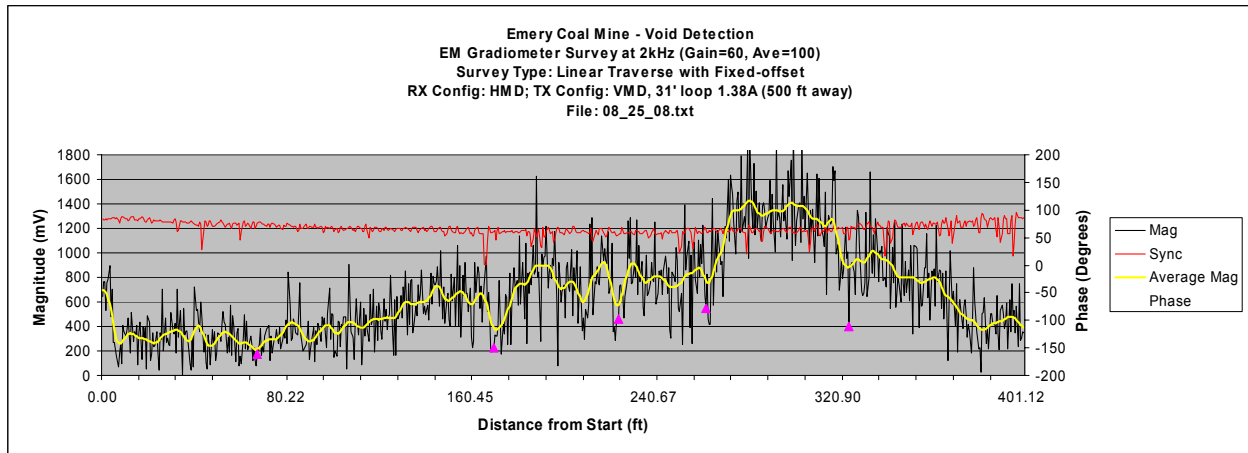


*Figure A-40. Area 6 2-kHz traverse response plot 2.*

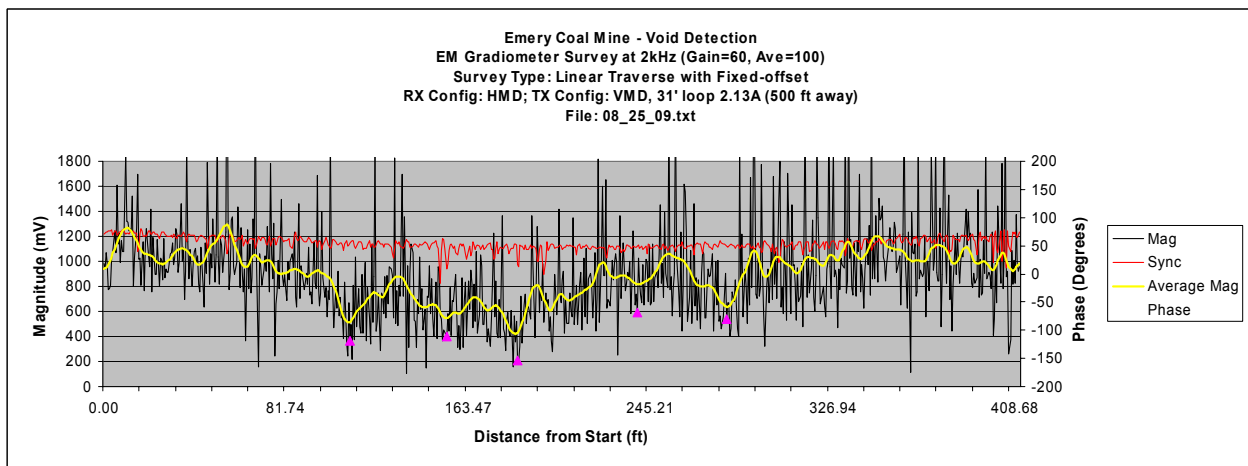


*Figure A-41. Area 6 2-kHz traverse response plot 3.*

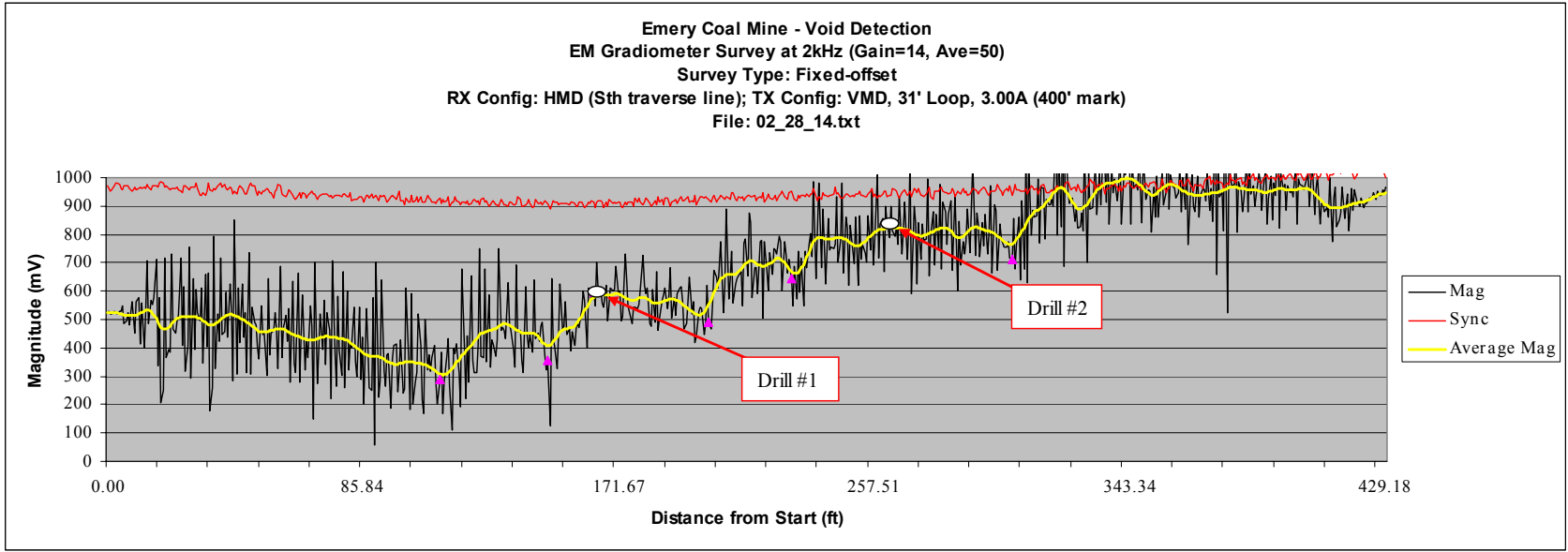


*Figure A-42. Old Workings Area 2-kHz traverse response plot 1.*



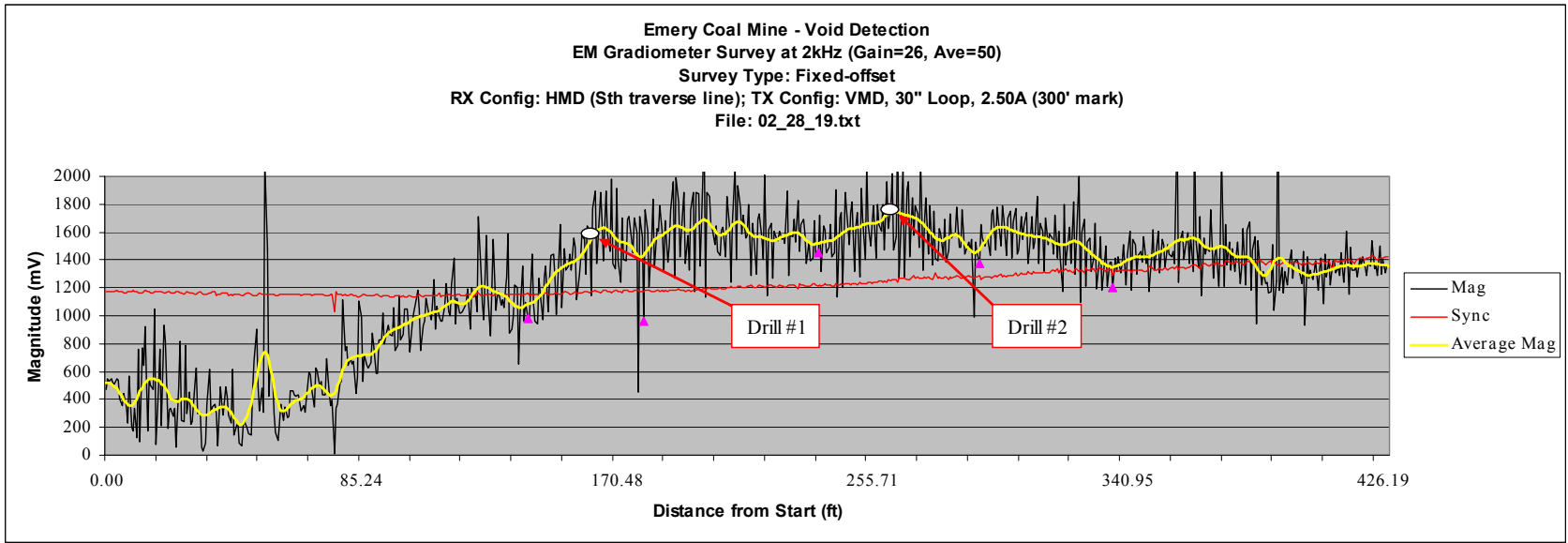


*Figure A-43. Old Workings Area 2-kHz traverse response plot 2.*



## APPENDIX B DELTAEM GRADIOMETER SPECIFICATIONS

### Detector

Detector type	Super-heterodyne
Gradiometer configurations	Horizontal gradient
Selectable operating frequencies of detection	2, 20, 80, 200 kHz
Depth range of detection penetration	0 to 300+ ft

### Mechanical

#### Weights

Receiver assembly with antennas and electronics	28.0 lb
Battery pack	5.0 lb
Transmitter electronics	1.4 lb
Transmitter antenna loop	5 lb (min) to 15 lb (max)
Transport, receiver assembly	Telescoping design

#### Dimensions

Carbon-fiber telescoping assembly	5 ft. long x 2.1 in. diameter (collapsed) 9 ft 3 in. long x 2.1 in. diameter (extended)
Receiver antenna rod	28 in. long x 1.5 in. diameter
Carbon-fiber assembly with antennas	14 ft long tip-to-tip (extended)
Transmitter antenna loop	4.5 in. high (max) x 30 in. diameter
Receiver electronics enclosure box	10.25 in. L x 5.75 in. high x 2.0 in. wide
Transmitter electronics enclosure box	8.0 in. L x 4.0 in. high x 2.0 in. wide

### Operational

Field maintenance	Replaceable modular design
Check status	Circuit monitoring and alert
Power source	12-VDC battery (10 Amp-hour)
Power consumption	1.45 A max (610 mA rcvr+840 mA PDA)
Battery types	Rechargeable nickel-metal hydride
Recharging capabilities	AC/DC adaptor
Operating time	8 hours continuous
Humidity level	95%
Temperature range, electronics	0 °C to 70 °C
Temperature range, PDA	0 °C to 40 °C
Vibration	MIL-STD-810E, <i>Transportation</i>

## APPENDIX C

Geology log data is given for coreholes near the Old Workings area, shown in Figure 76.

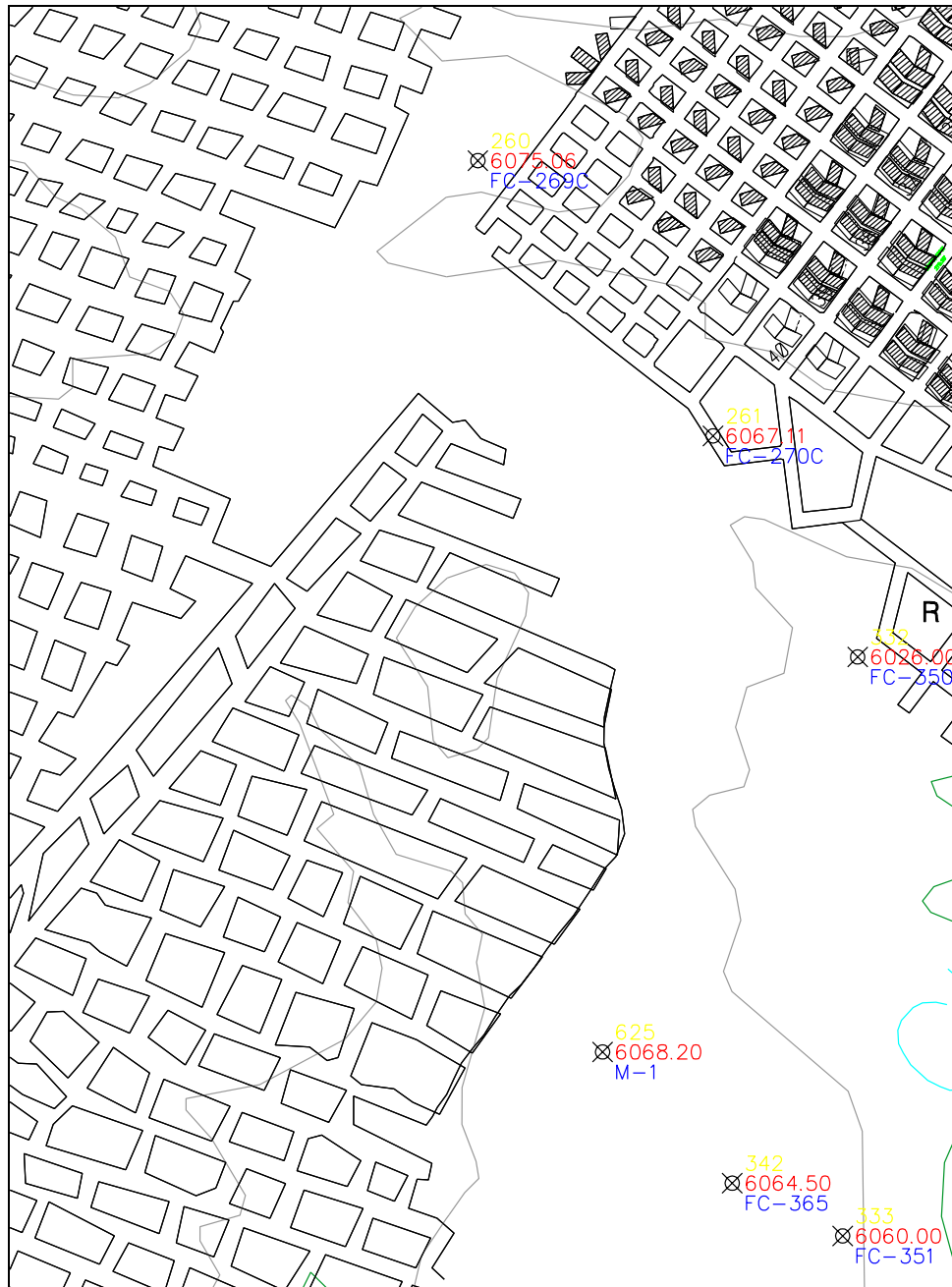


**Figure 76.** Locations of nearby corehole for the Old Workings Area

CONSOLIDATION COAL COMPANY

UNKNOWN

EMERY (211)

\*\*\* GEOLOGIST LOG \*\*\*

HOLE NO = FC- -269-C

-----

STATE = UTAH COUNTY = EMERY TWP = 022S RANGE = 006E SECT = 28

S ELEV = 6075.06 HOW DET = TRANSIT USGS QUAD = MESA BUTTE USGS SIZE = 71/2 MIN

N-COOR = 194713. E-COOR = 2071233. SOURCE = STATE LOC CODE = TELMETER ELOG = 12

MERIDIAN = SECT-NUM = CONTR = CONSOL DRILLER = ANDERSON DRILL CODE = ROTARY

FLUID = UNKNOWN FLOW = NONE CEMENTED = UNKNOWN WRAPPING = UNKNOWN CONTAINER = UNKNOWN

CORE COND. = UNKNOWN UNITS = ENGLISH SURFACE AZIMUTH DEG = .00 SURFACE DIP DEG = .00

INSPECTOR = E.KUHN DATE DRILLED = 040974 TO 040974 DATA SOURCE = CONSOL

COMMENTS = E-LOG ONLY

\*\*\* DATA ENTERED IN TO-DEPTHS \*\*\*

STRATA STRATA DEPTH STRATA SEAM CHARACTERISTICS





ELEV (TOP)	FROM	TO	THICK	CODE	LITHOLOGY	AND COMMENTS
6075.06	.00	11.00	11.00		SURFACE CASING, OVERBURDEN	
6064.06	11.00	112.00	101.00		SHALE	
5963.06	112.00	112.01	.01	TF	SANDSTONE	
5963.05	112.01	122.00	9.99		SANDSTONE	
5953.06	122.00	135.50	13.50		SANDY SHALE	
5939.56	135.50	165.00	29.50		SANDSTONE	
5910.06	165.00	170.70	5.70		SHALE	
5904.36	170.70	172.20	1.50	J1	COAL	
5902.86	172.20	173.70	1.50	J3	COAL	
5901.36	173.70	175.80	2.10		SHALE	
5899.26	175.80	182.00	6.20	UI	COAL	
5893.06	182.00	183.50	1.50		SHALE	
5891.56	183.50	192.00	8.50	LI1	COAL	
5883.06	192.00	197.30	5.30	LI5	COAL	
5877.76	197.30	200.00	2.70		SANDSTONE	
5875.06		200.00			BOTTOM HOLE	



CONSOLIDATION COAL COMPANY

UNKNOWN

EMERY (211)

\*\*\* GEOLOGIST LOG \*\*\*

HOLE NO = FC- -270-C

-----

STATE = UTAH COUNTY = EMERY TWP = 022S RANGE = 006E SECT = 28

S ELEV = 6067.11 HOW DET = TRANSIT USGS QUAD = MESA BUTTE USGS SIZE = 71/2 MIN

N-COOR = 194327. E-COOR = 2071563. SOURCE = STATE LOC CODE = TELMETER ELOG = 12

MERIDIAN = SECT-NUM = CONTR = CONSOL DRILLER = ANDERSON DRILL CODE = ROTARY

FLUID = UNKNOWN FLOW = NONE CEMENTED = UNKNOWN WRAPPING = UNKNOWN CONTAINER = UNKNOWN

CORE COND. = UNKNOWN UNITS = ENGLISH SURFACE AZIMUTH DEG = .00 SURFACE DIP DEG = .00

INSPECTOR = E.KUHN DATE DRILLED = 040974 TO 040974 DATA SOURCE = CONSOL

COMMENTS = E-LOG ONLY

\*\*\* DATA ENTERED IN TO-DEPTHS \*\*\*

STRATA STRATA DEPTH STRATA SEAM CHARACTERISTICS



ELEV (TOP)	FROM	TO	THICK	CODE	LITHOLOGY	AND COMMENTS
6067.11	.00	4.70	4.70		SURFACE CASING, OVERBURDEN	
6062.41	4.70	30.10	25.40		SHALE	
6037.01	30.10	30.11	.01	TF	SANDSTONE	
6037.00	30.11	31.00	.89		SANDSTONE	
6036.11	31.00	139.50	108.50		SANDSTONE	
5927.61	139.50	142.10	2.60		SHALE	
5925.01	142.10	144.00	1.90	J1	COAL	
5923.11	144.00	145.90	1.90	J3	COAL	
5921.21	145.90	147.80	1.90		SHALE	
5919.31	147.80	153.50	5.70	UI	COAL	
5913.61	153.50	155.00	1.50	UI	IMPURE COAL	
5912.11	155.00	161.00	6.00	LI1	COAL	
5906.11	161.00	167.10	6.10	LI5	COAL	
5900.01	167.10	167.70	.60		SHALE	
5899.41	167.70	168.20	.50		SANDSTONE	
5898.91	168.20	168.80	.60		SANDY SHALE	
5898.31	168.80	170.80	2.00		SANDSTONE	
5896.31	170.80	180.00	9.20		SANDY SHALE	
5887.11		180.00			BOTTOM HOLE	



CONSOLIDATION COAL COMPANY

UNKNOWN

EMERY (211)

\*\*\* GEOLOGIST LOG \*\*\*

HOLE NO = FC- -350-

-----

STATE = UTAH COUNTY = EMERY TWP = 022S RANGE = 006E SECT = 33

S ELEV = 6026.00 HOW DET = TRANSIT USGS QUAD = MESA BUTTE USGS SIZE = 71/2 MIN

N-COOR = 194017. E-COOR = 2071766. SOURCE = STATE LOC CODE = TELMETER ELOG = 12

MERIDIAN = SECT-NUM = CONTR = CONSOL DRILLER = DRILL CODE = ROTARY

FLUID = UNKNOWN FLOW = NONE CEMENTED = UNKNOWN WRAPPING = UNKNOWN CONTAINER = UNKNOWN

CORE COND. = UNKNOWN UNITS = ENGLISH SURFACE AZIMUTH DEG = .00 SURFACE DIP DEG = .00

INSPECTOR = DATE DRILLED = 112274 TO 112274 DATA SOURCE = CONSOL

COMMENTS = E-LOG ONLY

\*\*\* DATA ENTERED IN TO-DEPTHS \*\*\*

STRATA STRATA DEPTH STRATA SEAM CHARACTERISTICS



ELEV (TOP)	FROM	TO	THICK	CODE	LITHOLOGY	AND COMMENTS
6026.00	.00	12.00	12.00		SURFACE CASING, OVERBURDEN	
6014.00	12.00	83.00	71.00		SANDSTONE	
5943.00	83.00	84.50	1.50	J1	COAL WITH SHALE LAYERS	
5941.50	84.50	86.50	2.00	J3	COAL WITH SHALE LAYERS	
5939.50	86.50	88.00	1.50		SHALE	
5938.00	88.00	94.00	6.00	UI	COAL	
5932.00	94.00	94.80	.80	UI	IMPURE COAL	
5931.20	94.80	101.00	6.20	LI1	COAL	
5925.00	101.00	108.30	7.30	LI5	COAL	
5917.70	108.30	120.00	11.70		SILTSTONE	
5906.00		120.00			BOTTOM HOLE	

CONSOLIDATION COAL COMPANY

UNKNOWN

EMERY (211)

\*\*\* GEOLOGIST LOG \*\*\*

HOLE NO = FC- -351-

-----

STATE = UTAH COUNTY = EMERY TWP = 022S RANGE = 006E SECT = 33

S ELEV = 6060.00 HOW DET = TRANSIT USGS QUAD = MESA BUTTE USGS SIZE = 7 1/2 MIN

N-COOR = 193205. E-COOR = 2071745. SOURCE = STATE LOC CODE = TOPO ELOG = 12

MERIDIAN = SECT-NUM = CONTR = CONSOL DRILLER = DRILL CODE = ROTARY

FLUID = UNKNOWN FLOW = NONE CEMENTED = UNKNOWN WRAPPING = UNKNOWN CONTAINER = UNKNOWN

CORE COND. = UNKNOWN UNITS = ENGLISH SURFACE AZIMUTH DEG = .00 SURFACE DIP DEG = .00

INSPECTOR = DATE DRILLED = 112174 TO 112174 DATA SOURCE = CONSOL

COMMENTS = E-LOG ONLY

\*\*\* DATA ENTERED IN TO-DEPTHS \*\*\*





STRATA ELEV (TOP)	STRATA FROM	DEPTH TO	STRATA THICK	SEAM CODE	LITHOLOGY	CHARACTERISTICS AND COMMENTS
6060.00	.00	4.00	4.00		SURFACE CASING, OVERBURDEN	
6056.00	4.00	43.50	39.50		SANDSTONE	
6016.50	43.50	56.50	13.00		SANDY SHALE	
6003.50	56.50	95.00	38.50		SANDSTONE	
5965.00	95.00	96.50	1.50	J1	COAL	
5963.50	96.50	98.00	1.50	J3	COAL	
5962.00	98.00	100.00	2.00		SHALE	
5960.00	100.00	107.00	7.00	UI	COAL	
5953.00	107.00	108.00	1.00	UI	IMPURE COAL	
5952.00	108.00	112.00	4.00	LI1	COAL	
5948.00	112.00	120.50	8.50	LI5	COAL	
5939.50	120.50	123.10	2.60		SHALE	
5936.90	123.10	129.20	6.10		SANDSTONE	
5930.80	129.20	140.00	10.80		SANDY SHALE	
5920.00		140.00			BOTTOM HOLE	

CONSOLIDATION COAL COMPANY

UNKNOWN

EMERY (211)

\*\*\* GEOLOGIST LOG \*\*\*

HOLE NO = FC- -365-

-----

STATE = UTAH COUNTY = EMERY TWP = 022S RANGE = 006E SECT = 33

S ELEV = 6064.50 HOW DET = TRANSIT USGS QUAD = MESA BUTTE USGS SIZE = 71/2 MIN

N-COOR = 193279. E-COOR = 2071590. SOURCE = STATE LOC CODE = SURVEYED ELOG = 123

MERIDIAN = SECT-NUM = CONTR = DANIELS DRILLER = L.C.KNIGHT DRILL CODE = CNT CORE

FLUID = UNKNOWN FLOW = NONE CEMENTED = UNKNOWN WRAPPING = UNKNOWN CONTAINER = UNKNOWN

CORE COND. = UNKNOWN UNITS = ENGLISH SURFACE AZIMUTH DEG = .00 SURFACE DIP DEG = .00

INSPECTOR = DATE DRILLED = 042675 TO 042675 DATA SOURCE = CONSOL

COMMENTS =

\*\*\* DATA ENTERED IN TO-DEPTHS \*\*\*

STRATA STRATA DEPTH STRATA SEAM CHARACTERISTICS



ELEV (TOP)	FROM	TO	THICK	CODE	LITHOLOGY	AND COMMENTS
6064.50	.00	15.00	15.00		SURFACE CASING, OVERBURDEN	
6049.50	15.00	20.00	5.00		SANDSTONE	BRN
6044.50	20.00	58.60	38.60		SANDSTONE, GRAY	MGR CGR
6005.90	58.60	71.70	13.10		SANDY SHALE	DRK GRY
5992.80	71.70	110.00	38.30		SANDSTONE, GRAY	CAL MGR CGR SHY NBM
5954.50	110.00	110.30	.30		SHALE, CARBONACEOUS	COL SDY PYT
5954.20	110.30	112.00	1.70	J1	COAL WITH PYRITE STREAKS	
5952.50	112.00	114.00	2.00	J3	COAL WITH PYRITE STREAKS	
5950.50	114.00	114.95	.95		CLAY	GRY SDY SFT
5949.55	114.95	115.25	.30		SHALE, CARBONACEOUS	CLY
5949.25	115.25	121.00	5.75	UI	COAL	
5943.50	121.00	121.04	.04		SILTSTONE	
5943.46	121.04	128.00	6.96	LI1	COAL	
5936.50	128.00	128.04	.04		PYRITE	
5936.46	128.04	135.80	7.76	LI5	COAL	
5928.70	135.80	140.30	4.50		SANDY SHALE	GRY
5924.20		140.30			BOTTOM HOLE	

CONSOLIDATION COAL COMPANY

UNKNOWN

EMERY

(211)

\*\*\* GEOLOGIST LOG \*\*\*

HOLE NO = M - - 1-

-----

STATE = UTAH

COUNTY = EMERY

TWP = 022S

RANGE = 006E

SECT = 33

S ELEV = 6068.20

HOW DET = TOPO

USGS QUAD = MESA BUTTE

USGS SIZE = 7 1/2 MIN

N-COOR = 193463.

E-COOR = 2071408.

SOURCE = STATE

LOC CODE = TOPO

ELOG = 0

MERIDIAN =

SECT-NUM =

CONTR = USGS

DRILLER = CLARK

DRILL CODE = UNKNOWN

FLUID = UNKNOWN

FLOW = NONE

CEMENTED = UNKNOWN

WRAPPING = UNKNOWN

CONTAINER = UNKNOWN

CORE COND. = UNKNOWN

UNITS = ENGLISH

SURFACE AZIMUTH DEG = .00

SURFACE DIP DEG = .00

INSPECTOR =

DATE DRILLED =

TO 060179

DATA SOURCE = USGS

COMMENTS = USGS OFR 81-460, HOLES M-1 AND Q-5A

\*\*\* DATA ENTERED IN TO-DEPTHS

\*\*\*

STRATA

STRATA DEPTH

STRATA

SEAM

CHARACTERISTICS



ELEV (TOP)	FROM	TO	THICK	CODE	LITHOLOGY	AND COMMENTS
6068.20	.00	100.00	100.00		SURFACE CASING, OVERBURDEN	
5968.20	100.00	101.20	1.20		SILTSTONE	SDY
5967.00	101.20	125.00	23.80		SANDSTONE, GRAY, CROSSBEDDED	FGR CGR
5943.20	125.00	126.30	1.30		SHALE, CARBONACEOUS	
5941.90	126.30	128.20	1.90		SANDSTONE	BUR
5940.00	128.20	128.80	.60	J1	COAL WITH SHALE LAYERS	
5939.40	128.80	128.85	.05	J1	SILTSTONE	CAR
5939.35	128.85	129.45	.60	J1	COAL WITH SHALE LAYERS	
5938.75	129.45	129.50	.05		CLAY, BENTONITIC	
5938.70	129.50	131.45	1.95		SHALE	COL COS
5936.75	131.45	131.50	.05		CLAY, BENTONITIC	
5936.70	131.50	132.80	1.30	J3	COAL WITH SHALE LAYERS	
5935.40	132.80	133.00	.20		SHALE, CARBONACEOUS	
5935.20	133.00	133.60	.60		CLAY, BENTONITIC	
5934.60	133.60	139.55	5.95	UI	COAL	
5928.65	139.55	139.57	.02	UI	CLAY, BENTONITIC	
5928.63	139.57	140.10	.53	UI	COAL	
5928.10	140.10	140.11	.01		CLAY, BENTONITIC	
5928.09	140.11	146.60	6.49	LI1	COAL	
5921.60	146.60	155.10	8.50	LI5	COAL	
5913.10	155.10	155.50	.40		SHALE, CARBONACEOUS	SLY COS
5912.70	155.50	161.80	6.30		SANDSTONE	SLY NTP RTD
5906.40	161.80	219.00	57.20		NO ROCK RECOVERED	
5849.20	219.00	222.00	3.00		SILTSTONE	SDY BUR MAR
5846.20	222.00	223.20	1.20		SANDSTONE	FGR SLY BUR



5845.00	223.20	226.00	2.80		SANDSTONE	VFG FGR MAR
5842.20	226.00	233.20	7.20		SANDSTONE	FGR BUR
5835.00	233.20	234.60	1.40		SHALE	COL
5833.60	234.60	239.90	5.30	D	COAL	
5828.30	239.90	241.20	1.30		CLAY, BENTONITIC	
5827.00	241.20	243.25	2.05	C	COAL	
5824.95	243.25	243.35	.10	C	CLAY, BENTONITIC	
5824.85	243.35	243.85	.50	C	COAL	
5824.35	243.85	243.95	.10	C	CLAY, BENTONITIC	
5824.25	243.95	245.75	1.80	C	COAL	
5822.45	245.75	246.00	.25	C	CLAY, BENTONITIC	
5822.20	246.00	248.20	2.20	C	COAL	
5820.00	248.20	248.50	.30		SHALE	COL
5819.70	248.50	249.50	1.00		CLAYSTONE	RTD
5818.70	249.50	250.90	1.40		SILTSTONE	CLY RTD NTP BUR NBM
5817.30		250.90			BOTTOM HOLE	

## APPENDIX D

January 9, 2007

Jerry L. Jones  
Stolar Research Corporation  
848 Clayton Highway  
Raton, New Mexico 87740

Subject: Void Confirmation at the Emery Mine

Dear Mr. Jones,

As per the request of Stolar Research Corporation, EarthFax Engineering Inc. (EarthFax) advanced two bore holes to confirm the location of the abandoned mine workings at the Consol Energy's (Consol) Emery Mine near Emery Utah. This was accomplished using a rotary core drill rig operated by Prosonic Corporation during four separate occasions between November 16, 2006 and January 7, 2007. The drilling took place during weekends when the Emery Mine was closed and was therefore vacant of mine workers.

Since the drilling was performed within mine permit boundaries, safety was a high priority. All personnel on site were required to attend Consol's site-specific safety-training course on the hazards of working near mine workings. Personal protective equipment for each worker on site included a hard hat, padded gloves provided by Consol, steel-toed boots, safety glasses, hearing protection, and a reflective vest. Methane readings were taken with two gas detectors placed within ten feet of the boring during the entire drilling process. Water was used to flood the hole while drilling to keep the potential for methane low and to help detect small voids. A walky-talky style radio was kept on hand to keep in contact with the on-site Consol representative.

On four occasions during the completion of both bore holes drilling ceased due to the detection of a subsurface void. Each time the air at the surface of the bore hole was analyzed for methane as well as for air movement to assess if the void was mine related. Each time it was found that they were not mine voids, and the drilling resumed. Methane was not detected at any time during the drilling operation.

The bore holes were advanced to predicted depths provided to EarthFax by Consol (see table below). Hole #1 was advanced to 172' with no mine void encountered. Hole #2 was advanced to 174' with no mine void encountered. Both bore holes were advanced to at least 5 feet below the LI 5 coal seam to ensure no mine voids were missed. Refer to the enclosed geologic logs for contact depths encountered during drilling of Holes #1 and #2.

Predicted Depths	Hole # 1	Hole #2
Depth to Top of Ferron SS	36.3'	37.1'
Depth to Bottom of Ferron SS	141.3'	128.9'
Depth to Top of Void	153.5'	153.9'
Depth to BOC	168.5'	168.9'



**EarthFax**

**EarthFax  
Engineering, Inc.**  
Engineers/Scientists  
7324 So. Union Park Ave.  
Suite 100  
Midvale, Utah 84047  
Telephone 801-561-1555  
Fax 801-561-1861  
[www.earthfax.com](http://www.earthfax.com)



Both bore holes were filled with bentonite grout to the ground surface. Drill core from the completion of both bore holes was placed on four palates and staged on site.

If you have any questions, please let me know.

Sincerely,



James Hoggard, P.G.  
EarthFax Engineering, Inc

Enclosure



*Figure D-1. Drill rig on site.*

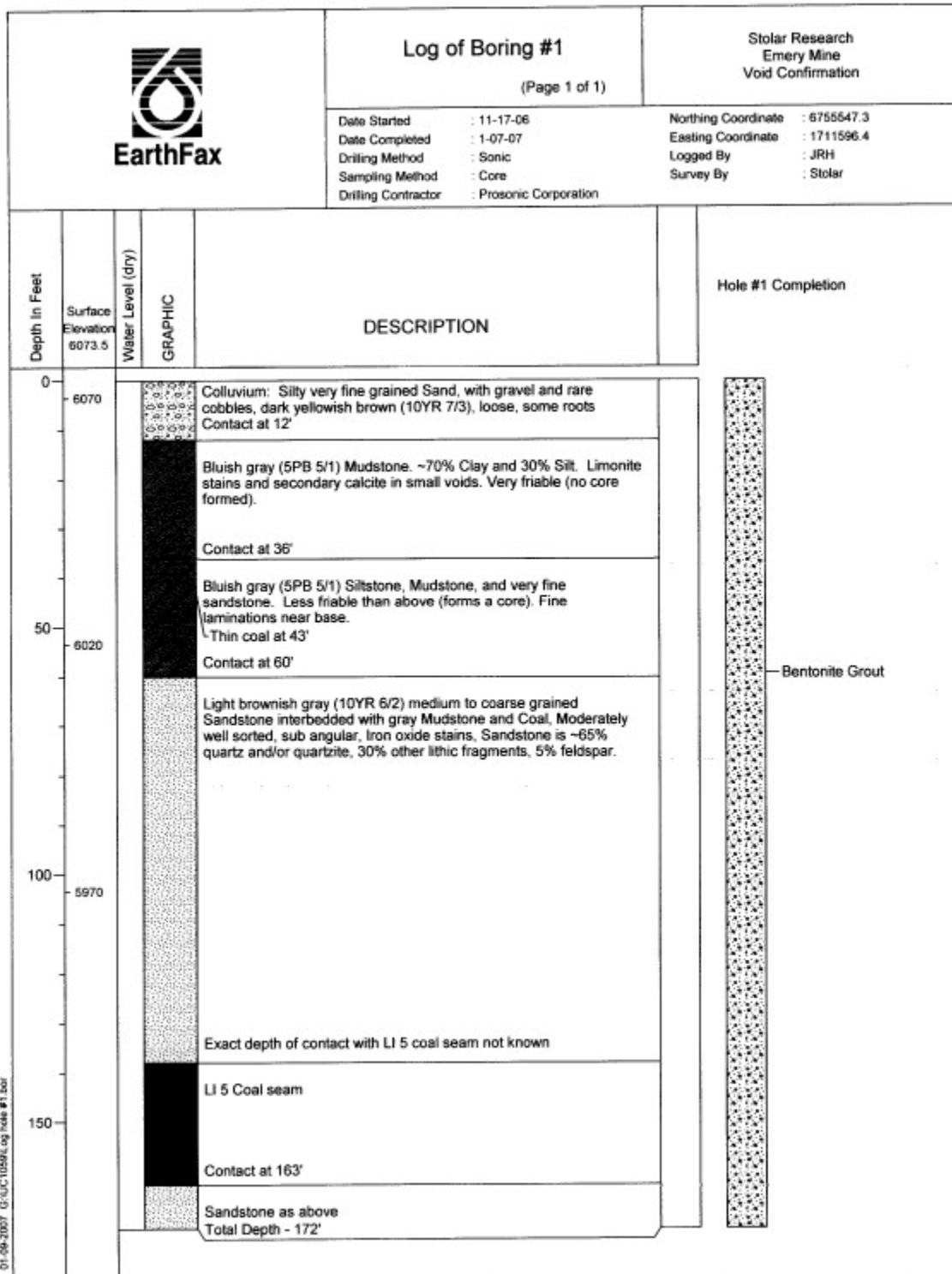


*Figure D-2. Confirmation drill hole 1 log.*

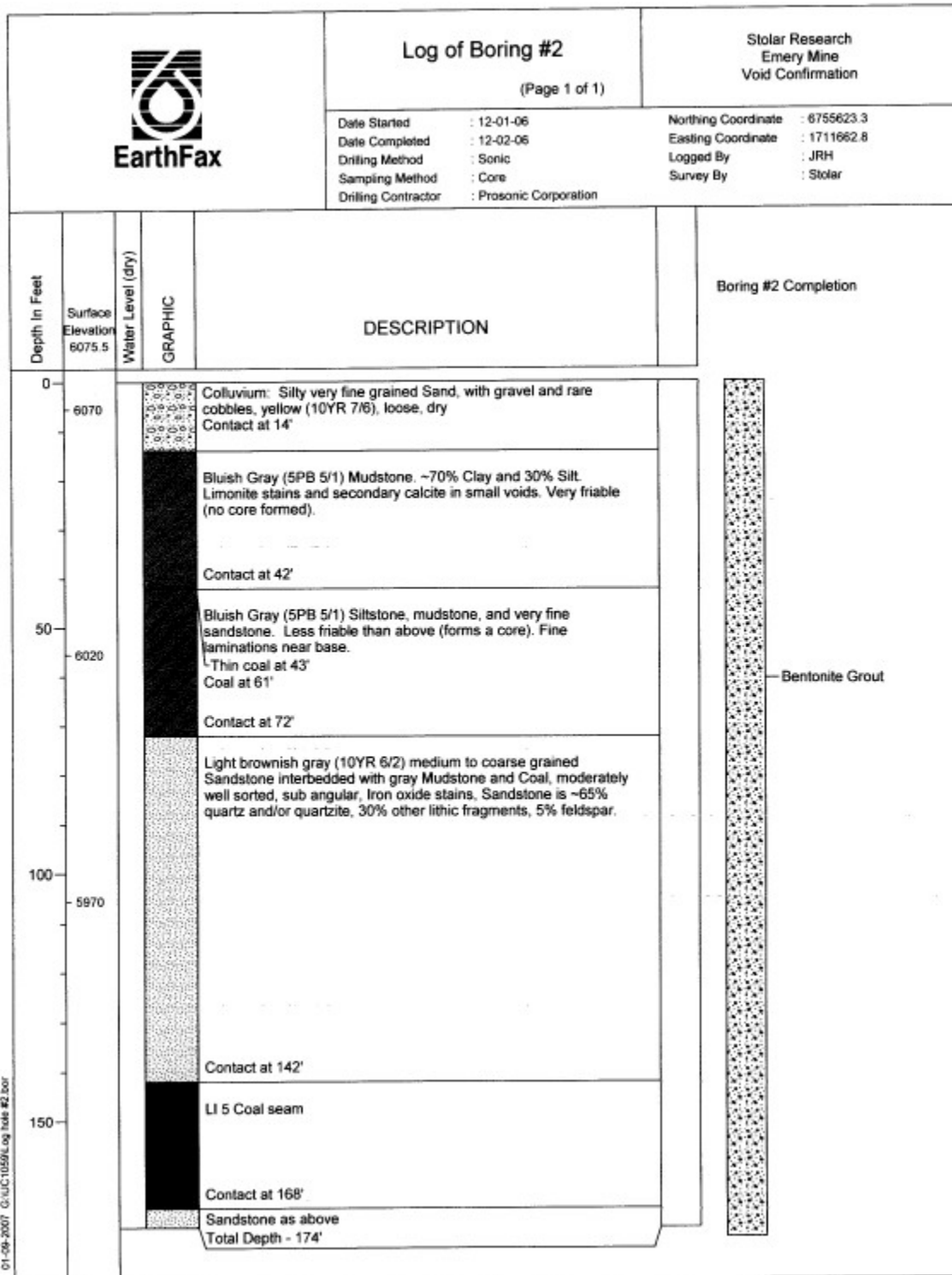


*Figure D-3. Confirmation drill hole 2 log.*